Molecular Control of Germ Plasm Localization in Zebrafish

Doctoral Thesis

Dissertation for the award of the degree

"Doctor rerum naturalium (Dr. rer. nat)"

in the GGNB program: Genes and Development

at the Georg August University Göttingen

Faculty of Biology

Submitted by

Nadia Rostam

Born in Sulaymaniyah/ Iraq

Göttingen, 2021

Members of the Thesis Advisory Committee

Prof. Dr. Ernst Wimmer

First member of the thesis committee (Supervisor) (Reviewer1).

Department of Developmental Biology, Georg August University Göttingen.

Dr. Roland Dosch

Second member of the thesis committee (Supervisor) (Reviewer2).

Institute for Human Genetics, Georg August University Göttingen.

Dr. Melina Schuh

Third member of the thesis committee

Department of Meiosis, Max Planck Institute for Biophysical Chemistry Göttingen

Members of the Examination Board

Prof. Dr. Rüdiger Behr

Deutsches Primatenzentrum (DPZ), Göttingen.

Prof. Dr. Gregor Bucher

Department of Evolutionary Developmental Biology, Georg August University Göttingen.

PD Dr. Gerd Vorbrüggen

Department of Developmental Biology, Georg August University Göttingen.

Date of oral examination: 18,08, 2021

Affidavit

Herewith I declare that I prepared the PhD thesis "**Molecular Control of Germ Plasm Localization in Zebrafish**" on my own and with no other sources and aids than quoted.

01.03.2022. _____

Nadia Rostam

Contents

Abbreviations

°C	Degrees Celsius
A	Adenine
aa	Amino acids
AJ	Apical junction
BB	Balbiani body
BSA	Bovine serum albumin
Buc	Bucky ball
C	Cytosine
C. elegans	*Caenorhabditis elegans*
cDNA	Complementary DNA
Cldn	Claudin
Co-IP	Co-immunoprecipitation
C-terminus	Carboxy-terminus
DAPI	4',6-diamidino-2-phenylindole
Dazl	Deleted in azoospermia like
DNA	Deoxyribonucleic acid
dpf	Days post fertilization
e.g.	*Exempli gratia*
EDTA	Ethylenediaminetetraacetic acid
EM	Electron microscopy
et. al.	*Et alii*
EtOH	Ethanol
FMA	Furrow microtubule array
G	Guanine
GFP	Green fluorescent protein
GP	Germ plasm

h	Hour
H2O	Water
hpf	Hours post fertilization
IDP	Intrinsically disordered protein
IDR	Intrinsically disordered region
IP	Immunoprecipitation
kDa	Kilodalton
M	Molar
MB	Midbody
MeOH	Methanol
mg	Milligram
min	Minute
ml	Millilitre
mRNA	Messenger RNA
MS	Mass spectrometry
n	Number
nl	Nanolitre
NMII	Non-muscle myosin II
N-terminus	Amino terminus
ORF	Open reading frame
Osk	Oskar
P	Proline
PBS	Phosphate-buffered saline
PBT	Phosphate-buffered saline Triton X-100
PFA	Paraformeldehyde
PGC	Primordial germ cell
PH	*Potentium hydrogenium*
PLAAC	Prion Like Amino Acid Composition

PLD	Prion like domain
p-NMII	Phosphorylated non-muscle myosin II
RNA	Ribonucleic acid
ROCK	Rhov Associated Protein Kinase
SD	Standard deviation
SDS	Sodium dodecyl sulfate
SH3	SRC Homology 3
T	Thymine
TJ	Tight junction
Tris	Tris (hydroxymethyl) aminomethane
UAS	Upstream activation sequence
UTR	Untranslated region
UV	Ultraviolet
YV	Tyrosine-valine
Zf	Zebrafish
ZO	Zonula occludens
µl	Microlitre
µm	Micrometer

Acknowledgements

First and foremost, I would like to express my sincere gratitude to my supervisor Dr. Roland Dosch for providing me the opportunity to start my PhD in his laboratory. I am very grateful for his guidance, support and encouragement and appreciate the knowledge that I learned from him.

This work would have been not completed without support and guidance of Prof. Ernst Wimmer, my second supervisor. Words cannot describe the importance of Prof. Wimmer in my PhD. I am very thankful for his scientific input and continuous support.

I would like to express my special thanks to Dr. Melina Schuh, who had a great impact on my PhD by giving me great ideas as a member of my thesis committee and being available for any other kind of help.

I am extremely thankful to Dr. Gerd Vorbrüggen, who voluntarily gave me a great amount of scientific advices and support during my PhD.

I would like to thank all the members of Dr. Dosch and Prof. Wimmer's laboratories for creating a friendly and supportive work atmosphere. Special thanks go to Roshan Perera, Hazem Khalifa and Alexander Goloborodko for being great friends and adding a lot of fun to my PhD life. In addition, I thank Gudrun Kracht for her technical support during my research.

I am also grateful for my students Julia Ochs, Srinithi Ranganathan, Julius Bahr and Armin Nikšić, who were a great help in this research.

My PhD would have been not started without encouragement from Dirk Hackel and financial support from DAAD, which I am very grateful for.

Last but not least, I want to express my heartfelt thanks and appreciation to my parents, siblings and friends who were a main reason for my success until here.

Abstract

Germ plasm (GP) consists of a maternally inherited ribonucleo-protein (RNP) condensate, which controls in many animals the formation of germline. Only the cells which contain GP commit to germ cell destinies, whereas all other cells will commit to somatic cell fates. Therefore, correct GP localization is important for germ cell specification, and its elimination is important for the development of soma. In this thesis, I show that zebrafish (*Danio rerio*) GP localization is similar to that of *Xenopus* but different from *Drosophila*. Bucky ball (Buc), the GP organizer in zebrafish, was used in this research as a molecular proxy to follow GP localization. The identification of Buc localization domain (BucLoc) is presented here as a tool to identify the protein interactome of Buc recruitment, which led to the identification of non-muscle myosin II (NMII) and tight junction (TJ) components such as ZO2 and Claudin-d (Cldn-d) as interacting candidates of Buc. The data here show that Buc colocalizes with TJ proteins ZO1 and Cldn-d. Moreover, TJ- like structures, at the cleavage furrows where the GP is anchored, was revealed under electron microscopy (EM). Furthermore, the detailed protein machinery anchoring GP at TJs is presented here. I am showing that multiple PxxP motifs in Buc interact with the SH3 domains of the TJ proteins ZO2a and ZO2b. I am showing a detailed mutation analysis of PxxP motifs in Buc, leading to the identification of the key motifs for interaction with SH3 domain and ultimate localization of GP at the TJs. Finally, overexpression of TJ-receptor Cldn-d created additional GP aggregates, whereas expression of a dominant negative version prevents the production of GP aggregates. Taken together, the data presented in this thesis discovered a comprehensive molecular mechanism for GP localization in zebrafish.

1. General Introduction

Reproduction is the fundamental feature of every living entity. This biological process has played a major role in the course of evolution and survival on our planet. Living organisms have adapted two types of reproduction, asexual and sexual. Asexual reproduction is the process which takes place in primitive organisms like bacteria. In this type of reproduction, only one parent is involved and as the result there is no genetic variation between the parent and its offspring. Different generations will contain identical genetic material (Crow 1994). In contrast, higher organisms like metazoans and other multicellular organisms reproduce by a more evolved reproduction process, sexual reproduction. These higher species have developed specialized cells called germ cells, which are exclusively dedicated for reproduction, allowing the rest of the cells to become soma and develop more specialized functions which in turn increases the overall fitness of multicellular organisms.

Precursors of germ cells have a unique capacity to undergo meiosis, which is essential for the formation of the two special types of cells that are required for sexual reproduction, the gametes (Strome and Updike 2015). Sexual reproduction involves two types of gametes, egg and sperm, which come from two parents. As the result, the resulted offspring from this kind of reproduction will contain genetic information from both parents and does not look identical to any of them. This type of reproduction has advantages over asexual reproduction, although it is a more complicated and energy costing process. Sexual reproduction provides the opportunity to mix and change genetic materials, incorporate more favourable mutations, and get rid of harmful mutations. These are all crucial factors during evolution, that increases overall species adaptation and survival (Crow 1994; Dosch 2015).

The process of sexual reproduction is facilitated through gonads in adults that produce gametes. When two gametes of two different sexes fuse, they form a zygote that will give rise to a whole embryo. During embryogenesis the embryo builds the precursor cells for their gonads, so called germ cells, that can then produce new gametes to give rise to the next generation. To survive, sexual organisms have to guarantee the correct germ cell specification, germ line development and fertility of their individuals (Ewen-Campen, Schwager, and Extavour 2010). Despite its importance, little is known about the mechanism behind germ cell specification in multicellular organisms. A better understanding of how this

process is organized and takes place will shade light on many critical biological questions that might lead to uncovering various aspects of cell specification and ultimately a better treatment for infertility.

1.1. Germ cell specification

Early embryogenesis is a very critical time point in the development of sexually reproducing organisms. It is a phase in which a single pluripotent cell, the zygote, commits to form the set of numerous unipotent cell types. Particularly, the one very important cell type 'germ cell' must be precisely specified, so that reproduction is assured. The separation of germ cells from somatic cells and the mechanism by which they specify is a central question in developmental biology (Extavour and Akam 2003; Ewen-Campen, Schwager, and Extavour 2010). Therefore, it is very precious to understand how different organisms specify germ cells.

During evolution, species have adapted two different strategies of germ cell specification: Induction and inheritance (Figure 1). The induction mode implies cells being specified to become germ cells as a response to paracrine signalling received from neighbouring cells. Vertebrates such as mammals, reptiles and urodeles use this mode to specify their germ cells (Extavour and Akam 2003). For example, in mice BMP4 signals from extraembryonic tissues induce germ cells specification in the epiblast just before the onset of gastrulation. BMP4 triggers the expression of BLIMP1, which is the key regulator of primordial germ cell specification (Saitou 2009).

In the inheritance mode of germ cell specification, mothers deposit cytoplasmic determinants which specify cells which receive them as germ cells. *Xenopus, Drosophila*, and zebrafish (*Danio rerio*) use this mode of germ cell specification. In zebrafish, mothers deposit germ plasm (GP) in oocytes, which later gets asymmetrically distributed during subsequent embryonic divisions (Bontems et al. 2009; Dosch 2015; Riemer et al. 2015).

1.2. Germ plasm

The history of inheritance mode of GP specification goes back to the GP theory that was established by August Weismann in the 19th century. According to him, inheritance is solely depending on the germ cells, which is what up to now accepted; however, he believed that inherited materials are stored in the nucleus. In 1910, Boveri discovered that GP is localized in the cytoplasm, not the nucleus (Riemer 2014; Weismann 1983). GP is the collection of maternal factors, RNAs and proteins, which are stored in the cytoplasm of the oocyte and gets transported to the embryo to control germ cell formation. Apart of germ cell specification, this unique process shows how mothers can genetically control the development of their offspring during embryonic development through cytoplasmic determinants (Dosch 2015).

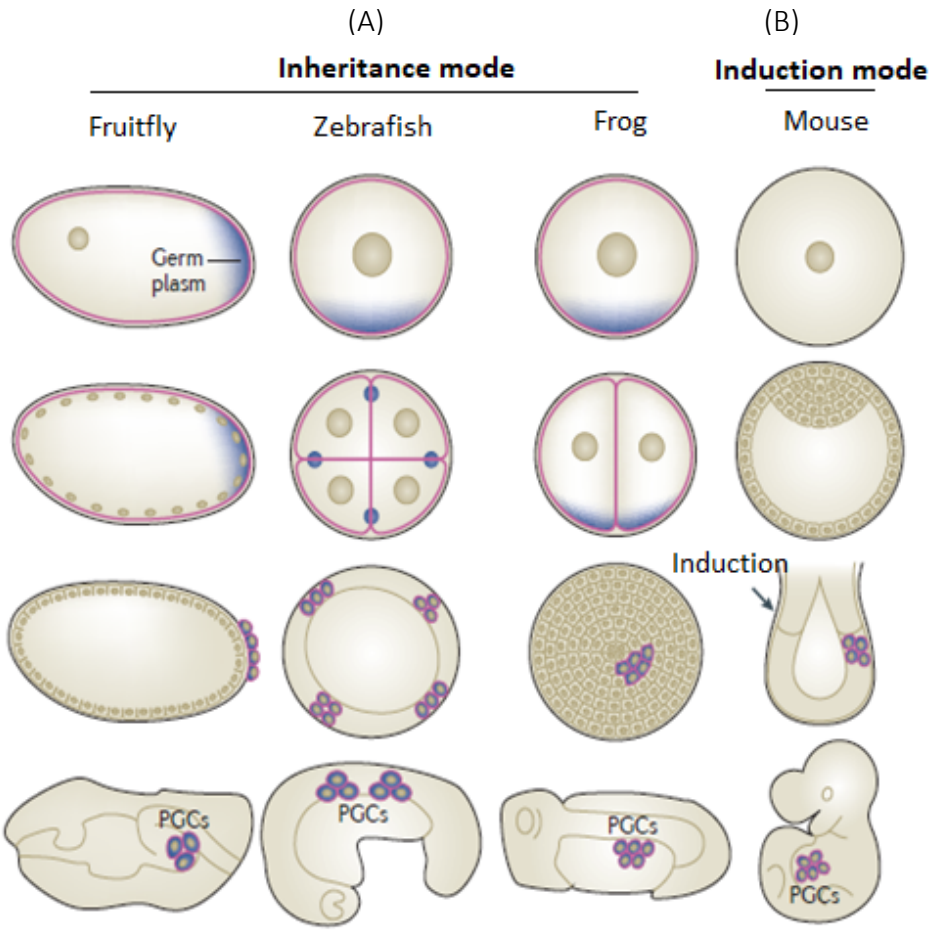

Figure 1. Primordial germ cell (PGC) formation in different animals with different mode of germ cell specification. A) Fruit fly, zebrafish and frog use inhertance mode of germ cell specifcaion while mouse uses induction mode. In the inheritance mode, GP is passed from oocyte to the PGCs in early embryos. Here, germ line is present at all stages. Germ line cells are outlined by pink circles and germ cells are shown in blue. B) Mice use induction mode of germ cell specification. In the induction mode, PGCs are newly induced by a subset of embryonic cells, in a later stage of development (modified after Strome, 2015).

For the first time, GP was seen in frogs eggs at the vegetal cortex (cited in Riemer, 2014). Later experiments showed the functionality of GP in germ line specification in frogs. It is shown that physical removal and UV-light irradiation of GP in the egg reduces the number of primordial germ cells in frogs or generates sterile embryos (Buehr and Blackler 1970; Smith 1966). However, fertility can be restored by the injection of vegetal cytoplasm into these sterile embryos (Wakahara 1977; Smith 1966). The same influence is seen when GP is removed from zebrafish oocytes (Hashimoto et al. 2004). Moreover, ectopic localization of GP at the anterior pole of Drosophila's egg cells (Illmensee and Mahowald 1974) and the animal pole of frog embryos (Tada et al. 2012) is shown to result in the ectopic formation of germ cells. These results mean that correct localization of maternal factors play a critical role in controlling germ cell formation in different animals, in whom GP is used for germ line specification.

1.2.1. Germ plasm localization during oogenesis

In the early oocyte, germ plasm is localized inside a highly specialized membraneless cytoplasmic structure called Balbiani body (BB) (Figure 2), termed mitochondrial cloud in frogs. The BB consists of an electron dense granular/fibrous material containing mitochondria, Golgi, endoplasmic reticulum, RNAs and proteins (Boke et al. 2016; Heasman, Quarmby, and Wylie 1984). This fascinating structure is shared among animals of different groups, although they have different modes of germ cell specification. BB was first discovered in oocytes from spiders and after that it became recognized in numerous other animals, invertebrates and vertebrates. In vertebrates, BB is present in a wide range of animal groups,

from frogs and birds till mice and humans (Kloc, Bilinski, and Etkin 2004; Pepling et al. 2007). Thus the localization mechanism of GP inside the eggs is quiet similar among animals, since they share the same structure, the BB. However, a more specific localization pattern is seen among them during embryogenesis.

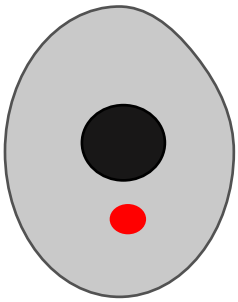

Figure 2. An exemplary oocyte containing the Balbiani body (BB). Nucleus is shown in black, BB is shown in red.

1.2.2. Germ plasm localization during embryogenesis

After fertilization and the onset of the embryonic development, animals show their own unique mechanism of GP localization, which is more diverse than during oogenesis. For example, in *Drosophila*, GP is also called pole plasm. In late oogenesis and in stage 1 embryo, pole plasm is localized to the posterior end of the egg or the embryo. Posterior migrating nuclei enter the pole plasm and budoff to form primordial germ cells, also called pole cells (Rongo and Lehmann 1996).

In *Xenopus*, GP is distributed at the vegetal cortex of the early embryo and it gets localized to the first four blastomeres after the first two cleavages. During the subsequent cell divisions, GP is localized at the cleavage furrows and gets asymmetrically distributed between the daughter cells which consequently produces a constant number of germ cells. In later stages, GP gets localized to the perinuclear region where it gives rise to the entire

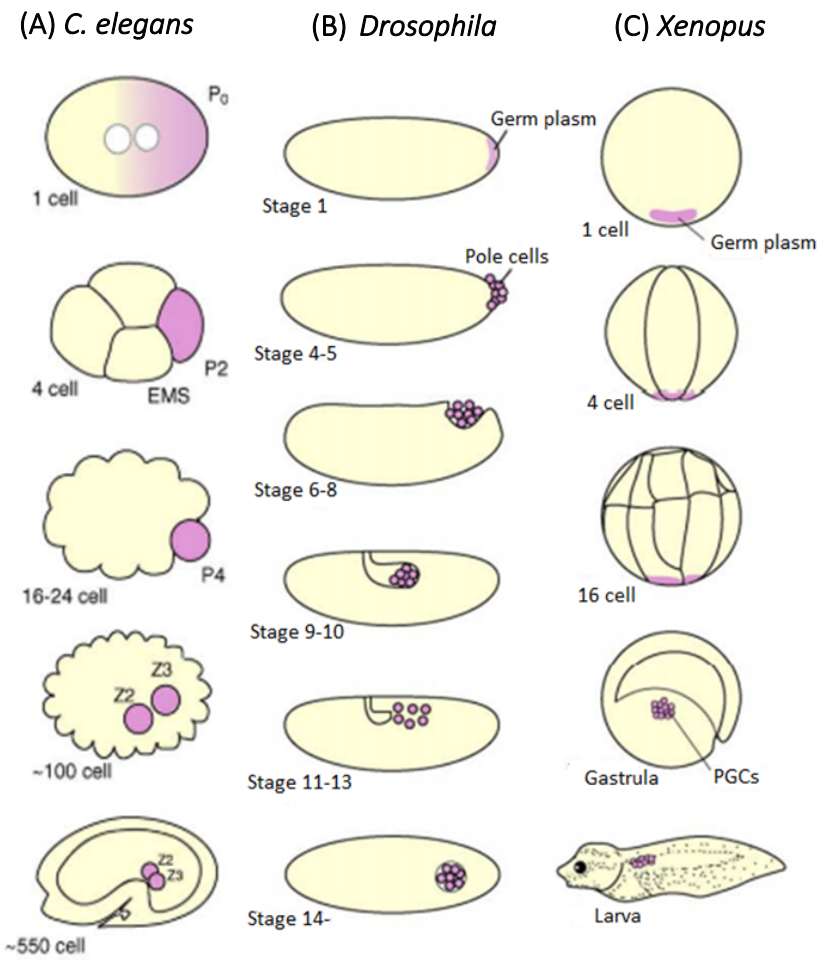

Figure 3. Early germ cell development in C. elegans, *Drosophila* and *Xenopus*.

A) The GP localization in *C. elegans* (also called P granule) is shown on the left side (in pink). GP is uniformly distributed in the oocyte, which later moves to the posterior end and becomes incorporated to the P1 blastomere after fertilization. Additional asymmetric divisions produce germline blastomere P4 which further divides to produce the PGCs, Z2 and Z3. B) The *Drosophila* GP (also called pole plasm) localization is shown in the middle (in pink). GP is assembled at the posterior pole of the egg, which is later embraced into the pole cells. The pole cells are then carried to the interior of the embryo during gastrulation and start their migratory journey towards the future gonadal region in the body cavity. C) The *Xenopus* GP localization is shown on the right side (in pink). GP is assembled at the vegetal cortex of the egg, which is later unequally distributed during the early cleavages, specifying PGCs. PGCs later migrate towards the genital ridges of the animal (Modified after Nakamura et al., 2010).

primordial germ cells pool of the organism, where they later migrate to the future gonad region (Taguchi et al. 2012). GP localization in zebrafish embryos is having it is own mechanism which is not the same as the other organisms, which is the topic of this thesis and will be explained in a separate section.

1.3. Germline development in zebrafish

1.3.1. Oogenesis

Zebrafish germ line development is determined by maternal factors which are stored in the ooplasm, the GP. Therefore, understanding this process requires understanding different stages of oogenesis. During oogenesis, GP undergoes different localization phases. In general, oogenesis in zebrafish is divided into five stages, namely stage I, II, III, IV, and V (Figure 4) (Dosch 2015; Pelegri 2003).

Stage I is subdivided into stage IA and IB, which are defined as pre-follicle phase and follicle phase, respectively. In stage IA, oocytes are rested inside a nest which is separated from the rest of the ovarian tissues and the follicles by a layer of pre-follicle cells. Oocytes of this stage are arrested at prophase of the first meiosis division and they have a huge nucleus and only a very little amount of cytoplasm which contains the disperse GP around the nucleus. In stage IB, oocytes have left the nest and occupied definite follicles. Oocytes of this stage are transparent and their cytoplasm is much more visible, accompanied by the assembly of GP. GP and all its contents is now aggregated inside the Balbiani body. Balbiani body is localized at the vegetal pole of the oocyte just beneath the nucleus. This defines the first polarity sign of an oocyte (Selman et al. 1993; Riemer et al. 2015). The animal pole is usually determined by the extrusion of the polar body which takes place during meiosis, this provides the first morphological indicator for oocyte asymmetry in zebrafish (Dosch 2015).

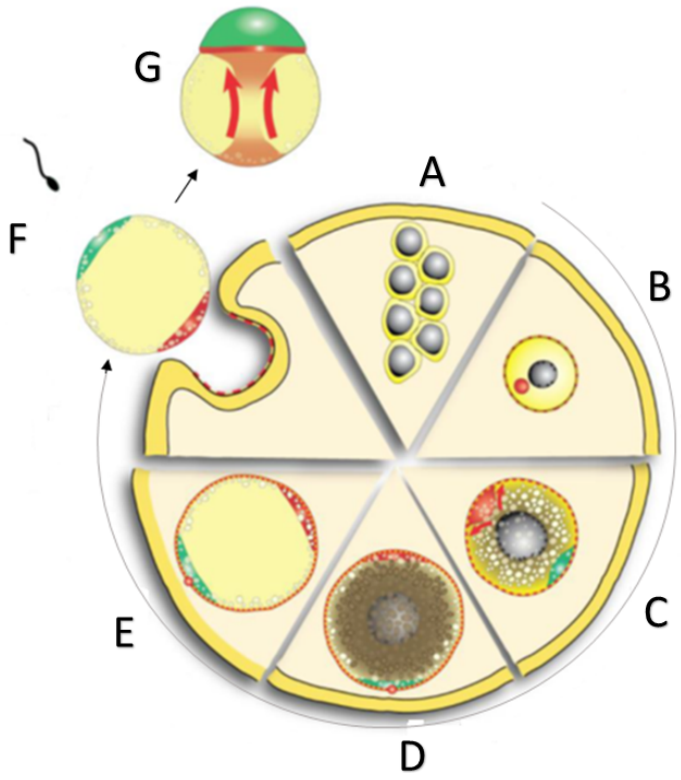

Figure 4: Schematic representation of GP localization during zebrafish oogenesis. A) stage IA oocyte (7-20 µm). B) Stage IB oocyte (20-140 µm), the Balbiani body is shown in red and the nucleus in black. C) Stage II oocyte (140-340 µm). D) Stage III oocyte (340-690 µm). E) stage IV oocyte (690-730 µm). F) Stage V oocyte (730-750). G) 1-cell stage embryo. The vegetal pole is facing the center of the scheme. Note: Ovulation occurs between (E) and (F) and fertilization occurs after stage (F) (modified from Bontems, 2009).

Stage II is known as cortical alveoli stage. At this stage, cortical alveoli begin to proliferate and yolk droplets become visible. This makes the ooplasm foamy and oocytes become translucent and lose their transparency. At the same time, Balbiani body starts to disassemble and its content gets distributed to the cortex. In stage III, the vitellogenesis stage, oocytes start to grow and increase in size prominently. This takes place due to sequestration of the yolk precursor protein, vitellogenin, and the accumulation of yolk granules. At this stage, GP distributes along the cortex (Selman et al. 1993; Riemer et al. 2015).

In stage IV, also called oocyte maturation, oocytes continue to grow and increase in size. Yolk particles lose their crystalline feature and the nuclear envelop disintegrates, leading the oocyte to escape the arrested phase and continue the first meiotic division, which will again

get arrested at the metaphase of second meiotic division. Oocytes are now called eggs, with GP remained at the cortex. At stage V, mature eggs are ovulated and micropyle canal is formed, determining the point for sperm entry and fertilization. At this stage, GP is still localized at the cortex. It is only after fertilization and egg activation, where at the 1 cell stage cytoplasmic streaming from the yolk pushes the GP up to distribute at the animal pole (Selman et al. 1993; Dosch 2015; Riemer et al. 2015; Howley and Ho 2000; Nair et al. 2013; Pelegri 2003).

1.3.2. Embryogenesis

During early embryogenesis, the BB will translocate to the first cleavage furrow. At two cell stage of the development, germplasm is located at two spots at the distal ends of first cleavage furrow, which then also moves to the second cleavage furrow after the second division. At the four cell stage, germplasm forms four distinct spots at the distal ends of the first and the second cleavage furrows. With the subsequent asymmetric cleavages, the germplasm will only be localized at the predefined four spots along the distal ends. Therefore, the same number of spots remain until 1000-cell stage, when GP starts to distribute symmetrically to both daughter cells in contrast

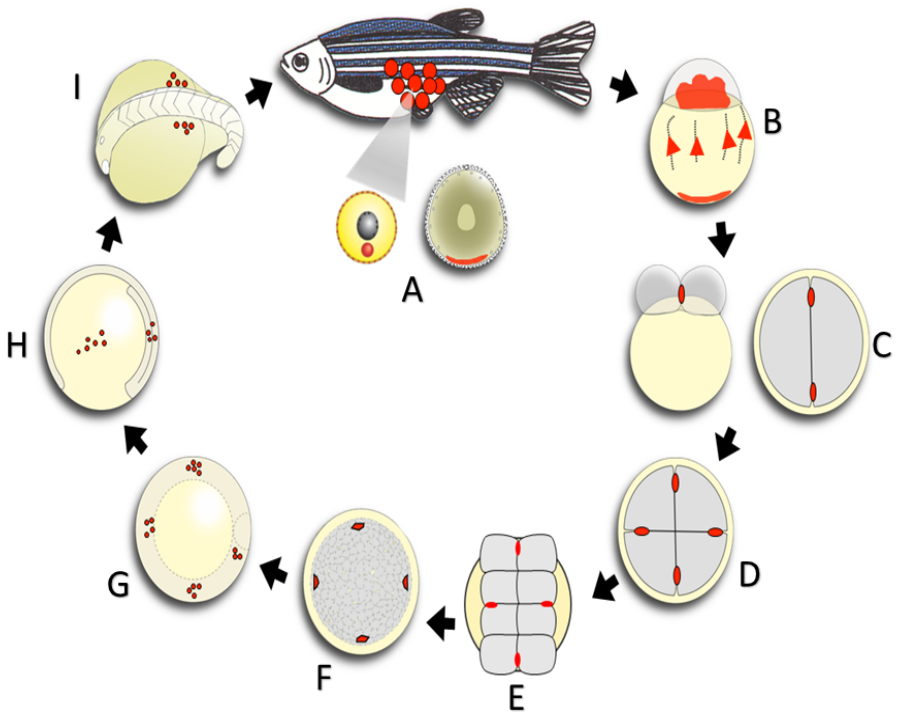

Figure 5. GP localization during zebrafish embryonic development. GP (A–E) or germ cells (F–I) are highlighted in red. A) An adult female fish harbouring several oocytes shown in red. The grey ray shows a magnified oocyte at stage IB (yellow colour with oocyte shown in red) and stage III oocyte next to it (in green). B) 1- cell stage embryo, showing cytoplasmic streaming of the GP components from the vegetal pole towards the animal blastodisc. C) 2- cell stage embryo from lateral view (left side) and animal view (right side). Note the distribution of the GP at two spots at the distal ends of the first cleavage furrow. D) 4- cell stage embryo from the animal view. Note the distribution of the GP at four distinct spots at the distal ends of the first and the second cleavage furrows. E) 8- cell stage embryo from the animal view. GP is still restricted to 4 distinct spots of the first and the second cleavage furrows. F) 512-cell stage embryo (2.75 hpf). Up to this stage, the embryo is having only 4 GP containing cells. From now on, germ cells start to divide symmetrically, producing four clusters of germ cells in the next stage. G) Embryo at gastrula stage. At this stage, four PGC clusters have formed. H) Embryo at 80% epiboly (8.4 hpf). At this stage, germ cells start to migrate dorsally (right side), which is indicated by the involuting hypoblast (lateral view, anterior to the top). I) Embryo at 15-somite stage (16.5 hpf). At this stage, PGCs have reached the prospective gonads, where they will differentiate into sperm in males or oocytes in females (A) (Modified after Dosch, 2015).

to the previous cleavages. This switch from asymmetric to symmetric distribution creates four primordial germ cells clusters (PGCs) which then migrate to gonadal anlagen where they differentiate to germ cells (Dosch 2015; Riemer et al. 2015; Raz 2003).

1.4. Molecular mechanism controlling the localization of germ plasm in zebrafish

Now we know that GP in zebrafish acts as a classical cytoplasmic determinant which controls germ cell formation and segregation, due to its asymmetric localization already during oogenesis and through embryogenesis. Cells that maintain this cytoplasmic determinant will be committed to germ line development, leaving the rest of the of the embryo to become the somatic tissues. This tells us how the correct localization of GP is important to develop germline as well as the whole embryonic tissues. Many crucial molecules for germline specification are shared among different species, such as Vasa, Nanos, and Piwi, revealing that the mechanism of specification is highly conserved (Ewen-Campen, Schwager, and Extavour 2010; Juliano, Swartz, and Wessel 2010). However, the molecular mechanisms controlling localization of GP is not well known and appear to vary among different species.

Here I am going to split the so far known molecular machinery for the localization in zebrafish into two different time frames as before, during oogenesis and embryogenesis.

1.4.1. During oogenesis

Very little is known about the assembly and distribution mechanisms of GP components during zebrafish oogenesis. It is reported that GP RNAs vasa, nanos1 and *dazl* colocalize with GP in the BB and are transported to the vegetal cortex during oogenesis (Kosaka et al. 2007). In addition, it is found that the GP component *brul* (*bruno-like*, homolog of *Drosophila bruno*) is also localized to the GP in zebrafish oocytes (Hashimoto et al., 2004; Suzuki et al., 2000). It is found that the RNA-binding protein Rbpms2, a homologue of Hermes which is a component of the mitochondrial cloud in *Xenopus*, is also colocalized in the Balbiani body of zebrafish oocytes. These results suggest a conserved feature between the mitochondrial cloud in *Xenopus* and the BB in zebrafish in the assembly and transport of RNA molecules (Kosaka et al. 2007).

The protein composition of GP is largely unexplored. In a rather recent maternal effect mutagenesis screen, a novel zebrafish specific gene called *bucky ball (buc)* was discovered to control early zebrafish development (Dosch et al. 2004). *buc* mutant oocytes show radial segregation of cytoplasm, loss of polarity, do not form BB and cannot develop beyond the 1 cell stage. Furthermore, Buc protein is localizing to the GP and GP RNAs *vasa, nanos1,* and *dazl* do not localize in *buc* mutants and it is shown that Buc protein, not RNA, is responsible for this localization. This suggests that Buc is essential for GP assembly during oogenesis (Bontems et al. 2009; Riemer et al. 2015).

1.4.2. During embryogenesis

The localization of GP RNA components is well studied in zebrafish; however, its protein localization is poorly understood. As I described previously, during early embryonic development GP is localized to the distal ends of the cleavage furrows. It is worth investigating how this occurs and what are the molecular features that anchors GP at the cleavage furrows, as this is still an unknown meth. *Vasa* RNA is well described in this sense

to colocalize with GP at the cleavage furrows (Yoon, Kawakami, and Hopkins 1997). The first protein that has been shown to colocalize with GP at early cleavage furrows was Brul (Hashimoto et al. 2006). Surprisingly *Brul* RNA is only localized to the GP at early cleavage furrows and disappears at 16-cell stage. It is not known how this localization is controlled at the molecular level.

Results from several studies, however, suggested that cytoskeletal components might define the localization of GP to the distinct spots. It is believed that GP components initially bind to actin filaments which together pushed out to the periphery of the early blastomeres by astral microtubules. This brings GP in close proximity so that it ultimately gets translocated to the cleavage furrows. It has been shown that furrow microtubular array (FMA) also plays role in the compaction of GP outwards along the cleavage furrows. It is known that defect in FMA formation abolishes *vasa* RNA localization to the cleavage furrows (Pelegri et al. 1999). Drug inhibition of actin components has also shown to show the same effect (Knaut et al. 2000). In addition to the role of cytoskeleton, proper cell division and cytokinesis is described to be crucial for correct localization of GP. It appears that mutants in Sas-6 and Aurora-B kinase, which have defect in cell division and cytokinesis respectively, fail to localize GP (Yabe et al. 2009; Yabe, Ge, and Pelegri 2007).

Taken together, the mechanism of GP localization during embryogenesis is not well understood. The novel protein Buc provided us a great tool to use it as a molecular proxy to follow this unknown process, since it is always localized with GP (Riemer et al. 2015). It is shown that the maternally expressed Kinesin-1 (Mkif5Ba) interacts with Buc and plays a major role in the transport of Buc to the cleavage furrows, using an unknown process (Campbell et al. 2015). In addition, it is known that remodelling and disassembly of FMA requires the activity of non-muscle myosin II (NMII), whose phosphorylation (pNMII) is essential for distal recruitment of GP at the cleavage furrows (Urven, Yabe, and Pelegri 2006). Nair et al. showed for the first time that pNMII colocalizes with GP RNAs (Nair et al. 2013) and we recently found that pNMII colocalizes with Buc in the oocyte and during embryogenesis (Rostam et al., 2021a, submitted). Phosphorylation of NMII is bound to the assembly of myosin filaments and contraction and inhibition of its phosphorylation cause defect in FMA, which suggests the role of phosphorylation in GP compaction. Similar defect in GP localization in zebrafish is seen using inhibitors of RhoA and Rock. This supports the role of RhoA/Rock pathway in

localization of GP through the phosphorylation of NMII, since ROCK is a kinase which phosphorylates NMII (Miranda-Rodríguez et al. 2017).

1.5. Bucky ball is a novel germ plasm marker

In a maternal screen to identify further maternal factors controlling early zebrafish development, Buc was found to have caused embryonic lethality in zebrafish. Buc mutants fail to grow beyond 1-cell stage. Mutant embryos at 1-cell stage show radially distributed cytoplasm and lose polarity compared to the wild type embryos where cytoplasm is located at the animal pole (Figure 6). Furthermore, these embryos do not have polarity and they resemble Buckminsterfullerene and hence they are referred to as Bucky ball (Dosch et al. 2004).

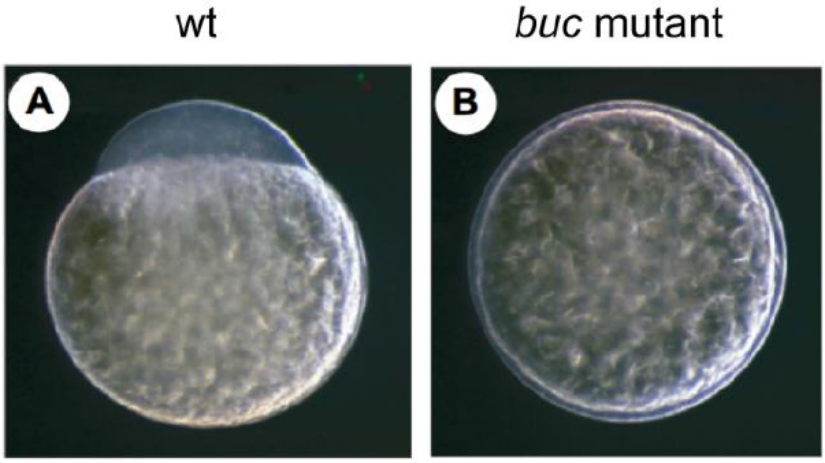

Figure 6. *buc* mutants show defect in the embryonic animal-vegetal polarity. A) A wild type (wt) embryo at 1- cell stage, showing the blastodisc at the animal pole. B) A *buc* mutant embryo at 1- cell stage. Note the radial distribution of the cytoplasm around the yolk and the complete loss of animal-vegetal polarity in this embryo. Both embryos are shown laterally, with the animal pole to the top (Figure from Dosch et al., 2004).

1.5.1. Molecular features of Buc

Buc is an intrinsically disordered protein which is rich in proline. Buc is homologue of velo1 in *Xenopus* and Oskar in *Drosophila*, although they do not share sequence similarities

(Krishnakumar et al. 2018; Riemer 2014). We know that Buc is necessary and sufficient for the localization of GP in zebrafish, but we do not know much about its structural features, especially since it is not dissolvable and tends to aggregate during purification. Therefore, to investigate this protein, we mostly use biochemistry, such as structural function analysis. Using biochemical approaches, we were able to identify the localization domain of the protein, which is localized at the N-terminal of the protein and is composed of 77 amino acids (aa), aa11-aa88, named BucLoc. BucLoc is sufficient to localize GP in zebrafish and a delta construct of the whole Buc protein lacking BucLoc is unable to localize (Rostam etl al., 2021a, submitted). Buc organizes GP assembly in zebrafish and is required for PGC formation, while its overexpression induces extra germ cell formation (Bontems et al. 2009). The question is now whether zebrafish, flies, and frogs use the same mechanism to localize GP or not.

1.6. Germ plasm localization is not conserved between vertebrates and invertebrates

It is recently addressed whether the GP organizers Buc, Xvelo and sOSK use the same localization mechanism. It is found that Xvelo gets localized to the GP when it is injected into zebrafish embryos, while sOSK fails to localize when it is injected to zebrafish embryos (Rostam et al., 2021a, submitted). This indicates that vertebrates use a different localization machinery than invertebrates. Moreover, it is previously shown that functional amyloid domains play a major role in germ cell formation in frogs and mice and it is known that BB in *Xenopus* forms amyloid like structures characterized by β-crosses (Boke et al. 2016; Berchowitz et al. 2015) . On the one hand, zebrafish BB is also thought to form amyloid aggregates (Kloc, Bilinski, and Etkin 2004), although this question has not been clearly addressed. On the other hand, during embryogenesis, GP in zebrafish tends to form liquid droplets instead amyloid structures (Riemer et al. 2015).

It is known that proteins that have these physical properties are mostly intrinsically disordered proteins which contain prion like domains. These proteins tend to phase separate and form aggregates (Kato et al. 2012; Kroschwald et al. 2015). Previous studies showed that the N-terminus (1aa- 100aa) of Buc containing BucLoc termed BUVE motif (for Buc-Velo) is strongly conserved during vertebrate evolution (Bontems et al. 2009; Krishnakumar et al. 2018; Boke et al. 2016). A recent study showed that BUVE motif is responsible for GP

localization to the BB in frog oocytes. And the same study showed that this localization of Velo1 in the BB is driven by the aggregation of prion-like domains (PLDs) in the BUVE motif (Boke et al. 2016). The PLDs in Xvelo are also conserved in BucLoc and it is previously thought that the same aggregation mechanism could be responsible for GP localization during zebrafish embryogenesis. However, the most recent data tells us that this is not the case. PLDs in Buc are not required for its localization. This means that localization and aggregation of GP are two separate mechanisms in zebrafish (Rostam et al., 2021a, submitted).

1.7. Aim of this work

GP localization retains to only four cells as the embryo develops, forming the entire germ line of the organism. However, the cellular structure controlling this specific localization was still unknown, which is the major question of this thesis. Buc was discovered as the first GP organizer in vertebrates, which mimics GP behavior. Overexpression of Buc causes ectopic GP formation and Buc mutants fail to form GP. Most importantly, Buc always colocalizes with the GP. This discovery allowed us to investigate the molecular mechanisms of GP localization in zebrafish in more detail. The aim of this work was the following.

1.7.1. Identify the cellular structure that anchors Buc

Up to now, the cellular structure which anchors Buc at the cleavage furrows early during embryogenesis was not known. The major aim of this work was to identify the structure at which Buc, and hence GP, anchors. Here, I am going to show that Buc is anchored at the cleavage furrows by tight junctions (TJ).

1.7.2. Characterize the protein machinery which anchors Buc

The protein machinery which anchors Buc at the defined spots, TJs, was also unknown for decades. A bigger aim of this work was to identify the protein interaction partners of Buc which localize GP. Here, I am going to present direct interaction partners of Buc, the TJ proteins, which clarifies the potential signaling pathway for GP localization in zebrafish.

1.7.3. Isolate proteins tethering Buc to the cleavage furrow

TJs also includes transmembrane receptors like Occludin and Claudins. The fish genome contains more than 50 Claudin genes, with very few of them expressed maternally. In this thesis, I am going to characterize Cldn-d as the receptor protein which recruits Buc to the TJs. I am going to show that interfering the function of Cldn-d alters GP aggregation.

2. Results

The results of this thesis are presented in three chapters, chapters 2.1 to 2.3. The first chapter (2.1) is a book chapter which is published by springer nature and as a part of the book series Methods in Molecular Biology (Title: Glyoxal Fixation as an Alternative for Zebrafish Embryo Immunostaining). The second chapter (2.2) is a manuscript which is currently under revision for *Development* (Title: Germ plasm anchors at tight junctions in the early zebrafish embryo). The third chapter (2.3) is a manuscript which is to be submitted (Title: Bucky ball Interacts with ZO2a and ZO2b to Direct the Localization of Germ Plasm to the Tight Junctions in Zebrafish).

Each chapter is preceded by a page describing the following:

- The main objective and conclusion of the manuscript in the context of the whole thesis.
- The status of the manuscript.
- Author contributions

References cited in each manuscript can be found at the end of each chapter.

References cited in the general introduction and the general discussion are listed at the end of the thesis.

2.1 Glyoxal Fixation as an Alternative for Zebrafish Embryo Immunostaining

The first experiments of this thesis involved numerous staining and imaging techniques to find out the cellular structure which Buc anchors to. When it comes to immunostaining in zebrafish, a huge problem is that there is a limited number of applicable antibodies in this species. Struggling to make the antibodies work and a huge amount of protocol optimization led to the development of a new fixative method which produces a better staining outcome. In this chapter, I am going to present glyoxal fixation as a novel method for zebrafish embryo immunostaining, which was never tested in this organism. Identification of this method is very useful as it can be tested on a wider range of antibodies, thereby increasing the number of applicable antibodies in this organism.

Authors: ***Nadia Rostam*** *and Roland Dosch.*

Status: Published as a book chapter by springer nature and as a part of the book series Methods in Molecular Biology, 2021.

DOI: https://pubmed.ncbi.nlm.nih.gov/33606236/.

Author contributions: Conceptualization: NR, RD; Methodology: NR; Investigation: NR; Visualization: NR; Resources: RD; Writing: NR; Review & Editing: NR, RD.

My specific contribution: Performing all the experiments, preparing the figures and writing the chapter.

Glyoxal Fixation as an Alternative for Zebrafish Embryo Immunostaining

***Nadia Rostam*[1,2,3]** *and Roland Dosch*[4]

[1]*Institute of Human Genetics, University of Göttingen Medical Center, Georg-August-Universität, Göttingen, Germany.* [2]*Department of Developmental Biology, Johann-Friedrich-Blumenbach Institute of Zoology and Anthropology, Göttingen Center of Molecular Biosciences, Göttingen, Germany.* [3]*Department of Biology, College of Science, University of Sulaimani (UoS), Sulaimaniyah, Iraq.* nadia.rostam@univsul.edu.iq. [4]*Institute for Developmental Biochemistry, University of Göttingen Medical Center, Georg-August-Universität, Göttingen, Germany. roland.dosch@med.uni-goettingen.de.*

Abstract

Immunohistochemistry has been widely used as a robust technique to determine the cellular and subcellular localization of proteins. This information ultimately helps to understand the function of these proteins and how biological processes are regulated. Antibodies applicable for labeling in zebrafish are limited, making immuno-staining challenging. Recently glyoxal fixation was rediscovered in tissue culture, mouse, rat, and Drosophila, expanding the list of effective antibodies for these species. Here, we compare a protocol for zebrafish staining using glyoxal as a fixative agent with PFA. We demonstrate that glyoxal fixation improves the antigenicity of some epitopes thereby increasing the number of useful antibodies in zebrafish.

Key words: Immunostaining, Zebrafish, Fixation method, PFA, Glyoxal, GP, Bucky ball

1. Introduction

Zebrafish has fast become an excellent vertebrate model for studying the function of proteins and complex biological processes in the context of an entire organism. To understand the function of a protein, it is crucial to know where and when it is expressed inside an organism or even inside a cell. Therefore, investigating localization and expression pattern of proteins using immunohistochemistry (IHC) is very important in identifying the function of genes, which can be achieved by immune labeling of fixed or frozen tissue samples or whole-mount samples. Up to today, IHC is a powerful and one of the most widely used tools in

detecting cellular and subcellular localization of proteins [1–5]. Principally, IHC works for a broad range of biological tissues and it is based on antigen detection using specific antibodies raised against the antigens of interest, which recognizes specific epitopes from proteins [2, 6]. In addition, this technique can be used more specifically to detect the activity of proteins, such as in their phosphorylated state, which is not possible with other methods like RNA in situ hybridization [7].

Whole-mount immunostaining of zebrafish embryos has significantly revealed the expression pattern of tissue-specific proteins. However, there is a shortage in the availability of antibodies for this organism, making IHC problematic in our field [8]. In addition, a major problem with this application is that detailed protocol optimization is needed based on the type of tissue investigated and the antibody used, especially because antibodies need different conditions to give the highest possible signal. Moreover, IHC is a multi-step technique which takes different levels of optimization and various combination of reagents is needed until maximum signal intensity from the antibodies is detected [6, 9].

For example, fixation is a critical step in immunohistochemistry which needs to be performed in a way that it keeps the balance between the integrity of the sample and antigenicity [10]. Previous studies have examined different protocols and fixative methods such as formalin, methanol, formaldehyde, and paraformaldehyde (PFA) for immunostaining [11–13]. More recently, it was shown that glyoxal fixation improves immune staining in tissue culture, mouse, rat, and Drosophila [14], but zebrafish was not tested in this study.

Here, we provide an alternative protocol for zebrafish embryo staining (Fig. 1). We show that glyoxal fixation provides better resolution, less background, and more intense signal production for protein visualization in zebrafish embryos but not for every antibody. We compared glyoxal and paraformaldehyde (PFA) fixation for Bucky ball (Buc) and tight junction protein Zonula occludens 1 (ZO1) antibodies. The ZO1 antibody gave a much better signal using glyoxal fixation, whereas Buc provides a strong signal using PFA fixation. We believe that our method can be extended to the staining of other tissue types of the zebrafish embryo, providing that optimal conditions for the antibodies are used.

2. Materials

2.1 Zebrafish Embryo Collection and Handling

1. Embryos of corresponding stage from wild-type zebrafish line maintained at standard conditions [15].

2. Stereomicroscope.

3. Plastic Petri dish.

4. Plastic Pasteur pipette 2 ml.

5. Eppendorf tubes 2 ml.

6. E3 medium: 5 mM NaCl, 0.17 mM KCl, 0.33 mM CaCl2, 0.33 mM MgSO4, 0.00001% methylene blue.

7. DUMONT forceps (size 5).

2.2 Embryo Fixation

1. PBS: 137 mM NaCl, 10 mM Na2HPO4, 2.7 mM KCl, 1.76 mM KH2PO4 (pH 7.4).
2. 4% PFA in 1 PBS: 4 mg PFA, 96 ml PBS.
3. 100% methanol (MeOH).
4. 100% ethanol (EtOH).
5. Glyoxal solution: 2.789 ml H2O, 0.789 ml 100% EtOH, 0.313 ml 40% Glyoxal, 30 µl 100% acetic acid (pH 6.5) (see Note 9).
6. Rotator at 4 C and room temperature (RT) conditions.

2.3 Blocking and Washings

1. 10% goat serum.
2. PBS/ 0.5% Triton X-100 (PBT) (see Note 1).
3. 2% Tween 20 in PBS: 2 ml Tween 20, 98 ml PBS (see Note 1).

2.4 Staining

1. Primary antibodies.
2. Secondary antibodies.

2.5 Imaging

1. FluoroDish 35 mm.
2. LSM780 confocal microscope (Carl Zeiss Microscopy, Jena).
3. ZEN 2011 software (Carl Zeiss Microscopy, Jena).
4. Murray's mounting medium: 2/3benzyl benzoate, 1/3 benzyl alcohol.

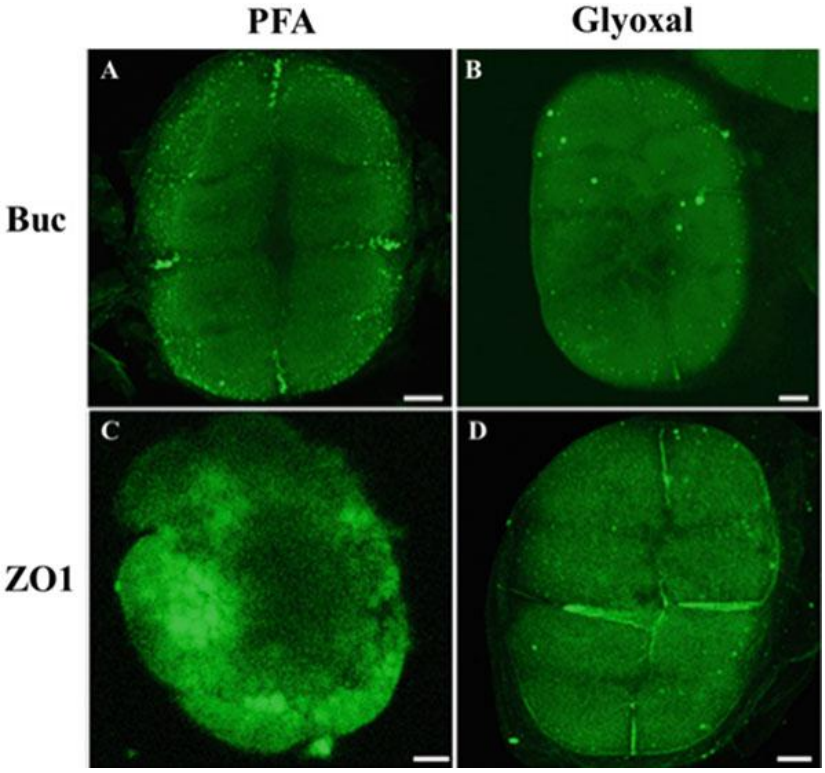

Fig. 1 Comparison of antibody staining of zebrafish embryos fixed with PFA and glyoxal. Labeling of PFA-fixed embryos (8-cell stage, animal view) is shown in the left column and of glyoxal-fixed embryos in the right column (see Note 6). The upper row shows Buc labeling (A and B) and the lower ZO1 (C and D). Buc antibody showed almost no signal with glyoxal fixation and a very strong signal with PFA fixation, while ZO1 antibody showed a much stronger signal with glyoxal fixation. Scale bars: 50 µm

3. Methods

3.1 Zebrafish Embryo Collection and Handling

1. Set up fish pairs the evening before embryo collection by separating each male from his female partner in a mating box overnight (see Note 11).
2. The next morning, put fish pairs together and let them mate and lay eggs.
3. Collect the eggs, keep them at 28 C to grow up to the desired cell stage.
4. Collect the embryos in a 2 ml Eppendorf tube containing E3 medium (see Note 12).

3.2 Embryo Fixation

Embryos were fixed using one of the following fixation methods

3.2.1 Glyoxal-Based Embryo Fixation

1. Prepare fresh glyoxal solution.
2. Keep the solution at 4 C.
3. Remove the E3 medium from the 2 ml Eppendorf tube containing embryos and replace it with glyoxal solution.
4. Keep the embryos on ice for 30 min.
5. Keep the embryos for another 30 min at RT.
6. Store at 4 C.

3.2.2 PFA-Based Embryo Fixation

1. Prepare 4% PFA solution from frozen aliquots.
2. Replace the E3 medium from the 2 ml Eppendorf tube containing embryos with 4% PFA.
3. Rock the embryos on a rotator at 4 C overnight.
4. Discard the PFA and replace it with PBS. Wash the embryos twice 10 min with PBS, each time for 10 min.
5. Gradually dehydrate the embryos in a MeOH/PBT series and store at least overnight or until used for staining at 20 C.

3.3 Immunostaining

1. Rehydrate the embryos in a MeOH: 0.5% PBT series (50%, 75%, 87.5%, 100%) for PFA-fixed embryos and an EtOH: 0.5% PBT series (50%, 75%, 87.5%, 100%) for glyoxal-fixed embryos.
2. Manually dechorionate the embryos using a pair of forceps and remove damaged embryos (see Note 2).
3. Transfers embryos into a 24-well tissue culture plate (see Note 8 and Note 13).

4. Replace the PBT with 500 µl fresh 0.5% PBT + 10% goat serum and rock for 2 hrs at RT (see Note 7).

5. Replace the blocking solution with 500 µl 0.5 PBT + 2% BSA + 10% goat serum and the appropriate dilution of the primary antibodies.

6. Rock embryos overnight at 4 C.

7. Replace the primary antibody solution with 2 ml 2% Tween 20 and rock at RT for 15 min (repeat three times) and wash once with 2 ml of 0.5% PBT for 15 min.

8. Replace the PBT with 500 µl 0.5% PBT/10% goat serum and the appropriate dilution of the fluorescently labeled secondary antibodies.

9. Cover the dish with aluminum foil to protect from light and rock for 2 hrs at 4 C.

10. Replace the primary antibody solution with 2 ml 2% Tween 20 and rock at RT for 15 min (repeat three times) and wash once with 2 ml of 0.5% PBT for 15 min.

11. Gradually dehydrate the embryos in a 0.5% PBT: MeOH series for PFA-fixed embryos and a 0.5% PBT: EtOH series for glyoxal-fixed embryos.

12. Embryos are ready to be imaged or stored at 20 C until imaging.

3.4 Imaging

1. Transfer the embryos from the dish into an imaging FLuoroDish.

2. Remove MeOH/EtOH

3. Add a drop or more of Murray's clearing medium into the FluoroDish, covering the embryos (see Note 10).

4. Wait for about 5 min until the embryos become clear and image with confocal microscope

4. Notes

1. We used a combination of two different detergents, Tween 20 and Triton, since this gave our samples a clearer and less damaged texture. Tween 20 is a soft detergent while Triton is harsher, when used alone they are either not effective enough or harmful. Therefore, washing three times with Tween 20 preserves the texture of the embryos and one final wash with Triton effectively washes out the remaining Tween 20.

2. Manually dechorionating the embryos better preserves their morphology; therefore, we recommend avoiding dechorionation using chemicals like Pronase.

3. Glyoxal-fixed embryos have a much clearer morphology after fixation. This makes them easier to deyolk, since the dark embryos are easily distinguishable from the transparent yolk compared to the dark yolk after PFA fixation (Fig. 2a, b). We recommend glyoxal fixation method if it works for your antibodies.

4. It is much easier to deyolk glyoxal-fixed embryos than PFA-fixed embryos. In the case of glyoxal, the yolk is stickier and more elastic, which is easier to remove, compared to the brittle yolk after PFA fixation (Fig. 2c, d). Fragile PFA-fixed embryos are also problematic since auto-fluorescent sticky yolk globules cause unwanted background during imaging.

5. Glyoxal-fixed embryos are very easy to dechorionate and deyolk. Pressing the embryo with a forceps bursts the embryo out of the chorion. This procedure simultaneously deyolks the embryo (Fig. 2d).

6. Glyoxal fixation gives less background during imaging.

7. We highly recommend blocking with serum derived from the same species as the secondary antibodies to get the least possible background.

8. We recommend using an embryo sucker to transfer embryos during deyolking and mounting (Fig. 2e).

9. Glyoxal-fixed embryos can be stored in a 4 C fridge for more than a week before staining. However, because of the easy and less time-consuming nature of this method,

we prefer making fresh glyoxal always and staining embryos within few days after fixation.

10. Murray's mounting medium is toxic and should be handled very carefully. Wear gloves and work inside a hood while dealing with this substance.

11. Fish should be kept under 14 hrs light and 10 hrs dark condition before setting them up.

12. We prefer using 2 ml tube for embryo collection since these tubes have round bottoms, which make the movement and transfer of the embryos in them easy.

13. During embryo transfer with embryo sucker, it is important to suck some medium up before sucking up the embryos. This will keep the embryos in the fluid and prevents them from moving up and sticking to the rubber tube. It is better not to suck the embryos beyond the glass capillary, because they might get stuck at the rim at the capillary–tube transition.

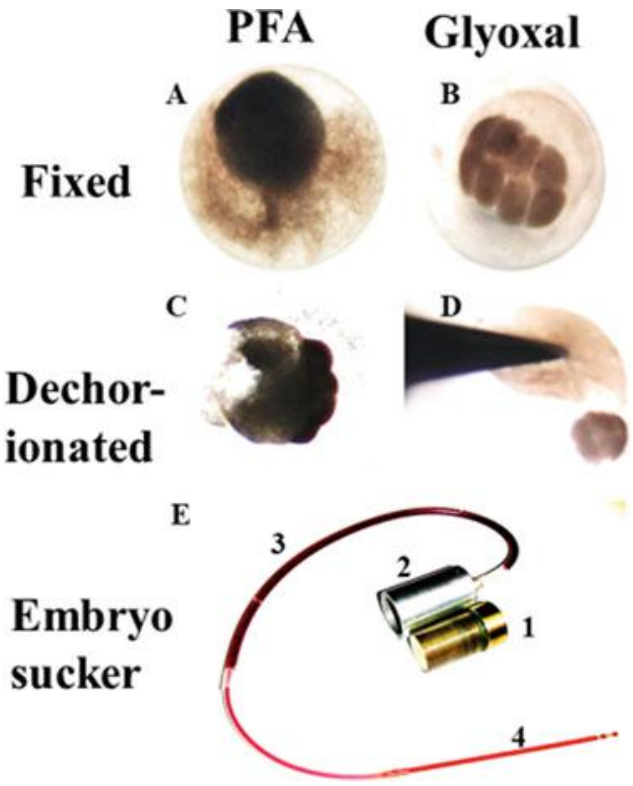

Fig. 2 Zebrafish embryo fixation using PFA and glyoxal.

PFA fixation is shown in the left column and glyoxal fixation in the right. (a) After fixation with PFA embryos look dark and grainy. (b) A glyoxal-fixed embryo, which looks more transparent. The yolk becomes transparent with glyoxal fixation, which makes it easier to differentiate it from the embryo. Embryonic cells are clearly visible. (c) A manually dechorionated PFA-fixed embryo (see Note 3), showing aggregated granules of yolk around the broken yolk of the embryo. This commonly happens since embryos fixed with PFA are more fragile (see Note 4). (d) A glyoxal-fixed embryo after dechorionation, which is much more simple than with PFA. Careful pressing with forceps (dark triangle) on one chorion side, until it bursts, makes the embryo jump out without the yolk (see Note 5). As deyolking and dechorionation is a single-step process, auto-fluorescent yolk globules around the embryo are absent. (e) Embryo sucker. Using this instrument for embryo transfer preserves the texture of the embryos and prevents their destruction. Embryo sucker is composed of three parts. Part (1) is a metal screw which fits in part (2). The screw needs to be attached to part 2 during usage. Screwing and unscrewing the screw pushes and pulls pressure inside the rubber tube (3), which provides the needed force for sucking up and transferring out the deyolked or dechorionated embryos. To make this construction airtight, the screw is lubricated with grease, e.g., Vaseline. Part (3) is an extension rubber tube which can hold extra fluid medium for the embryos and provides surface area for producing enough pressure. Part (4) is a glass capillary tube. During embryo transfer, the screw should be locked first, and then the tip of the capillary tube should be held close to the embryos, unscrewing the screw sucks the embryos along with a minimal amount of embryonic medium up into the tube. Finally, the embryos can be pushed out by unscrewing.

References

Han R, Li Z, Fan Y, Jiang Y (2013) Recent advances in super-resolution fluorescence imaging and its applications in biology. J Genet Genomics 40:583–595. https://doi. org/10.1016/j.jgg.2013.11.003

Waldvogel HJ, Curtis MA, Baer K et al (2007) Immunohistochemical staining of post-mortem adult human brain sections. Nat Pro-toc 1:2719–2732. https://doi.org/10.1038/ nprot.2006.354

Inoue D, Wittbrodt J (2011) One for all-a highly efficient and versatile method for fluo-rescent immunostaining in fish embryos. PLoS One 6:1–7. https://doi.org/10.1371/jour nal.pone.0019713

Barlow AL, MacLeod A, Noppen S et al (2010) Colocalization analysis in fluorescence micro-graphs: verification of a more accurate calcula-tion of Pearson's correlation coefficient. Microsc Microanal 16:710–724. https://doi. org/10.1017/S143192761009389X

Childs GV (2014) History of Immunohisto-chemistry. Elsevier Inc., Amsterdam

Zhang H, Wen W, Yan J (2017) Application of immunohistochemistry technique in hydrobio-logical

studies. Aquacult Fish 2:140–144. https://doi.org/10.1016/j.aaf.2017.04.004

Perdana (2018) 済無No title. J Chem Inf Model 53:1689–1699. https://doi.org/10.1017/CBO9781107415324.004

Deflorian G, Cinquanta M, Beretta C et al (2009) Monoclonal antibodies isolated by large-scale screening are suitable for labelling adult zebrafish (Danio rerio) tissues and cell structures. J Immunol Methods 346:9–17. https://doi.org/10.1016/j.jim.2009.04.012

Yang J, Xu X (2012) Immunostaining of dis-sected zebrafish embryonic heart. J Vis Exp 59: e3510. https://doi.org/10.3791/3510

Thomask U (2003) Immunocytochemistry of the amphibian embryo – from overview to ultrastructure. Int J Dev Biol 383:373–383

Moon IS, Cho SJ, Jin IN, Walikonis R (2007) A simple method for combined fluorescence in situ hybridization and immunocytochemistry. Mol Cells 24:76–82

Novak AE, Ribera AB (2003) Immunocyto-chemistry as a tool for zebrafish developmental neurobiology. Methods Cell Sci 25:79–83. https://doi.org/10.1023/B:MICS.

Ferna´ndez J, Fuentes R (2013) Fixation/per-meabilization: new alternative procedure for immunofluorescence and mRNA in situ hybri-dization of vertebrate and invertebrate embryos. Dev Dyn 242:503–517. https:// doi.org/10.1002/dvdy.23943

Richter KN, Revelo NH, Seitz KJ et al (2018) Glyoxal as an alternative fixative to formalde-hyde in immunostaining and super-resolution microscopy. EMBO J 37:139–159. https:// doi.org/10.15252/embj.201695709

Alestro¨m P, D'Angelo L, Midtlyng PJ, et al (2019) Zebrafish: housing and husbandry recommendations. Lab Anim 0:1–12. https:// doi.org/10.1177/0023677219869037

2.2 Germ plasm anchors at tight junctions in the early zebrafish embryo

Buc was discovered as the first GP organizer in vertebrates, which mimics GP behavior. Overexpression of Buc causes ectopic germ plasm formation and Buc mutants fail to form germ plasm. Most importantly, Buc always colocalizes with GP, allowing me to use this to investigate the molecular mechanisms of GP localization. This manuscript found a specific domain of Buc, which is 77 amino acids long at the N-terminal of the protein (11aa-88aa), necessary and sufficient for GP localization in this organism, termed BucLoc. Moreover, a mass spectrometry analysis of BucLoc found candidates of cellular structures binding to Buc. Therefore, detailed colocalization, imaging and functional analyses were used to identify the exact cellular structure to which GP anchors. Results discovered TJ as the anchoring partner for localizing GP in this organism.

Authors: ***Nadia Rostam****, *Alexander Goloborodko, Stephan Riemer, Andres Hertel, Dietmar Riedel, Gerd Vorbrüggen, Roland Dosch*

**Corresponding author: Nadia Rostam (nrostam@gwdg.de).*

Status: Under revision for Development, 2022.

DOI: https://doi.org/10.1101/2021.03.24.436784

Author contributions: Conceptualization: RD; Methodology: NR, AG, SR, AH; Investigation: NR, AG, SR, AH, DR; Visualization: NR, AG, SR, AH, DR; Validation: NR; Formal Analysis: NR, AG, SR; Resources: RD; Writing– Original Draft: NR, RD, GV; Writing – Review & Editing: NR, RD, GV; Supervision: RD; Project Administration: RD; Funding Acquisition: RD.

My specific contribution in the data: Main Figure 5, 6,7, 8. Supplementary Figure 8, 9, 10, 11.

Germ plasm anchors at tight junctions in the early zebrafish embryo

Nadia Rostam*[1,2], *Alexander Goloborodko*[3], *Stephan Riemer*[3], *Andres Hertel*[4], *Dietmar Riedel*[5], *Gerd Vorbrüggen*[2,4], *Roland Dosch*[1,3]

[1]*Institute of Human Genetics, University Medical Center, Göttingen, Germany.* [2]*Department of Developmental Biology, Johann-Friedrich-Blumenbach Institute of Zoology and Anthropology, Göttingen Center of Molecular Biosciences, University of Göttingen, Göttingen, Germany.* [3]*Institute for Developmental Biochemistry, University Medical Center, Göttingen, Germany.* [4]*Department of Molecular Developmental Biology, Max Planck Institute for Biophysical Chemistry, 37077 Göttingen, Germany.* [5]*Laboratory of Electron Microscopy, Max Planck Institute for Biophysical Chemistry, 37077 Göttingen, Germany.*

Abstract

The zebrafish germline is specified during early embryogenesis by inherited maternal RNAs and proteins collectively called germ plasm. Only the cells containing germ plasm will become part of the germline, whereas other cells will commit to somatic cell fates. Therefore, proper localization of germ plasm is key for germ cell specification and its removal is critical for the development of soma. The molecular mechanism underlying this process in vertebrates is largely unknown. Here we show that germ plasm localization in zebrafish is similar to *Xenopus* but distinct from *Drosophila*. We identified non muscle myosin II (NMII) and tight junction (TJ) components such as ZO2 and Claudin-d (Cldn-d) as interaction candidates of Bucky ball (Buc), which is the germ plasm organizer in zebrafish. Remarkably, we also found that TJ protein ZO1 colocalizes with germ plasm and electron microscopy (EM) of zebrafish embryos uncovered TJ like structures at the cleavage furrows where the germ plasm is anchored. In addition, injection of the TJ-receptor Cldn-d produced extra germ plasm aggregates whereas expression of a dominant negative version inhibits germ plasm aggregate formation. Our findings support for the first time a role of TJs in germ plasm localization.

Keywords: Germ plasm localization, zebrafish, tight junctions, Bucky ball, ZO proteins, Claudin-d.

Introduction

Germ plasm consists of a maternally inherited ribonucleo-protein (RNP) condensate, which controls in many animals the formation of germline (Strome and Updike 2015; Tristan Aguero, Susannah Kassmer, Ramiro Alberio, Andrew Johnson 2017). Germ plasm thereby acts as a classical cytoplasmic determinant during embryonic development with the following activities: (I) In the zygote, germ plasm is asymmetrically localized, which after the cleavage period, leads to the formation of a subpopulation of embryonic cells containing germ plasm. (II) These cells will be reprogrammed to differentiate into primordial germ cells (PGCs), while other cells without germ plasm adopt a somatic fate *e.g.* neuron, muscle etc. Proper segregation of germ plasm allows its accumulation in presumptive PGCs, whereas it is subsequently degraded in prospective somatic cells.

The molecular activities in germ plasm specifying PGCs seem to be largely conserved during evolution, because many components like Vasa, Nanos and Piwi are present throughout most animal genomes (Ewen-Campen, Schwager, and Extavour 2010; Juliano, Swartz, and Wessel 2010). By contrast, it is currently unknown whether the molecular mechanisms controlling localization of germ plasm is also conserved during evolution.

The positioning of germ plasm during embryogenesis is best understood in invertebrates, because of their powerful molecular-genetic tools. In *C. elegans*, the entry of sperm determines embryonic polarity (Otto and Goldstein 1992; Strome and Wood 1983), which eventually leads to asymmetric localization of germ plasm and germline specification (Strome and Updike 2015; Seydoux 2018). In the fly *Drosophila*, local translation of the germ plasm organizer Oskar (Osk) recruits germ plasm components to the cellular cortex of the posterior pole (Anne Ephrussi 1992; Kim-Ha et al. 1993; Trcek and Lehmann 2019). Among vertebrates using germ plasm for germline specification, some key discoveries of its localization were made in the frog *Xenopus laevis* (Tristan Aguero, Susannah Kassmer, Ramiro Alberio, Andrew Johnson 2017; Houston 2013). In *Xenopus laevis* it was shown that during oogenesis the germ plasm first accumulates at the prominent Balbiani body (BB), also called mitochondrial cloud (Heasman, Quarmby, and Wylie 1984). Then, germ plasm gets anchored at the vegetal pole and after fertilization is passively inherited during the cleavage period of the most vegetal blastomeres (Tristan Aguero, Susannah Kassmer, Ramiro Alberio, Andrew Johnson 2017;

Ressom and Dixon 1988). At the blastula stage, germ plasm positive cells internalize into the embryo and then start their migratory journey until they reach the gonads. However, the molecular structure tethering germ plasm to the vegetal pole during the cleavage period of *Xenopus* embryogenesis is not known.

In zebrafish egg, germ plasm accumulates also first at the Balbiani Body and subsequently localizes to the vegetal pole like in *Xenopus* (Moravec and Pelegri 2020; Raz 2003; Dosch 2015). However in contrast to *Xenopus*, after fertilization germ plasm streams together with cytoplasm during 'ooplasmic segregation' into the forming blastodisc at the animal pole of the zebrafish embryo (Welch and Pelegri 2014). Subsequently, germ plasm localizes to the cleavage furrows at the four-cell stage, forming four aggregates in close proximity to apical ends of the furrows (Raz 2003; Yoon, Kawakami, and Hopkins 1997; Olsen, Aasland, and Fjose 1997). Indeed, maternal mutants affecting the first embryonic cleavages also interfere with germ plasm recruitment (Yabe, Ge, and Pelegri 2007; Nair et al. 2013). The first described cytoskeletal structure tethering germ plasm in zebrafish was described as furrow-associated microtubule-array (FMA) (Jesuthasan 1998; Pelegri et al. 1999). However, the FMA starts to disassemble after the third cleavage, leaving the molecular identity of the cellular structure anchoring germ plasm after the eight-cell stage unresolved.

Molecular and genetic screens identified the proteins which are specifically localized to these four germ plasm spots, *e.g.* zebrafish Piwi (Ziwi) (Houwing et al. 2007), phosphorylated non muscle myosin II (p-NMII)(Nair et al. 2013) and Bucky ball (Buc) (Bontems et al. 2009; Campbell et al. 2015; Riemer et al. 2015; Roovers et al. 2018). Buc appears to exert a central role during germline specification, because it acts as a germ plasm organizer by recruiting other germ plasm components and thereby triggers germline specification (Bontems et al. 2009; Marlow and Mullins 2008; Heim et al. 2014; Krishnakumar et al. 2018). Buc interacts through Kinesin Kif5Ba with microtubules, which is essential for Buc transport towards the cleavage furrows (Campbell et al. 2015). However, it is not clear, which cellular structure anchors Buc after its transport to the four germ plasm spots in the early embryo.

Here, we show that the germ plasm nucleators Buc and its *Xenopus* homolog Velo1 use conserved mechanisms for their localization, whereas *Drosophila* Osk localizes by a distinct mode. We mapped the localization motif in the Buc protein and used the isolated peptide to purify interactors from zebrafish embryos. Among numerous proteins, we identified subunits

of the NMII complex, which is a known cytoskeletal component of adherens junctions, tight junctions and midbodies (Liu et al. 2012; Vicente-Manzanares et al. 2009). In addition, ZO2 and the adherence receptor of tight junctions (Cldn-d) was identified as Buc associated proteins. Furthermore, we discovered that TJ protein ZO1 colocalizes with the four germ plasm aggregates at the cleavage furrows at the 8-cell stage. Electron microscopy (EM) of zebrafish embryos uncovered TJ like structures at the cleavage furrows that are in proximity to germ plasm at the 8-cell stage. Moreover, overexpressing the tight junction receptor Claudin-d (Cldn-d) led to the formation of ectopic germ plasm aggregates in zebrafish embryos. Taken together, our results indicate TJ as the cellular structure which recruits germ plasm at the onset of zebrafish embryogenesis.

Results

Zebrafish Buc and Xenopus Velo1 localize similarly in zebrafish embryos

Consistent with its function as a germ plasm organizer, Buc localizes to the germ plasm throughout early embryogenesis (Riemer et al. 2015; Heim et al. 2014; Bontems et al. 2009). To address whether this localization mechanism is conserved between zebrafish and *Xenopus*, we injected mRNA encoding GFP-fusions of these germ plasm organizers into 1-cell zebrafish embryos (Fig. 1A). At 2.5-3 hours post fertilization (hpf), we analyzed if the GFP-fusion proteins colocalize with the germ plasm using an antibody against the endogenous Buc proteins, which is tightly associated with the germ plasm (Bontems et al. 2009) and an antibody detecting □-Catenin to label the membrane of the cleavage furrows. Western blot of *in vitro* translated proteins confirmed the specificity of the Buc antibody (Supplementary Fig. 1). Injections of mRNA encoding Buc-GFP colocalized with zebrafish germ plasm recapitulating the positioning of the germ plasm (Fig. 1B, C, Supplementary Fig. 2A) (Bontems et al. 2009). Similarly, Velo1-GFP colocalized with the germ plasm (Fig. 1B, D, Supplementary Fig. 2B), suggesting that zebrafish Buc and *Xenopus* Velo1 are targeted by a similar molecular machinery for germ plasm localization. To test if the localization mechanism also detects the invertebrate germ plasm organizer sOsk, mRNA of sOsk fused to GFP was injected as well. In contrast to Buc and Velo1, sOsk-GFP did not overlap with the germ plasm in injected zebrafish embryos (Fig. 1B, Supplementary Fig. 2C), but instead localized to the nuclei as previously shown in insect cells and *Drosophila* embryos (Jeske, Müller, and Ephrussi 2017; Kistler et al.

2018) similar to control injections of a GFP that resulted in a ubiquitous subcellular localization including the nucleus (Fig. 1B, E, Supplementary Fig. 2C, D). These results suggest that zebrafish Buc and *Xenopus* Velo1 are localized by a conserved machinery, which does not recognize *Drosophila* sOsk. To test if this non-overlapping localization mechanism is also true for Buc in *Drosophila,* we tested if ectopic localization of Buc to the anterior pole in *Drosophila* embryos is sufficient to recruit endogenous germ plasm and the subsequent formation of ectopic PGC as shown for sOsk. (Anne Ephrussi 1992). We fused the *buc* ORF to GFP and a *bicoid*-3'-UTR to direct its translation to the anterior pole of *Drosophila* embryos (Supplementary Fig. 3A). As a positive control, we used *sosk* ORF fused to *bicoid*-3-UTR (*sosk*) (Tanaka and Nakamura 2008). Indeed, immunolabelling of stage 4-5 fly embryos showed that sOsk-GFP is anchored at the anterior cortex of the embryos causing the formation of ectopic PGCs (Supplementary Fig. 3B, D) by the ectopic localization of germ plasm including Vasa protein at the anterior pole (Supplementary Fig. 4). By contrast, Buc was neither localized to the embryo cortex nor did it ectopically aggregate germ plasm or form perinuclear foci (Supplementary Fig. 3E; Supplementary Fig. 4). These results show that Buc is also not recognized by the localization machinery in *Drosophila* that anchors sOsk to the cortex, suggesting that zebrafish and flies use different mechanisms for germ plasm localization.

The Buc localization signal is part of the conserved N-terminal BUVE motif

To identify the protein domain of Buc responsible for its localization to the four germ plasm aggregates, we generated systematic deletions of Buc fused to GFP (schematically shown in Fig. 2A), injected the mRNA into zebrafish 1-cell stage zygotes and scored the number of embryos with GFP foci at 3 hpf as depicted in Fig. 1A.

An N-terminal fragment (aa 1-361, Fig. 2A) which corresponds to the previously identified buc^{p43} mutant allele localizes correctly and with the same penetrance as full-length Buc (Fig. 2A, B, C, Supplementary Fig. 5A). Next, we split this fragment into two halves (aa1-158 and 159-361) and analyzed their localization. Buc1-158 localized, whereas Buc159-361 showed ubiquitous fluorescence, similar to control embryos injected with GFP mRNA (Fig. 2A, B, Supplementary Fig. 5B, C). We then split Buc1-158 into two fragments and in addition removed the first ten amino acids (Buc11-88), which show a low conservation in teleost evolution (Škugor et al. 2016). Buc11-88 was sufficient to recapitulate germ plasm

localization, whereas Buc89-158 showed no specific localization (Fig. 2A, B, E, Supplementary Fig. 5D). Further splitting of Buc11-88 disrupted the localization activity of both resulting fragments (Fig. 2A, B, Supplementary Fig. 5E, F), suggesting that aa 11-88 contains the residues sufficient to target the protein to the germ plasm spots. To confirm that Buc does not contain other motifs involved in localization, we generated a deletion of the isolated motif aa11-88 (BucΔ11-88) in full length Buc. This protein did not localize (Fig. 2A, B, F). We therefore concluded that aa11-88 is sufficient and necessary for the localization of Buc and named the protein-region BucLoc. This domain is part of the so called BUVE domain a region within Buc that shows the highest homology to *Xenopus* Velo1 (Bontems et al. 2009; Boke et al. 2016; Krishnakumar et al. 2018).

Prion-like domains in the BucLoc motif are not required for Buc localization

The BUVE domain was recently shown to be responsible for Velo1 localization to the BB during *Xenopus* oogenesis (Boke et al. 2016). Furthermore, the localization of Velo1 to the BB is driven by aggregation of two prion-like domains (PLDs) within the BUVE motif (Boke et al. 2016). A Sequence alignment of Buc with Velo1 showed the conservation of the aromatic amino acids of the PLDs in Buc between aa24-30 and 64-71 (Fig. 3A, marked in red), suggesting that these domains might also be required for the formation of the four germ plasm aggregates at the 8-cell stage.

To investigate the importance of these two potential PLD domains in Buc, the colocalization of deletion variants with the germ plasm was analyzed. Therefore, mRNA of deletion variants of the BucLoc domain (shown schematically in Figure 3D) fused to mCherry were injected into 1-cell embryos and the colocalization to germ plasm aggregates marked by Buc-GFP was examined at 3 hpf. As a positive control we used the entire BucLoc domain (aa11-88) that shows colocalization with the endogenous germ plasm (Fig. 3B, C, quantification in E). To narrow down the localization motif further, the N-terminal 20 amino acids were removed deleting the N-terminal PLD domain (aa21-30). Indeed, Buc 31-88 showed a slight reduction in germ plasm localization (Fig. 3D, E, Supplementary Fig. 6). However, when we deleted in addition ten C-terminal amino acids (Buc31-78), localization was restored to nearly wild-type frequency (Fig. 3D, E, Supplementary Fig. 7B). By contrast, deleting four additional N-terminal

amino acids (Buc35-78) almost completely abrogated localization (Fig. 3D, E). These results suggest that the first PLD does not seem to be necessary for localization.

To examine the role of the second PLD, we generated internal deletions in Buc31-78. When we removed the second PLD (Δ64-71), no fluorescence could be detected in the embryos (Supplementary Fig. 7C) suggesting that aa64-71 might affect protein stability or translation. Therefore, we analyzed two variants with five amino acid deletions within the second PLD domain. Strikingly, removing parts of the second PLD (Buc⍰62-66 or Buc⍰67-71) caused no clear reduction in germ plasm localization (Fig. 3D, E, Supplementary Fig. 7D, E). In contrast, when we kept the second PLD domain intact, but removed C-terminal sequences (Buc31-71), the localization efficiency dropped to 15% (Fig. 3D, E, Supplementary Fig. 7F). These results suggest that the two PLD motifs, which control Buc's aggregation into the Balbiani body during oogenesis (Boke et al. 2016), are not required for positioning Buc to the four germ plasm aggregates in the embryo.

Identification of the BucLoc interactome

As Buc forms clusters with the germ plasm in the proximity of the cleavage furrows, we aimed to identify the cellular structure that is essential for its anchorage. As our results show that BucLoc domain is sufficient for the localization of Buc to the germ plasm foci, we used this protein motif as a bait to identify cellular binding partners directly by co-immunoprecipitation followed by mass spectrometry analysis. Embryos were injected at 1-cell stage with mRNA encoding BucLoc-GFP, lysed at the stage of the formation of germ plasm foci and immunoprecipitated using GFP-tag (Fig. 4A). Embryos injected with mRNA encoding GFP were used as a negative control, and transgenic embryos for full length Buc-GFP were used to control for mRNA overexpression.

In this analysis, we found 1817 protein candidates that potentially interact with full length Buc and BucLoc but not with GFP. From those, 213 proteins were strongly enriched for BucLoc interaction (Fig. 4B, Supplementary Table 1 for the full list of candidates of the mass spectrometry) and represent therefore candidates for the subcellular network required for germ plasm localization. Among the candidates that were strongly enriched was Myosin Light Chain (Fig. 4C), which is a subunit of the Non-Muscle Myosin II (NMII) protein complex. Interestingly, phosphorylated NMII (p-NMII) colocalizes with germ plasm RNAs at the 2- and

4-cell stage in zebrafish embryos (Nair et al. 2013). To investigate if p-NMII also colocalizes with Buc and could therefore play a role in germ plasm localization we performed immunohistochemistry for Buc and p-NMII. Indeed, we found that Buc colocalizes with p-NMII in early stage IB oocytes (Fig. 4D) and during zebrafish embryogenesis (256 cell stage, Fig. 4E, F).

As the NMII associates with various cellular structures (Liu et al. 2012; Vicente-Manzanares et al. 2009; Nair et al. 2013), we therefore screened the list of potential BucLoc interactors for a defined subcellular localization. We detected ZO2 and ZF-A89 as highly enriched in the pull-down assay, the latter is a homolog of Cldn-d (UniProtKB/Swiss-Prot record; description: *Claudin-like protein ZF-A89*) (Supplementary table 1). This suggest that we might have purified components of tight junctions. Claudins are adherence receptor essential for the formation of TJs, suggesting that Buc and germ plasm aggregate at TJs within the cleavage furrows. These results confirm that our immunoprecipitation experiment has purified candidates involved in anchoring Buc in the forming germ plasm foci.

Buc colocalizes with tight junction protein ZO1 and Cldn-d

To further confirm the localization of Buc to TJs, we used an antibody specifically detecting the zona occludens protein ZO1 shown to directly interact with Cldn proteins to mark the TJ for colocalization analysis. As controls, we used an antibody against E-Cadherin to label the adherens junction and Kif23 to label the midbody. Fascinatingly, Buc perfectly colocalized with the TJ marker ZO1 (Fig. 5D, Supplementary Fig. 8C), whereas no overlap could be detected with E-Cadherin Fig. 5B, Supplementary Fig. 8A) or Kif23 (Fig. 5C, Supplementary Fig. 8B). These data show that Buc localizes to the ZO1-positive foci at the cleavage furrows suggesting colocalization of the germ plasm aggregates with TJs. To investigate the localization of Cldn-d, we generated an antibody. Colabeling of 8-cell embryos with Buc and Cldn-d antibodies showed partial overlapping signals of both proteins (Supplementary Fig. 9). By contrast, at germ plasm free cleavage furrows we did not detect Buc and Cldn-d colocalization. These data support a role of Cldn-d in tethering Buc at the germ plasm cleavage furrows of early zebrafish embryos. To confirm this colocalization independently, we analyzed the localization of Cldn-d in zebrafish embryos after injection of mRNA of a *cldn-*

d fusion with m-Cherry. Cldn-d-m-Cherry showed similar localization as the double staining of Buc and Cldn-d (Supplementary Fig.10).

Taken together, our data show that Buc colocalizes to Cldn-d and ZO1-positive foci at the cleavage furrows supporting the idea that the TJ protein complex might probably be functionally involved in the association of Buc and the germ plasm.

Electron microscopy showed TJ-like structures at early cleavage furrows

To verify that the ZO1- and Buc-positive structures at the distal cleavage furrows of the 8-cell embryos are TJs we used electron microscopy to search for characteristic TJs structures at the cleavage furrows of 8-cell stage embryos. Indeed, electron microscopy showed electron-dense membrane sections resembling TJ-like structures at the cleavage furrows where germ plasm is localized (Fig. 5E). In contrast, we did not find these structures at those cleavage furrows, where germ plasm is not accumulated (Fig. 5F). This finding supports the results of the staining with the antiserum against ZO1, that also showed four spots at the 8-cell stage embryos. The result of the electron microscopy shows in addition for the first time, that early zebrafish embryos have TJ-like structures already at the 8-cell stage.

The tight junction receptor Cldn-d anchors germ plasm

Claudins are one family of receptors, which physically connect the TJ in the epithelial and endothelial tissues of vertebrates. Claudins are transmembrane proteins that bind to the PDZ domains of scaffolding zonula occludens (ZO) proteins through their cytoplasmic C-terminal YV (Tyrosine-Valine) motifs (Furuse et al. 2014; Mccarthy et al. 2000). More than 50 claudins are identified in teleost fishes with restricted tissue expression patterns (Kolosov et al. 2013).

The zebrafish genome encodes only five ZO proteins with numerous functions during early zebrafish embryogenesis (Kiener, Sleptsova-Friedrich, and Hunziker 2007; Schwayer et al. 2019). Fascinatingly only two Claudins, Cldn- and -e are listed in the Zfin database (https://zfin.org/), which are maternally expressed (Supplementary Fig. 11). Moreover, the role of the maternally expressed *Xenopus* homolog Xcla was previously characterized including a dominant-negative version of the receptor (Brizuela, Wessely, and De Robertis

2001). Based on the colocalization of Buc with TJs and the interaction of ZO1 with Cldn-d, we addressed the hypothesis that Cldn-d could act as a membrane anchor for germ plasm.

To analyze a potential function of Cldn-d in germ plasm tethering, we injected *cldn-d* mRNA into 1-cell zebrafish embryos transgenic for Buc-GFP to detect germ plasm localization *in vivo*. Compared to uninjected control embryos, the injection of *cldn-d* mRN*A* led to a significantly higher number of Buc-GFP positive spots at 2-3 hpf (Fig. 6A, B, E). To control the specificity of mRNA overexpression, we injected the same concentration of Cldn-a, but did not detect a change of germ plasm spots similar to uninjected controls (Fig. 6A, C, E). Moreover, quantification of the fluorescent intensity of control and injected embryos showed no significant difference suggesting a change in the localization rather than a change in the levels of Buc (Fig. 6G). Together these results indicate that Cldn-d might be involved in germ plasm tethering in the early zebrafish embryo.

The C-terminal amino acids Tyrosine and Valine are crucial for the interaction of Claudins with ZO proteins (Itoh, Furuse, and Morita 2014). We therefore generated a Cldn-d mutant lacking the interaction motif (C-terminal YV, named Cldn-dΔYV), which was previously shown to act as a dominant-negative form of Cldn-d (brizuela, 2001). Notably, *cldn-dΔYV* injected embryos showed a significantly reduced number of germ plasm spots in comparison to uninjected embryos (Fig. 6A, D, E). However, c*ldn-dΔYV* injected embryos displayed severe developmental defects, in which the cells did not attach to each other suggesting that the dominant-negative receptor might also disrupt TJs formed during later embryogenesis (Fig. 6D, D').

To exclude that the reduced number of germ plasm foci in *cldn-dΔYV* injected embryos is a secondary result caused by a defect in cell attachment, we targeted its expression to two blastomeres in a 16-cell embryo. Injection of *cldn-dΔYV* mRNA into 16-cell stage embryos still reduces the number of germ plasm spots. At this stage, the junctions are matured and the germ plasm containing cells can easily be distinguished from somatic cells, since they hold the central position in the marginal row of four blastomeres ('middle blastomeres'). We injected *cldn-dΔYV* into two middle blastomeres surrounding one germ plasm spot (Fig. 7A) using uninjected and wild-type *cldn-d* injected embryos as controls. The number of Buc spots was counted right after injection (16-cell stage) and then followed up in regular time intervals (see table 2 in the Supplementary). In this assay, embryos developed normally and did not show

developmental defects (Fig. 7B, C). Interestingly, we still observed a significant reduction in the number of germ plasm spots in *cldn-dΔYV* injected embryos (Fig. 7B, C, D) compared to uninjected and *cldn-d* injected controls (Fig. 7D). More than 35% of *cldn-dΔYV* injected embryos lost a germ plasm spot, whereas only 6% of the embryos injected with *cldn-d* showed germ plasm spot reduction (Fig. 7D, table 1 in the Supplementary). These results support our model that TJs might be involved in recruiting germ plasm to the cleavage furrows and that the Cldn-d receptor might be component of TJs in the early zebrafish embryo (Fig. 8).

Discussion

Our data show that the localization machinery of germ plasm is different between vertebrates and invertebrates. We identified that the N-terminal BucLoc domain (aa11-88), is necessary and sufficient for the localization of Buc to the four germ plasm aggregates at the furrow channels at the 8-cell stage embryo. Our colocalization and protein-protein interaction data from the immunoprecipitations suggest that Buc together with other germ plasm components are linked to de novo forming TJs at cleavage furrows.

Our results showed that (i) myosin light chain co-immunoprecipitated with Buc and that p-NMII is colocalizing with Buc protein, suggesting that germ plasm might get anchored to one of the cellular structures through NMII (Fig. 4). (ii) Co-immunoprecipitations of Buc co-purified ZO and Claudin (Fig. 4). (iii) Germ plasm colocalizes with the TJ protein ZO1 and Cldn-d (Fig. 5; Suppl. Figure8,9,10). (iv) EM-micrographs show the presence of TJ-like structures at the cleavage furrows in the 8-cell zebrafish embryo (Fig. 5). (v) *cldn-d* injection causes the formation of a higher number of germ plasm spots, whereas Cldn-d with a mutated interaction motif for ZO proteins (C-terminal YV motif) functions as a potential dominant negative resulting in fewer germ plasm spots (Fig. 6; Fig. 7). These results strongly support the model that newly forming TJs at the cleavage furrows represent the anchorage hub for the germ plasm in zebrafish. This localization might be critical to achieve a threshold concentration for phase-transition, which plays an important role during germ plasm aggregation (Kistler et al. 2018; Trcek and Lehmann 2019; Krishnakumar et al. 2018).

Evolutionary conservation of germ plasm anchorage among vertebrates

Invention of multicellularity requires cell adhesion and germ plasm for sexual reproduction. With our finding, it will be possible to address whether germ plasm localization at TJs was already used at the origin of Metazoa or whether it is a derived mechanism acquired during vertebrate evolution. The isolated BucLoc motif does not show homologies to known protein domains, which did allow to deduce its biochemical function. However, it proposes vertebrate species, which might use a similar localization mechanism for Buc like the zebrafish.

Our data suggest that the tethering of germ plasm is conserved among vertebrates, as we observed identical positioning in *Xenopus* and zebrafish, but not in *Drosophila*, suggesting a similar anchorage mechanism in fish and frogs. In contrast, *Drosophila* sOsk is not targeted by the vertebrate localization system. Therefore, our results show that the localization machinery of germ plasm is different between vertebrates and invertebrates. Despite the functional equivalence of Buc and Osk which is previously shown (Krishnakumar et al. 2018), we here provide evidence that Buc and Osk proteins use different mechanisms to localize germ plasm. Germ cell specification activity of these germ plasm nucleators looks conserved, whereas the mechanism of their localization seems to adapt to the architecture of the embryo. Therefore, different localization mechanisms are consistent with the different shapes of early embryos.

TJs as an anchorage hub for germ plasm

Anchoring of the germ plasm to the TJs is different from anchoring to the posterior cell cortex in *Drosophila* oocytes and embryos long before cellularization take place. The posterior localization of germ plasm is essential for the specific embedding into budding PGC at the posterior pole in early *Drosophila* embryos. However, in zebrafish embryos the role of germ plasm anchorage is different. The observed accumulation and linkage to the TJs keep the germ granules concentrated in one spot of the cytoplasm, thereby inhibiting symmetric distribution of germ plasm during the following cell divisions. This anchorage results in the preservation of only four PGC up to the 512 cell stage. Only after the mid-blastula transition (MBT), germ plasm is symmetrically inherited when the PGC start to divide forming four clusters of PGCs (Knaut et al. 2000; Dosch 2015; Wolke et al. 2002). At that time the germ plasm is localized

into perinuclear clusters, enabling a symmetric distribution during PGC divisions (Strasser et al. 2008). Therefore, the anchorage to the TJs has to be released at a later stage, as the PGC start dividing and the germ plasm needs to be inherited symmetrically by both daughter cells to ensure their fate.

A release of the germ plasm aggregate from the TJ could be a consequence of the modification of Claudins, Buc or of other unknown bridging protein(s). We believe that our results show a specific function of Cldn-d, as injection of Cldn-d caused a significant increase in the number of germ plasm spots, whereas Cldn-a had no effect. Furthermore, co-immunoprecipitation experiments revealed a specific interaction of Buc with Cldn-d but not with Cldn-a. This differential biological activity could be caused by the particular capability of Cldn-d to form *de novo* TJs in the early cleavage furrows, but we would rather favor a model in which the interaction of Cldn-d with the germ plasm is specific. This model could explain the release of the germ plasm from TJs by exchange or dilution of the maternal Cldn-d with other claudins, starting at the onset of zygotic expression. Surprisingly, overexpression of claudins did not make significant change in the overall quantification of BucGFP (Figure 6G), suggesting the alteration in the number of germ plasm spots as the result of changing the number of junctions where Buc can anchor, rather than the stability of the protein. Future experiments have to address the mechanism by which germ plasm is inherited symmetrically into both daughter PGCs after MBT.

Function of Buc in germ plasm anchorage at the TJs

Sequence analysis of Buc did not reveal any characterized domain within the protein (Bontems et al. 2009; Krishnakumar et al. 2018). However, sequencing of *buc*^{p106re} allele revealed a mutation in the 6th exon of Buc genomic locus, which would cause a deletion of only 37 C-terminal amino acids, suggesting an essential role of its C-terminal end. Within this C-terminus Arginine residues are dimethylated, thereby enabling the direct interaction of Buc with the zebrafish Tudor homologue Tdrd6 (Roovers et al. 2018). Tdrd6 interacts with the known RNAs enriched in the germ plasm and it was shown that it is involved in the loading of germ plasm components into PGCs. Furthermore, high-resolution microscopy showed that Tdrd6 and Buc form particles with germ plasm mRNA in which Buc is localized in the core of the particle, whereas Tdrd6 is mostly positioned at the periphery of the particles at the 4-cell

stage when the germ plasm start to accumulate at the cleavage furrows. These data suggested that Buc cooperate with Tdrd6 like Osk with Tudor in the aggregation of the germ plasm.

Buc is also interacting with Vasa as shown by co-immunoprecipitations and experiments using split Cherry, suggesting that Buc and Vasa bind directly within the N-terminal 360 amino acids (Krishnakumar et al. 2018). Furthermore, the N-terminal half of Buc is also able to interact with *nanos3*-3'-UTR RNA. However, it is unknown whether Buc can directly interact with mRNA of the germ plasm, because it does not contain any characterized RNA binding motif.

Sequence comparison with 15 related Buc proteins revealed a conserved 100 amino acid N-terminus, which was named BUVE motif (Buc-Velo) (Bontems et al. 2009). The BUVE domain was shown to be essential for the formation of the amyloid-like aggregates in the BB in *Xenopus* oocytes. The BUVE domain contain potential prion like domains (PLD) (Alberti et al. 2009), which were shown to be essential for the aggregation process, based on the fact that the replacement of critical residues with charged amino acids inhibited the aggregation. These results suggested that the BUVE domain of Velo1 and Buc is required for amyloid-like germ plasm aggregation in the BB. However, Velo1 variants in which the potential PLDs were replaced with unrelated PLDs were inactive, whereas the replacement with the related sequences from zebrafish Buc were active, revealing a sequence specificity (Boke et al. 2016). Surprisingly intrinsic disorder prediction of Buc showed that N- terminus (aa 1–150) is the largest ordered sequence in Buc (Krishnakumar et al. 2018). *Drosophila* Osk was recently shown to form aggregates in an ectopic system (insect S2 cells) although Osk does not display any PLD domains (Jeske, Müller, and Ephrussi 2017; Boke et al. 2016). Nevertheless, we tested for the role of the predicted PLDs within the N-terminus when we identified the region between aa11 and 88 to be essential and sufficient for the localization of Buc to the 4 germ plasm spots at the cleavage furrows (Fig. 2). The detailed mapping showed however, that none of these two potential PLDs within this sequence are essential, but short stretches C-terminal of them (Fig. 3). This result does not exclude that the PLDs are involved, as the additional regions might be required for the proper presentation of the PLDs. However, co-immunoprecipitation and Mass spectrometry analyses showed that the domain between aa 11-88 interacts with about 213 peptides including myosin light chain and Cldn-d (Fig. 4). 213 peptides are an unexpected high number of interactions and includes probably a number of

indirect interactions. We therefore prefer to interpret these results in a different way, whereby the BUVE domain including the BucLoc represents a protein-protein interaction module that indirectly enables the formation of a protein RNA complex essential for germ plasm aggregation. Future experiments will identify the mechanisms and the direct interaction partners of Buc.

Buc and TJs in biomolecular condensates

Increasing evidence suggest that germ granules in many different organisms are formed by phase separation. Germ plasm consists of spherical units of protein RNA aggregates that show a highly dynamic exchange with the surrounding cytoplasm (recently reviewed in (Dodson and Kennedy 2020; So, Cheng, and Schuh 2021)**.** Indeed, the BucLoc motif was previously shown to play a crucial role in aggregating the Balbiani body in the *Xenopus* oocyte, which is probably the largest biomolecular condensate in the animal kingdom (Boke et al. 2016). However, our results show that the Prion-like domains in the BucLoc motif, which control Balbiani body assembly, are not required for germ plasm anchoring in the embryo. Nonetheless, our previous data show that Buc forms liquid-like condensates in the embryo (Riemer et al. 2015; Roovers et al. 2018; Krishnakumar et al. 2018),suggesting that aggregation does not control its embryonic localization.

Interestingly, ZO Proteins also induce the assembly of liquid-like condensates (reviewed in (Canever, Sipieter, and Borghi 2020; Citi 2020). The condensation of ZO proteins in cell culture and zebrafish embryos induces the assembly of TJs revealing an unexpected activity in the cytoplasm to control the formation of TJs (Schwayer et al. 2019; Beutel et al. 2019). Our finding that Buc and ZO1 colocalize raises the question whether Buc indeed autonomously induces condensates or whether this activity is mediated by ZO1. However, we previously showed that Buc condensates in HEK293 cells, which do not form TJs, supporting Buc's autonomous phase separation activity (Krishnakumar et al. 2018).

Fascinatingly, we show that the injection of *cldn-d* had a similar activity on forming extra germ plasm spots compared to the injection of Buc (Bontems et al. 2009). Surprisingly, overexpression of Claudins did not significantly change the overall quantity of BucGFP-fluorescence (Figure 6G), suggesting the alteration in the number of germ plasm spots as the result of changing the number of junctions where Buc can anchor, rather than the stability of

the protein. In this scenario, the maternal load of Cldn-d is limited and just sufficient to form four spots. Indeed, the loss of spots after injection of dominant-negative Cldn-d seems to support this hypothesis. Taken together, our results support an essential function of Buc generating a multiprotein hub at the newly forming TJs that allows the anchorage of germ granules.

Conclusion

In conclusion, we found that vertebrates and invertebrates utilize different germ plasm localization mechanisms, with evolutionary conservation between vertebrates. We discovered that TJs anchor germ plasm during early zebrafish embryogenesis and that germ plasm in zebrafish is anchored to the TJs and via Cldn-d receptor protein. Microinjection of *cldn-d* induced extra germ plasm spots. Currently we believe that NMII interaction with Buc drives the localization of germ plasm into the TJs, as shown in the following model (Fig. 8).

Materials and methods

Zebrafish handling and manipulation

Zebrafish (*Danio rerio*) was used as an animal organism in this study, AB*TLF (wild-type) and

Buc-GFP transgenic zebrafish line(Riemer et al. 2015). Fish were raised and maintained according to the guidelines from (Westerfield, 2000) (Westerfield M. 2000) and regulations from Georg-August University Goettingen, Germany.

Microinjection

Previously synthesized capped RNA was diluted with 0.1M KCl and 0,05% phenol red (Sigma Aldrich, Hannover). 2nl of RNA was injected into 1- cell stage embryos using PV820; WPI injecting apparatus (Sarasota, USA). Injected embryos were incubated in E3 medium at 28°C until they reached the developmental stage of the phenotype evaluation.

Sixteen- cell injection assay of Cldnd- ΔYV

To study whether non-functional Cldn-d has an influence on matured TJs, we conducted *cldn-dΔYV* injections in 16-cell embryos. In this assay, we injected the RNA directly into two cells next to a germplasm localizing tight junction. As a control we used uninjected and *cldn-d* RNA injected embryos. The number of Buc spots was counted right after injection and then followed up in regular time periods. Detailed description of the injection procedure at 16- cell stage is previously published (Krishnakumar et al. 2018; Bontems et al. 2009).

Drosophila handling and manipulation

Flies were kept and crossed at room temperature or 25 °C. To collect embryos, the flies were kept in cages with apple juice agar plates at 25 °C. Experiments were approved by the Lower Saxony State Office for Consumer Protection and Food Safety (AZ14/1681). The pUASp *bcd*3'UTR plasmid expressing sOsk (Tanaka and Nakamura 2008) was used to replace the *sosk* ORF with Buc ORF-GFP. A germline- specific *mat -Gal4VP16* driver was used to express UASp-based transgenes in oogenesis. Antibody staining and fluorescent *in-situ* hybridization was performed as described (Pflanz et al. 2015). The antibodies used were anti-PY20 (1/500, Biomol), rabbit anti-GFP (1/1000, Synaptic Systems, Göttingen, Germany) and anti-Vasa (1/5000 (Pflanz et al. 2015)). Anti-mouse and anti-rabbit antibodies coupled to Alexa 488, 568 or 647 were used as secondary antibodies (Invitrogen, 1/1000). Embryos were imbedded in DPX to provide clearing and to protect from bleaching.

Biochemical methods

Co-immunoprecipitation (Co-IP)

CO-IP was performed to identify Buc protein interactome. Each sample was prepared from 500 deyolked high stage embryos after homoginization on ice in lysis buffer (10 mM Tris (pH 7.5), 150 mM NaCl, 0.5 mM EDTA, 0.5 % NP-40, 1x complete protease inhibitor cocktail (Roche, Mannheim)). The supernatant was subsequently used for the Co-IP using a GFP-binding protein coupled to magnetic beads (GFP-Trap_M; ChromoTek, Planegg-Martinsried) following manufacturers instructions. After pulling down, the magnetic beads and their bound proteins were either incubated with 2x SDS loading buffer for 5 min at 96 °C and

analyzed via SDS-PAGE and western blotting or sent for mass spectrometry (Core Facility of Proteome Analysis, UMG, Goettingen), as described previously (Krishnakumar et al. 2018).

Selection criteria for specifically interacting proteins

In total, 3464 protein candidates interacted. From those, 1817 candidates were identified that interacted with both Buc-GFP and BucLoc-GFP. We were not interested in every candidate for interaction with Buc-GFP, as they might interact with any other region outside of BucLoc. Therefore, we applied a set of criteria to identify significant interacting candidates with BucLoc. First, any peptide below a background threshold of five in BucLoc-GFP was considered as not significant and were sorted out. Furthermore, only proteins with counts in BucLoc-GFP that were at least twice as high as in the negative control GFP were considered as significant. To further reduce overexpression artefacts, enrichment in the positive control and in the sample had to be within a magnitude of +/- 4-fold. Applying these selection criteria, the number of potential BucLoc interaction proteins could be restricted to 213 interaction candidates (see the Supplementary for the full list of mass spectrometry candidates).

Immunohistochemistry

Embryos were fixed and stained as previously described (Riemer et al. 2015) with the following antibody concentrations.

Table 1: Antibodies used for immunostaining.

Antibody	Dilution
guinea pig-α-Buc (Biogenes, Berlin)	1:5000
Mouse-α-B-catenin (Merck, Kenilworth, USA)	1:1000
Mouse-α-E-cadherin (BD Transduction Laboratories, Franklin Lakes, New Jersey, USA)	1:50
rabbit-α-p-NMII (Cell Signaling Technology, Danvers, USA)	1:50
Mouse-α-Kif23 (Gene Tex, Irvine, California, USA)	1:50

Rat-α-ZO1 (Santa Cruz, Dallas, Texas, USA)	1:100
Rabbit -α-DDX4 (Bioss, USA)	1:300
goat-α-guinea pig Alexa Fluor 488 (Life Technologies, Carlsbad, USA)	1:500
goat-α-rabbit Alexa Fluor 594 (Life Technologies, Carlsbad, USA)	1:500
Cldn-d	1:25

Western blotting

Western blotting was performed to detect the specificity of Buc antibody as described before (Krishnakumar et al. 2018). Fluorescent signal was detected with Li-Cor Odyssey CLx Infrared Imaging system (Li-Cor, Lincoln, USA) and analyzed with the Image Studio Software (Li-Cor, Lincoln, USA). Western blots with *in vitro* translated proteins confirmed that the Buc antibody did not cross-react with GFP or other proteins and thus specifically highlights endogenous germ plasm (Supplementary Fig. 1).

Table 2: Antibodies used for western blotting.

Antibody	Dilution
guinea pig-α-Buc (BioGenes, Berlin)	1:5000
mouse-α-GFP (Merck, Kenilworth, USA)	1:2500
goat-α-guinea pig 800CW (IRDye, Li-Cor)	1:20000
goat-α-mouse 680CW(IRDye, Li-Cor)	1:20000

In-vitro translation

Proteins were synthesized with the TnT SP6 Quick Coupled Transcription/ Translation System (Promega, Madison, Wisconsin, USA).

Molecular biology methods

Cloning

The template of all the constructs that are used in this study were amplified from reverse transcribed cDNA which was made from total ovarian RNA. Constructs are cloned with either restriction digestion or gate way cloning.

Imaging

Images were taken by SteREO Lumar.V12 (Carl Zeiss Microscopy, Göttingen) and LSM780 confocal microscope and analyzed with xio Vision Rel. 4.8 software and ZEN2011 software (Carl Zeiss Microscopy,Göttingen), as described before (Riemer et al. 2015). Electron microscopy was performed at the facility for transmission electron microscopy (Max Planck Institute for Biophysical Chemistry, Göttingen). Qunatification of confocal images was done with imageJ software.

Bioinformatics

Sequence alignment

Pairwise sequence alignment was used to compare protein sequences, using Needleman-Wunsch algorithm with the EMBL-EBI alignment software EMBOSS Needle (McWilliam et al. 2013).

PLD prediction

Fold amyloid (Fernandez-Escamilla et al. 2004), APPNN (Família et al. 2015), FISH amyloid (Gasior and Kotulska 2014), and Aggrescan (Conchillo-Solé et al. 2007) algorithms were used to predict PLDs in BucLoc.

Analysis of mass spectrometry data

Overlaps in protein interactions between each Co-IP sample were analyzed using a Venn diagram generator (http://jura.wi.mit.edu/bioc/tools/venn3way/index.php). The Kyoto

Encyclopedia of Genes and Genomes (KEGG, http://www.genome.jp/kegg/) has been used to classify the BucLoc-GFP interaction candidates in collaboration with Dr. Thomas Lingner.

Statistics

All the statistical analysis of the experiments have been carried out in Microsoft Excel and the Prism software (GraphPad Software, La Jolla, USA). Error bars indicate the standard deviation of averages. For each injection experiment, at least three independent replicates were used.

Availability of data and materials

The datasets used and/or analysed during the current study are available from the corresponding author on reasonable request.

Competing Interests

The authors declare that they have no competing interests.

Funding

This work was supported by a GZMB stipend, a GGNB bridging fund (SR), the German Academic Exchange Service, DAAD https://www. daad.de/en/) (NR), the Deutsche Forschungsgemeinschaft (DO 740/2-3) (http:// www.dfg.de), the GGNB Junior Group Stipend and the 'Forschungsfo¨rderungsprogramm' of the University Medical Center Go¨ttingen (RD). The funders had no role in study design, data collection and analysis, decision to publish, or preparation of the manuscript.

Acknowledgements

We are thankful to Prof. E. A. Wimmer for providing the facilities to perform this research and G. Kracht for technical assistance. Authors would also like to thank Dr. Sabine Klein for the useful input on this manuscript.

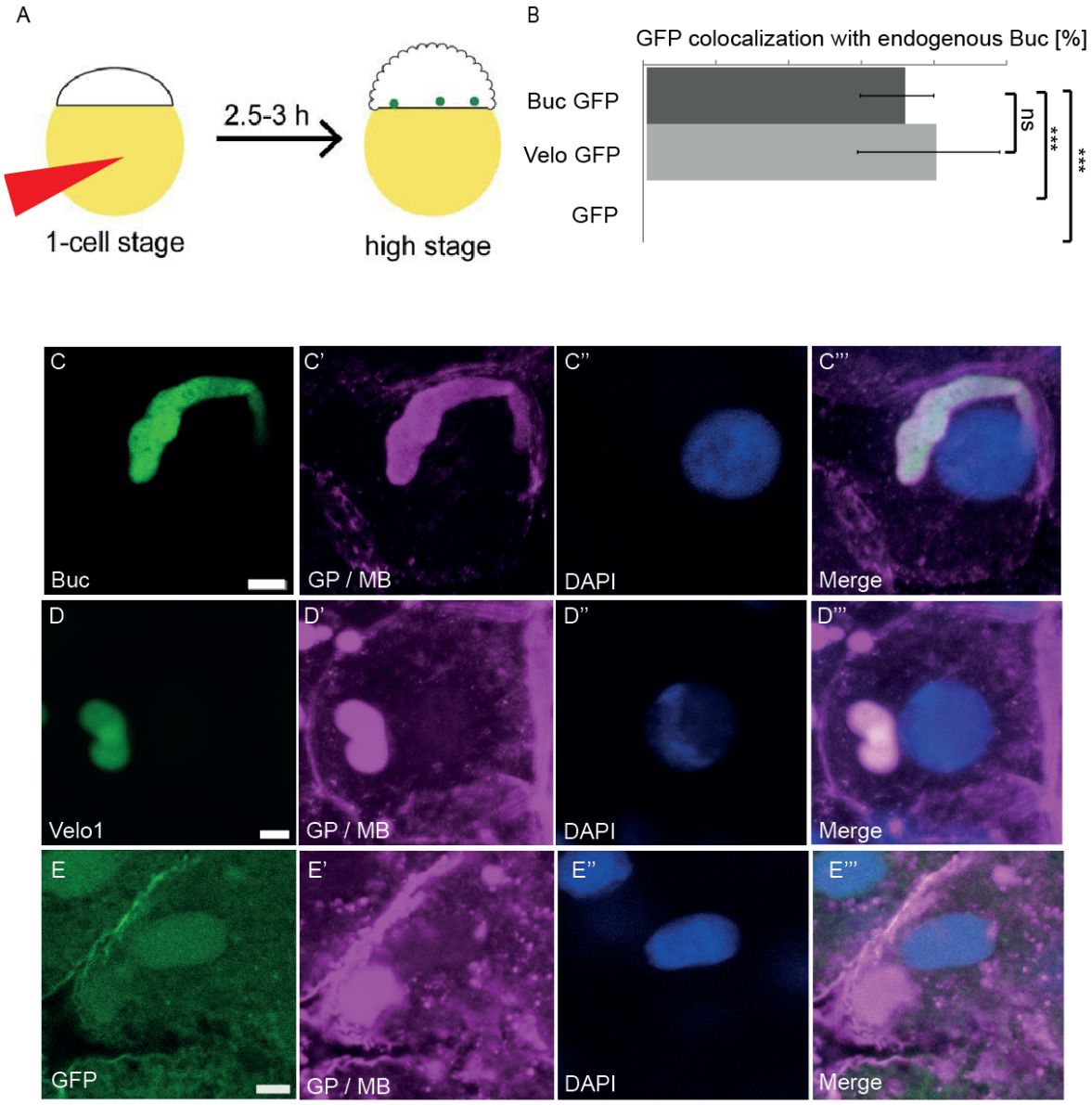

Figure 1. Buc and Velo1 localize to zebrafish germ plasm.

(A) Scheme of zebrafish colocalization assay. RNA encoding GFP fusions of germ plasm organizers Bucky ball (Buc) and Velo1 was injected into 1-cell stage and scored at high stage for localization with endogenous Buc (green dots) by immunohistochemistry. (B) Quantification of colocalization assay. GFP fusions of Buc (71±10.1%) and Velo1 (79.7±19.5%; p=0.6), but not showed colocalization with endogenous Buc. (C-E) Magnified germ plasm spot of embryo at high stage (full embryos are shown in the Supplementary Fig. 2). Colocalization of GFP (1st column, green) with endogenous Buc (germ plasm, GP; and □-catenin to label membranes, MB; magenta) and nuclei (DAPI, blue) was determined by immunohistochemistry. n (Buc: 33, Xvelo:39, GFP: 32). Error bars represent standard deviation (SD). Scale bars: 5 µm.

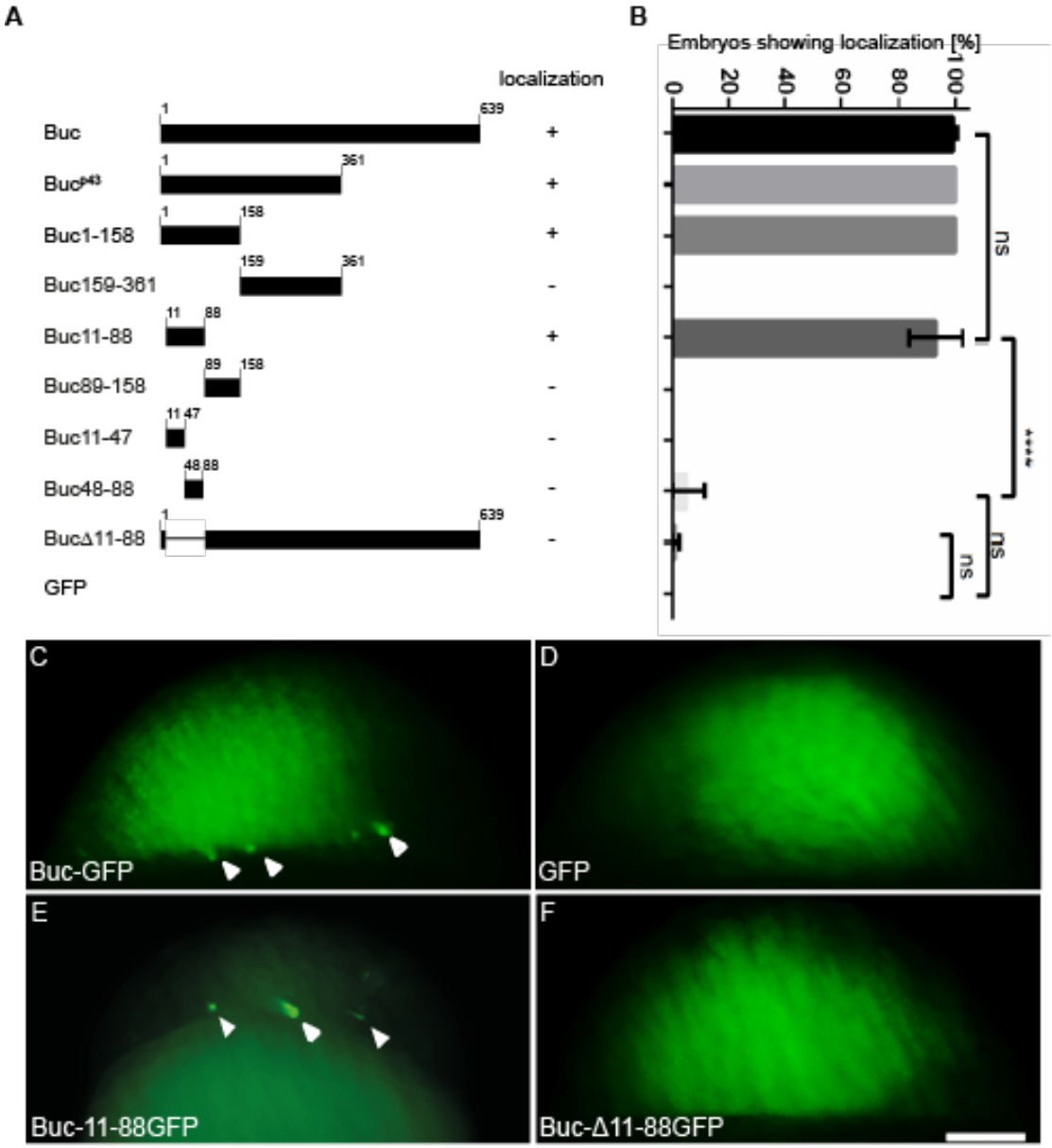

Figure 2. Buc11-88 is necessary and sufficient for Buc localization in zebrafish embryos.

In this localization assay RNA was injected into 1-cell stage embryos and scored at high stage for localization of fluorescence in living embryos as shown in Fig. 1A. (A) Schematic representation of Buc protein deletions and summary of their localization (+/-). Numbers indicate amino acids. (B) Quantification of the localization assay. Buc11-88 localized (90.9±10.1%) similarly to WT Buc (99.1±1.3%) (P=0.8). BucΔ11-88 did not localize (0.9±1.6%) compared to WT Buc (P=0.009) and Buc11-88 (P=0.01. (C-F) Blastomeres of living high stage embryos oriented as shown in Figure 1A expressing the indicated constructs. Note protein localization of Buc-GFP (D; arrowheads) or Buc11-88 (F; arrowheads), whereas a GFP-control or BucΔ11-88 show ubiquitous fluorescence (E, G). n (Buc-GFP: 98, GFP: 94, Buc-11-88GFP: 181, Buc-Δ11-88: 230). Error bars represent SD. Scale bar: 100 μm.

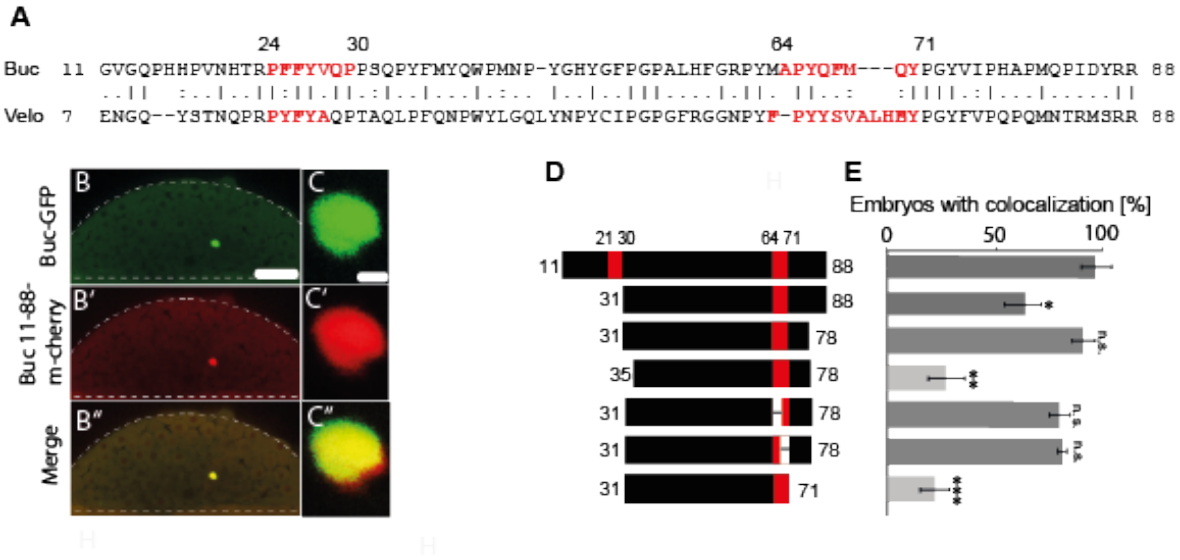

Figure 3. Aggregation and localization of BucLoc are separate activities.

(A) Alignment of Buc11-88 with the N-terminus of *Xenopus* Velo1 (aa7-88). Red letters highlight the prion-like domains previously discovered in Velo1 (Boke, 2016) and their corresponding amino acids in Buc. (B-B'', C-C'') BucLoc (11-88)-m-cherry colocalizes in transgenic embryos with endogenous Buc-GFP to the germ plasm. (B-B'') Living sphere stage transgenic Buc-GFP embryo injected at 1-cell stage with RNA encoding BucLoc-m-cherry, showing colocalization. Embryo is shown on the lateral view with the animal pole to the top, outlined by the white dashed line. (C-C'') Magnification of the localized spot of germ plasm shown in (B-B''). (D) Summary of BucLoc mapping showing that PLDs are not important for the localization of Buc. Prion-like domains are shown with red boxes. (E) Quantification of BucLoc mapping and 5aa deletions in (D). Buc31-88 (60.1± 7.9%) and Buc31- 71 (21.1± 6.4) show significantly less localization compared to Buc11- 88 (P= 0.01 and 0.0004). There was no significant difference between the localization of Buc11-88 and Buc 31-78 (P=0.41), excluding the role of the first PLD in localization. 5aa deletions of Buc31-78 showed that residues other than second PLD are important in the localization of Buc. Buc31-78 Δ 31-35 (30.0± 10) showed significantly less localization compared to Buc31- 78 (P=0.009). Colocalization of constructs in (D) is shown in Supplementary figure 7. n (Buc11-88: 30, Buc31-88: 30, Buc31-78: 30, Buc35-78: 30, Buc31-78Δ62-66: 30, Buc31-78 Δ67-71: 30, Buc31-71). Error bars represent SD. Scale bars (B): 50 µm, (C): 2 µm.

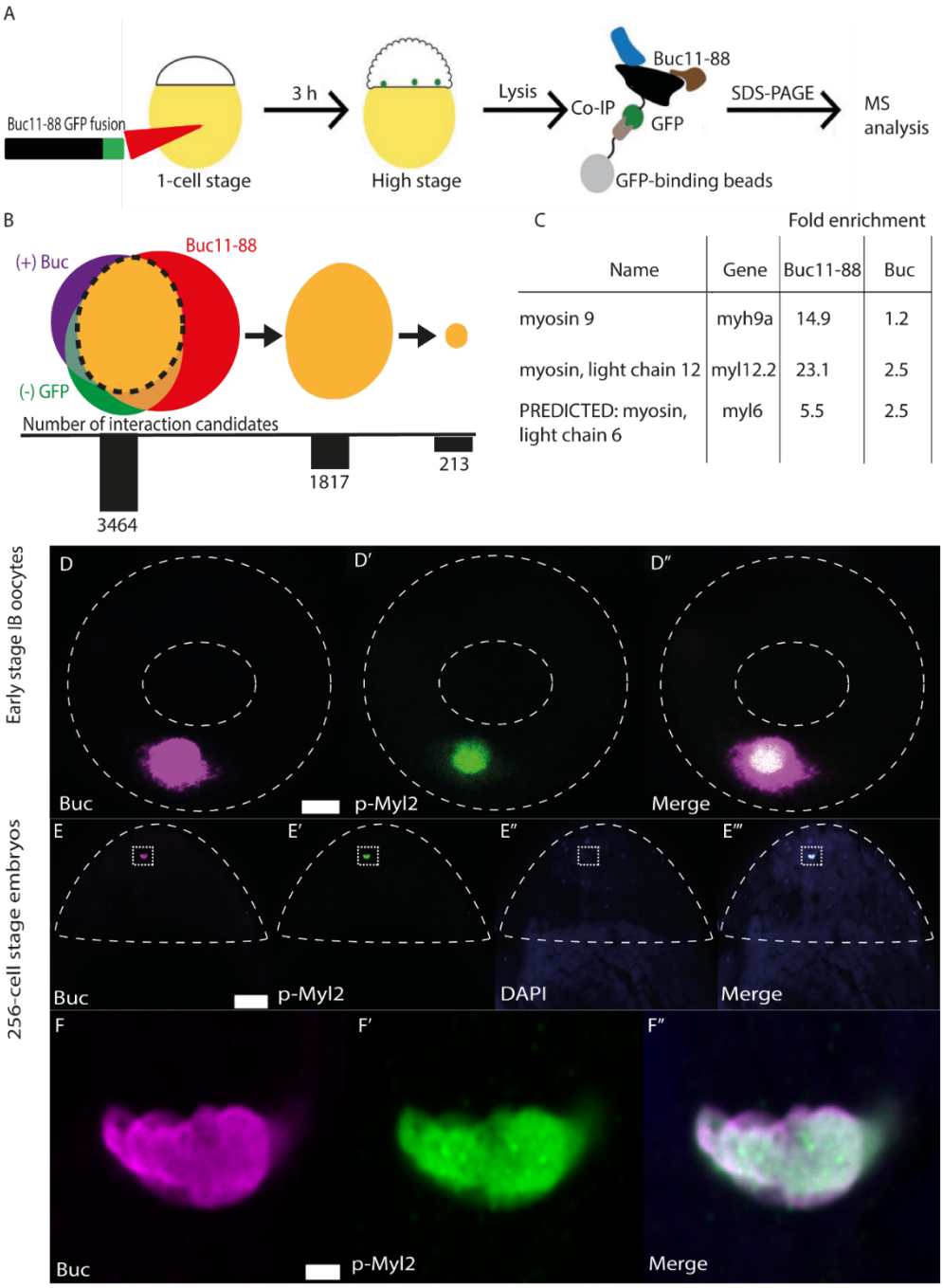

Figure 4. Non-muscle myosin II (NMII) colocalizes with Buc.

Colocalization of Bucky ball (Buc) and phosphorylated myosin light chain 2 (p-Myl2) was determined by immunostaining. (A) Schematic representation of mass spectrometry of BucLoc. Wild type embryos (n: 500) were injected with RNA encoding for BucLoc-GFP and lysed at high stage. Embryos of the transgenic Buc-GFP line were used as positive control. GFP RNA injected embryos were used as negative control. Subsequent to lysis, an IP against the GFP-tag was carried out. Interacting proteins were identified by mass spectrometry. (B) 3464 proteins were identified in the mass spectrometry, of which 1817 candidates interacted with both Buc-GFP and BucLoc-GFP and 213 specifically with BucLoc-GFP (for selection criteria see Material and Methods). (C) Fold enrichment of myosin light chain in the mass spectrometry. (D-D'') Colocalization at early stage (IB) oocyte stage. 1st column -

Buc (magenta), 2nd column – p-Myl2 (green), 3rd column - merge (white). (E-E'') Show colocalization in embryo (256 cells). 1st column - Buc (magenta), 2nd column - Myl2 (green), 3rd column - DAPI (blue) and 4th column - merge (white). (F-F'') Show magnification of germ plasm spot in E-E''. Scalebars (D-D''): 10 µm, (E-E'''): 50 µm, (F-F'''): 2 µm.

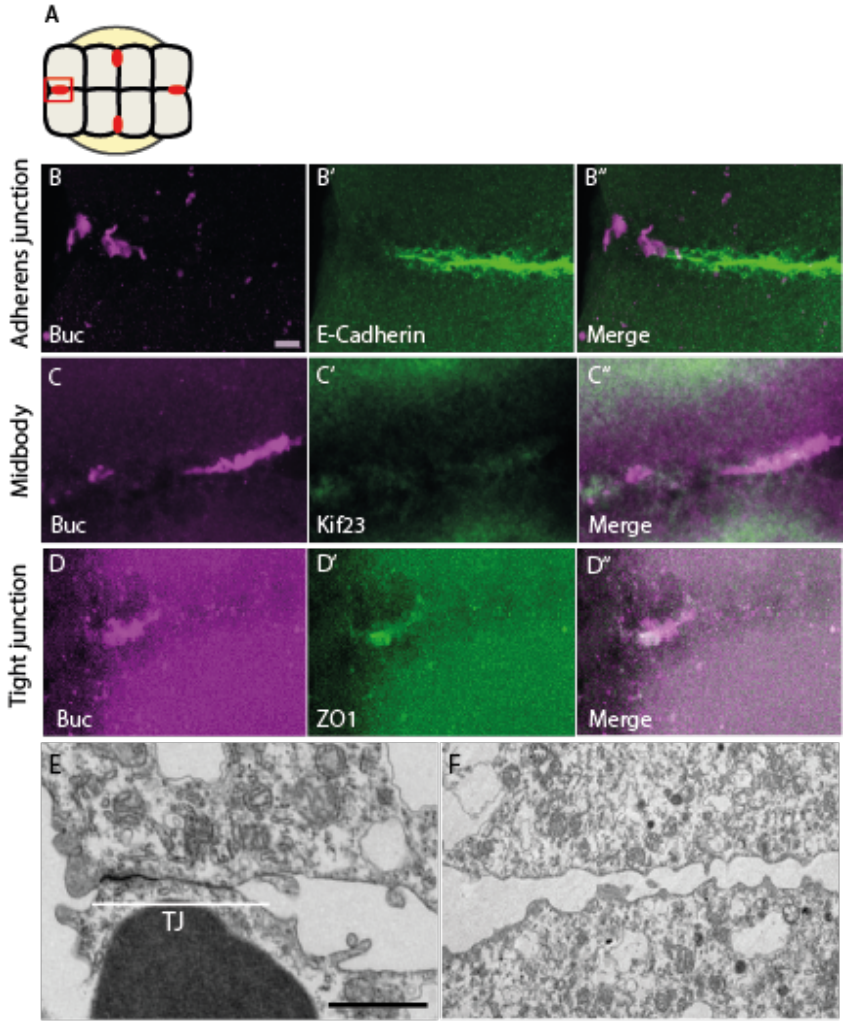

Figure 5. Buc colocalizes with TJ protein ZO1 and electron microscopy of early cleavage furrows shows TJ-like structures.

Colocalization analysis of Buc with different cellular structure markers at 8-cell stage. (A) A representative cartoon showing an 8-cell stage embryo from the animal view. The red dots show where germ plasm is localized the cleavage furrows. The cleavage furrows which do not have red dotes do not contain germ plasm. The red box represent the cleavage furrows which are shown in the following pictures. (B, C, D) Magnification of one of the cleavage furrows containing germ plasm (full embryo staining is shown in Supplementary Fig. 7). 1st column - Buc (magenta), 2nd column – respective cellular structure (green), 3rd column - merge. (B-B'') Immunostaining for Buc and adherens junction marker E-cadherin; (C-C'') Buc and midbody marker Kif23; (D-D'') Buc and tight junction marker ZO1. (E) Electron microscopy of germ plasm containing cleavage furrow. Note: TJ-like structures are observed in this cleavage furrow as shown with the upper white line but no germ plasm

granules are shown here. (F) Electron microscopy of a non-germ plasm containing cleavage furrow. Scale bars (B, C, D): 5 µm, (E, F): 1 µm.

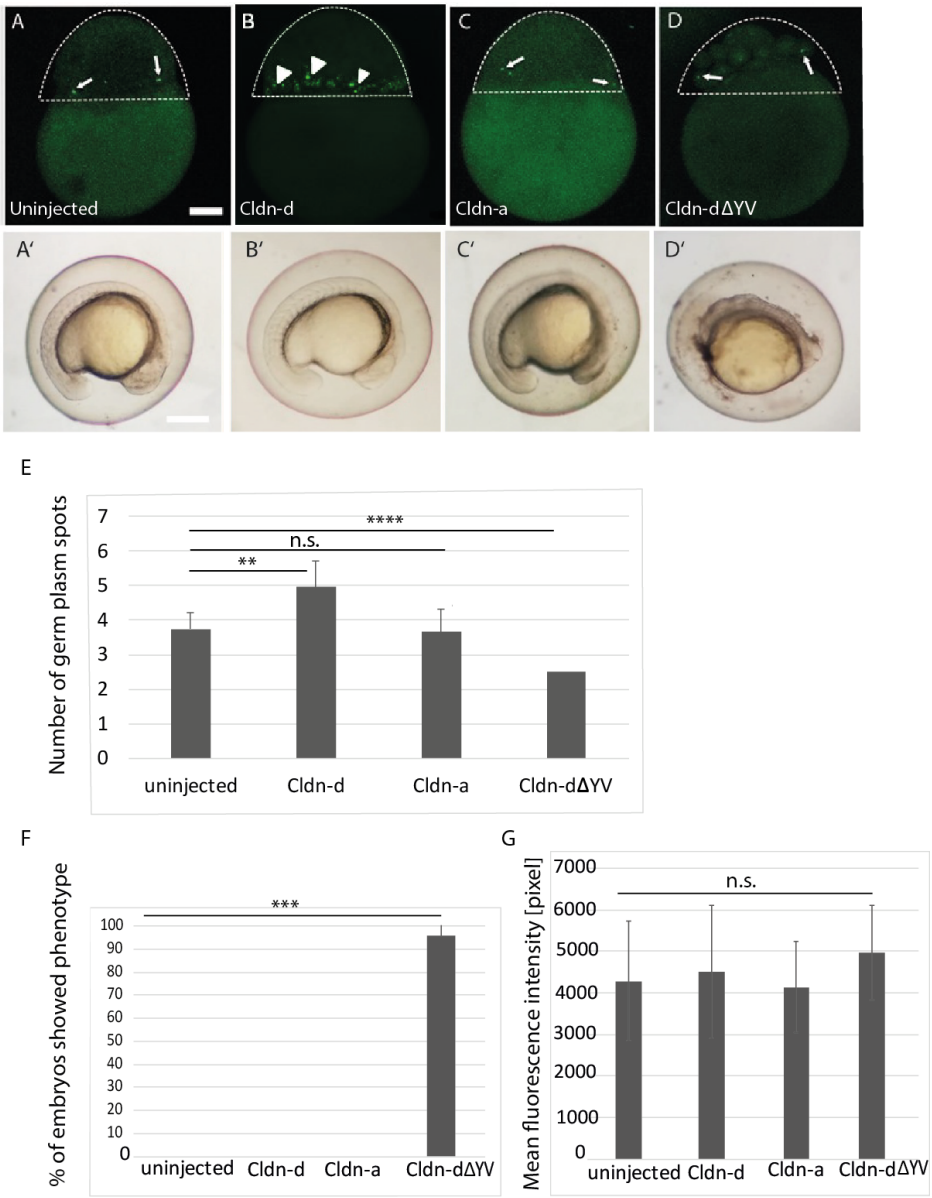

Figure 6. Cldn-d induces ectopic germ plasm foci.

Over expression of Cldn-d in zebrafish embryos at 1- cell stage. A) An uninjected embryo from Buc-GFP transgenic line at 2hpf. Buc is localized in germ plasm spots. Arrows show germ plasm spots. B) Over expression of Cldn-d produces additional germ plasm spots (arrow heads). C) Embryo injected with c*ldn-a* show no effect in comparison to control (A). D) Injection of *cldn-dΔYV* produces a strong phenotype in zebrafish embryos. One embryo is shown here which has developmental defect and its blastomers are not properly attached to each other. Germ plasm spots are shown with arrows. A'-D') Developed embryos from (A-D) at 1 dpf (day post fertilization). A') An uninjected embryo, B') A *cldn-d* injected embryo, C') a c*ldn-a* injected embryo and D') a *cldn-dΔYV* injected embryo showing developmental defects. E) Quantification of the average number of germ plasm spots in uninjected

and injected embryos. c*ldn-a* injection showed no significant difference to uninjected control (P-value: 0.3), with average number of spots (3.66 ± 0.65) and (3.74 ± 0.48), respectively. *cldn-d* injection caused a significantly higher number of germ plasm spots (4.96 ± 0.76) compared to controls (P- value: 0.004) and *cldn-dΔYV* injection resulted in significantly lower number of germ plasm spots (2.49 ± 0.62) compared to controls (P- value: 0.00003) and c*ldn-a* injected embryos (P- value: 0.0049). Note germ plasm spots in A, B, and D (arrows) and ectopic germ plasm spots in C (arrow heads). F) Quantification of total number of control and injected embryos showing defect in development. Embryos injected with c*ldn-dΔYV* showed significant developmental defect compared to uninjected and embryos injected with c*ldn-d* and *cldn-a* (P- value: 0.0003). The percentage of c*ldn-dΔYV* injected embryos that showed developmental effect was (95.8± 5.89). n (*cldn-d:* 76, *cldn-dΔYV*: 169, *cldn-a:* 86, uninjected: 161). G) Quantification of total fluorescence in injected and control embryos. No significant difference was recorded between control and *cldn-d*, *cldn-a* or *cldn-dΔYV* injected embryos (P-value: 0.5, 08 and 0.7, respectively). n (*cldn-d:* 22, *cldn-dΔYV*: 24, *cldn-a:* 18, uninjected: 21) Error bars represent SD. **: P- value ≤ 0.01, ** : P- value ≤ 0.01, *** : P- value ≤ 0.001, n.s.: non-significant. Scale bars: 50 µm.

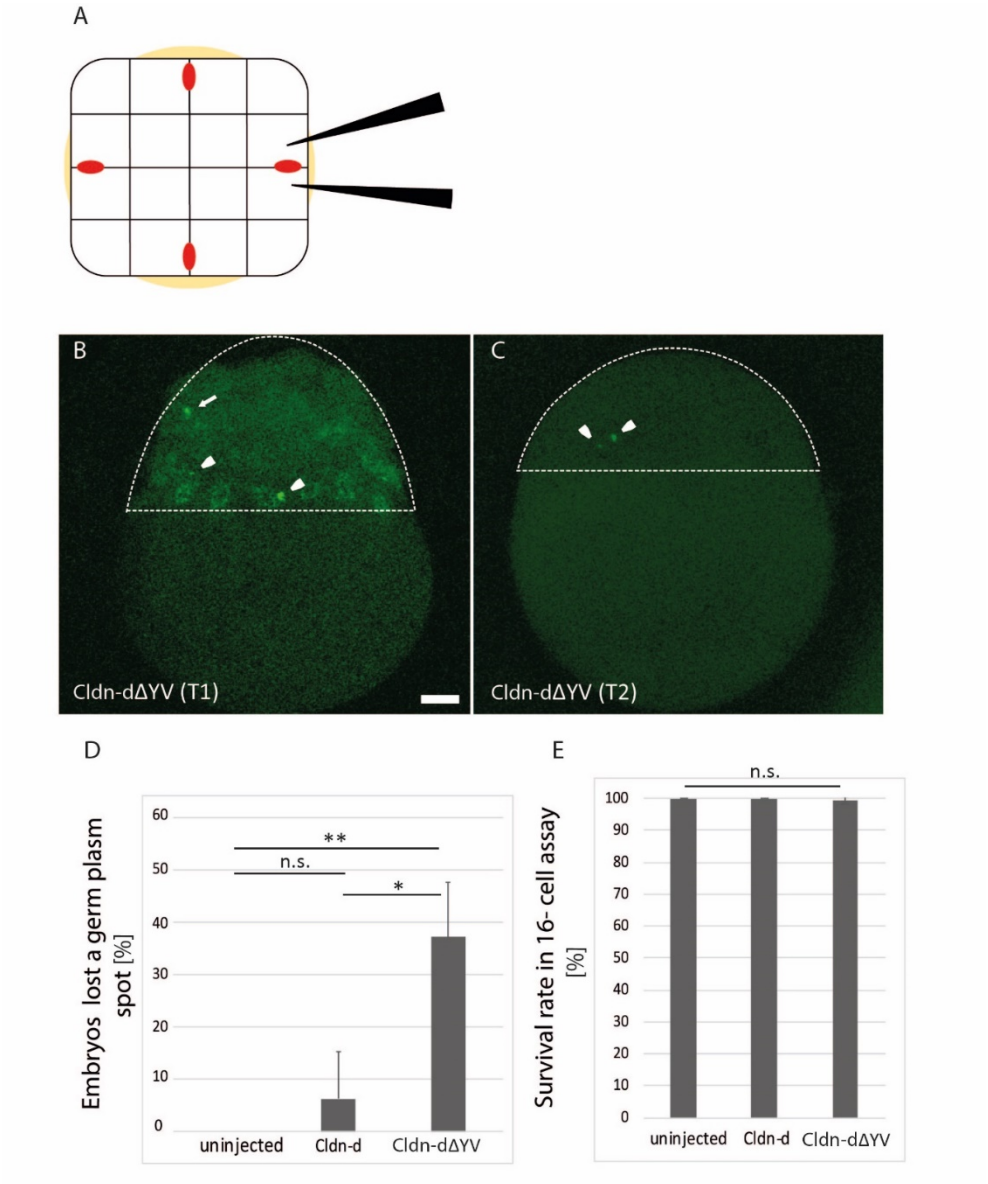

Figure 7. Cldn-dΔYV reduces the number of germ plasm spots.

A) Schematic representation of 16- cell injection assay. The embryo is shown in animal view, germ plasm is shown as red spots. Two middle blastomeres surrounding a single germ plasm spot were injected. B) A *cldn-dΔYV* injected embryo from Buc- GFP transgenic line showing 3 Buc spots in lateral view. C) The same embryo shown in B at 2 hpf. One Buc spot disappeared (white arrow in B), while the other spots are sustained (arrowheads in B and C). D) Quantification of embryos which lost a germ plasm spot. *cldn-dΔYV* injected embryos lost a germ plasm spot (35.1 ± 11.2%) which was significantly higher than *cldn-d* injected (6.12 ± 10.8%; p=0.014) or uninjected (0 ± 0.0%; p=0,0024) embryos. No significant difference was seen between Cldn-d and uninjected embryos (P-value: 0.37). E) Percentage of embryo survival rate in 16- cell assay. There was no significant difference in the survival rate between injected and control embryos (P- value: 0.43). n (*cldn-d:* 49, *cldn-dΔYV*: 94, uninjected: 57) (see supplementary table 2). Error bars represent SD. *** : P- value ≤ 0.01, ** : P- value ≤ 0.01, *, n.s.: non-significant. Scale bar: 50 µm.

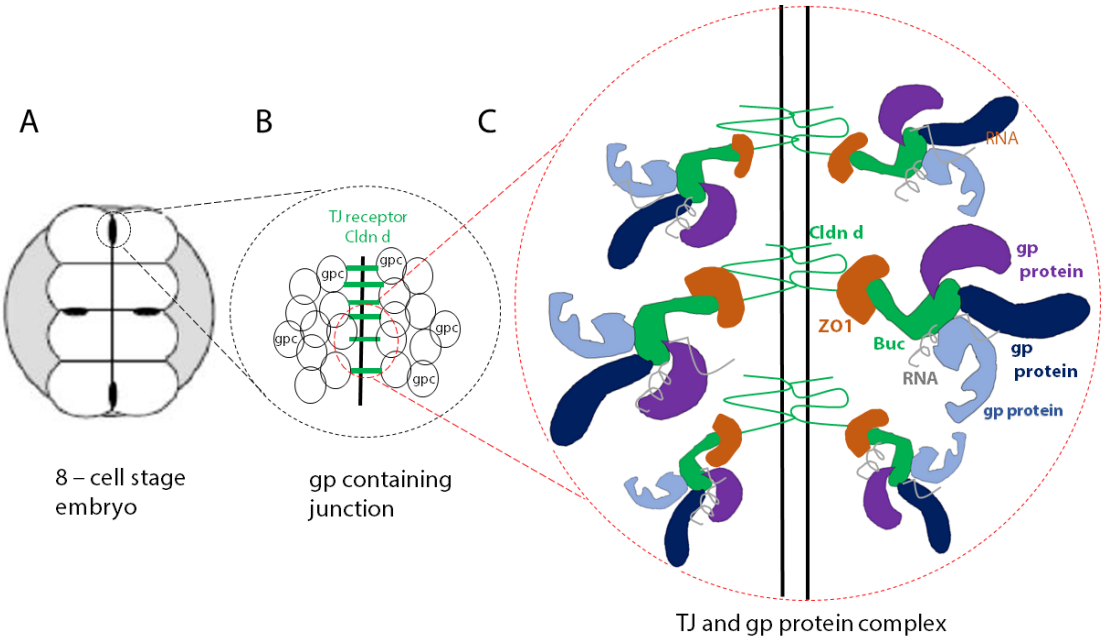

Figure 8. Proposed model for germ plasm localization in zebrafish.

TJs anchor germ plasm at early cleavage furrows in zebrafish embryos. A) Schematic representation of a zebrafish embryo at 8-cell stage. Germ plasm is shown in four black spots. B) Magnification of a germ plasm spot from the embryo in (A). Complex containing germ plasm and TJ proteins (gpc) are anchored to the cleavage furrows by the TJ receptor Cldn-d (green). C) Representative magnification of the dashed red circle in (B). Buc in a complex with other germ plasm (gp) proteins and RNA interacts with the C-terminal end of Cldn-d. Note that it is currently not known whether Buc binds directly to ZO1.

Supplementary data

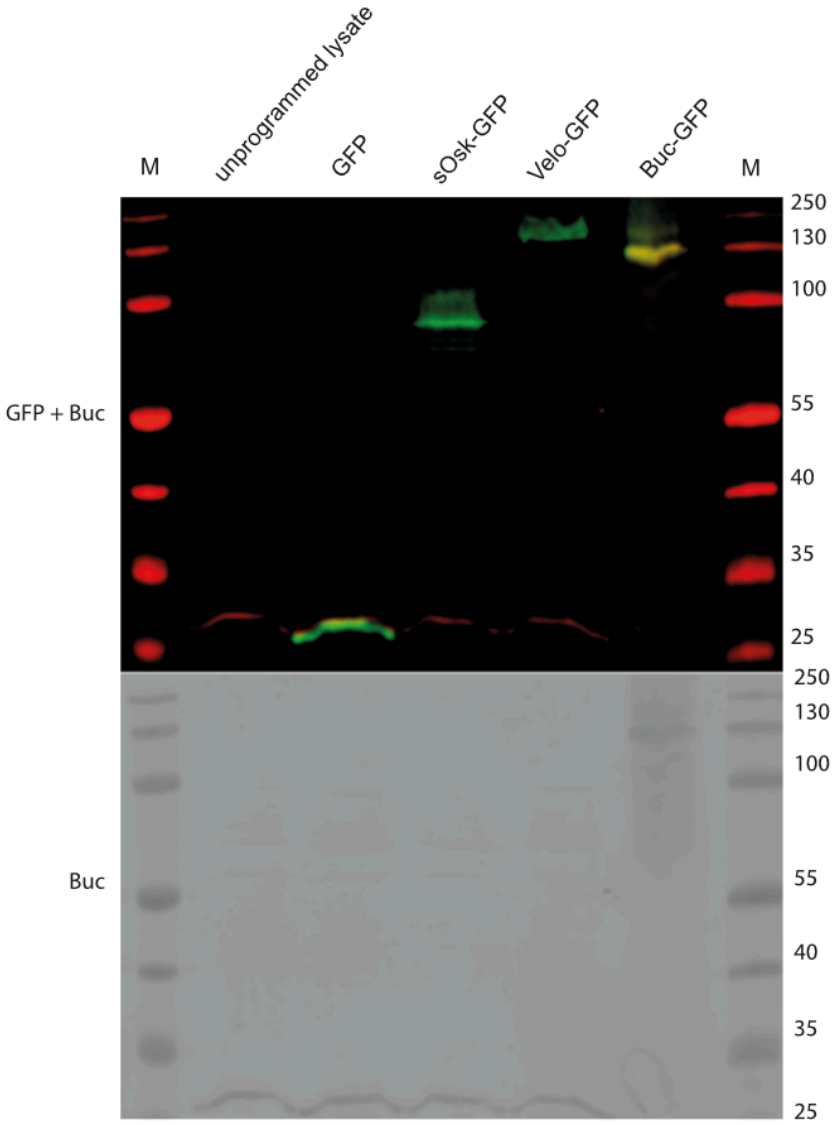

Supplementary figure 1. The Buc antibody does not cross-react with GFP, *Xenopus* Velo or *Drosophila* Oskar.

Western blot showing anti-Buc (red in upper panel and black in lower panel) or anti-GFP (green in upper panel) antibody staining of *in vitro* translated GFP, sOsk-GFP, Velo-GFP and Buc-GFP. Unprogrammed lysate was used as negative control for protein translation. Buc-GFP is visualized by both anti-Buc and anti-GFP antibodies (yellow in merged panel and black in lower panel), whereas Velo-GFP, sOsk-GFP and GFP are only recognized by anti-GFP antibody, but not by anti-Buc antibody.

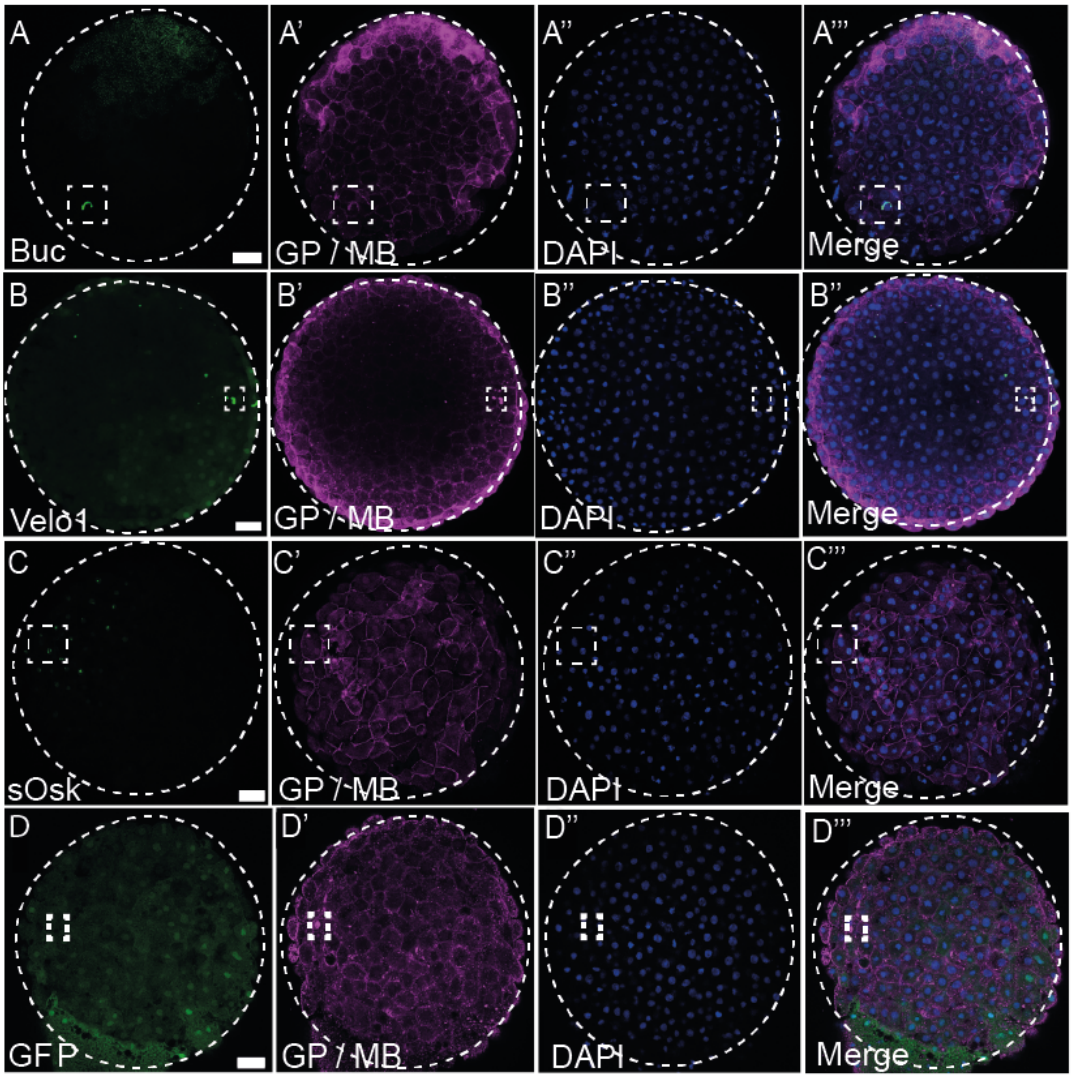

Supplementary figure 2. Germ plasm localization is conserved in vertebrates.

Panels (A,B,C,D) show embryos at high stage from the animal view. Dotted circles outline the embryos. Dotted rectangles show magnified areas in figure 1. Colocalization of the GFP with endogenous Buc was determined by immunohistochemistry: 1st column – injected GFP fusions (green), 2nd column – endogenous Buc and beta-catenin (magenta), 3rd column – DAPI (blue) and 4th column – merge. Buc-GFP (A-A''') and *Xenopus* Velo1 (B-B''') colocalize with endogenous germ plasm, whereas *Drosophila* Osk(C-C''') shows nuclear localization. The GFP control shows ubiquitous low level fluorescence (D-D'''). Scalebars: 50 µm.

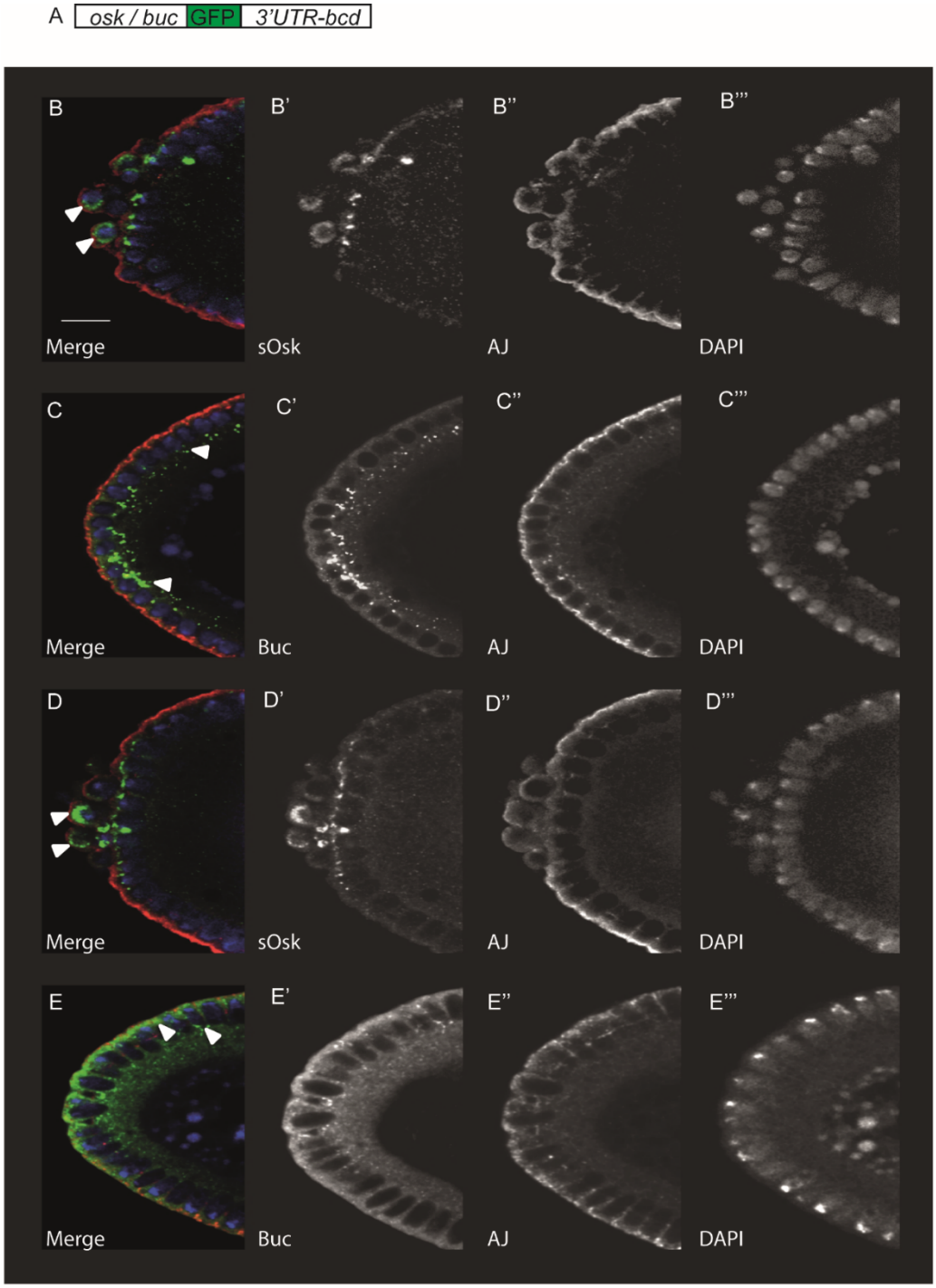

Supplementary figure 3. Transgenic Buc- and Oskar-GFP Drosophila embryos show different localization patterns.

A) Scheme of transgenes to study Bucky ball (Buc) and short Oskar (sOsk) localization. Transgenic flies were generated expressing Buc-GFP or sOsk ectopically at the anterior pole of the embryo by fusion of the constructs to the *bicoid* 3'UTR. (B-E) Localization of sOsk and Buc-GFP was investigated by immunohistochemistry: 1st column – merge, 2nd column –expressed protein, 3rd column – apical junctions (AJ), 4th column – DAPI. Anterior pole of immunostained embryos expressing the indicated transgenic constructs at stage 4 (B, C) and 5 (D, E). sOsk (B, B', D, D') localizes in condensed aggregates

at the most distal part of the anterior pole (white arrowheads), whereas Buc-GFP (C, C', E, E') distributes in a gradient along the cortex of the anterior pole (white arrowheads). Scale bar: 10 µm.

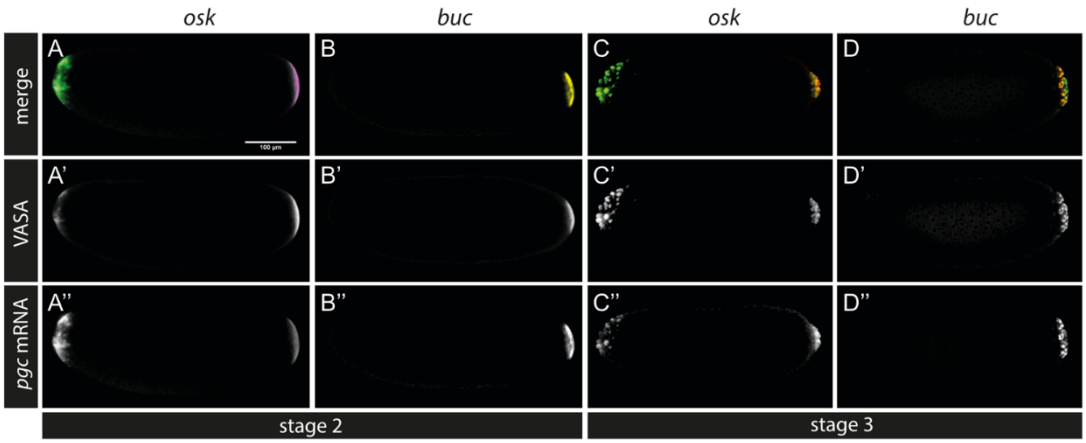

Supplementary figure 4. Vasa protein and pgc mRNA recruitment in transgenic flies.

Vasa protein and *pgc* mRNA labeling of the transgenic embryos showed that sOsk specified ectopic PGCs, whereas Buc transgenics did not recruit Vasa protein or *pgc* mRNA at the anterior pole. (A-A'' , B-B'') show VASA and *pgc* labeling of sOsk and Buc in stage2 transgenic flies. (C-C'' , D-D'') show VASA and *pgc* labeling of sOsk and Buc in stage3 transgenic flies. Scale bar: 100 µm.

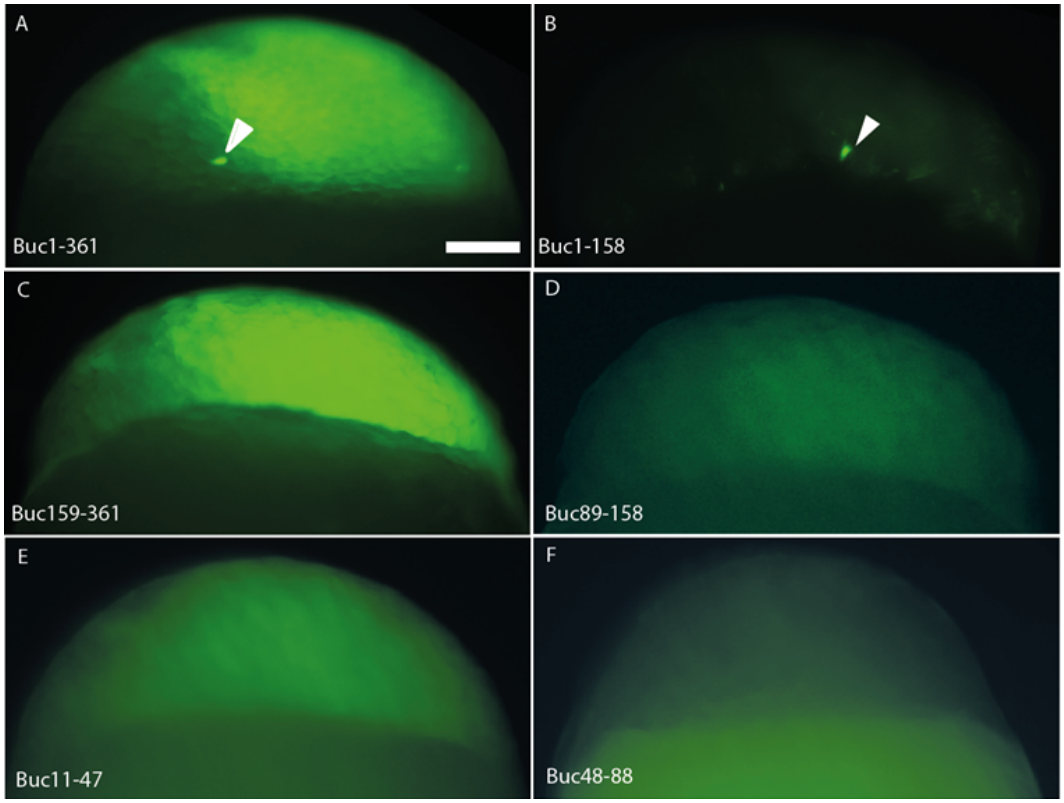

Supplementary figure 5. Systematic mapping of Buc localization motif.

(A) N-terminal fragment of Buc (aa1-361) (white arrowhead) (100%). (B) Buc1-158 localizes (white arrowhead) (100%). (C) Buc159-361 is ubiquitous (0%). (D) Buc89-158 is ubiquitous (0%). (E) Buc11-47 is ubiquitous (0%). (F) Buc48-88 is ubiquitous (6.0±6.7%). Scale bar: 50 µm

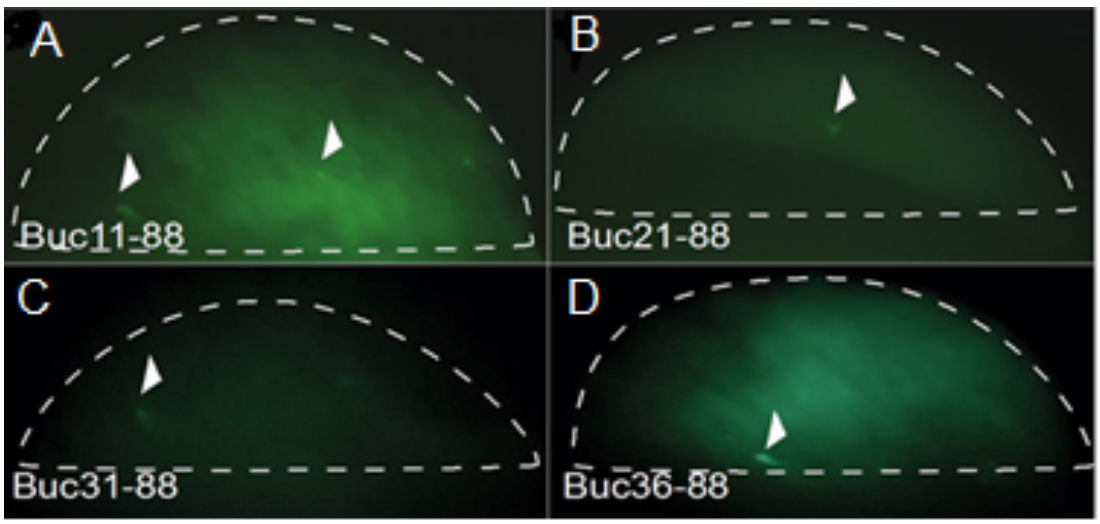

Supplementary figure 6. Aggregation and localization of BucLoc are separate activities.

(A-D) Show embryos at high stage from the lateral view. Embryos are outlined by the dashed white line. Injected constructs showed fluorescent aggregates (white arrowheads). (A) Buc11-88 (91.4±6.8%). (B) Buc21-88 (67±4.0%). (C) Buc31-88 (60.1±7.9%). (D) Buc36-88 (52.2±13).

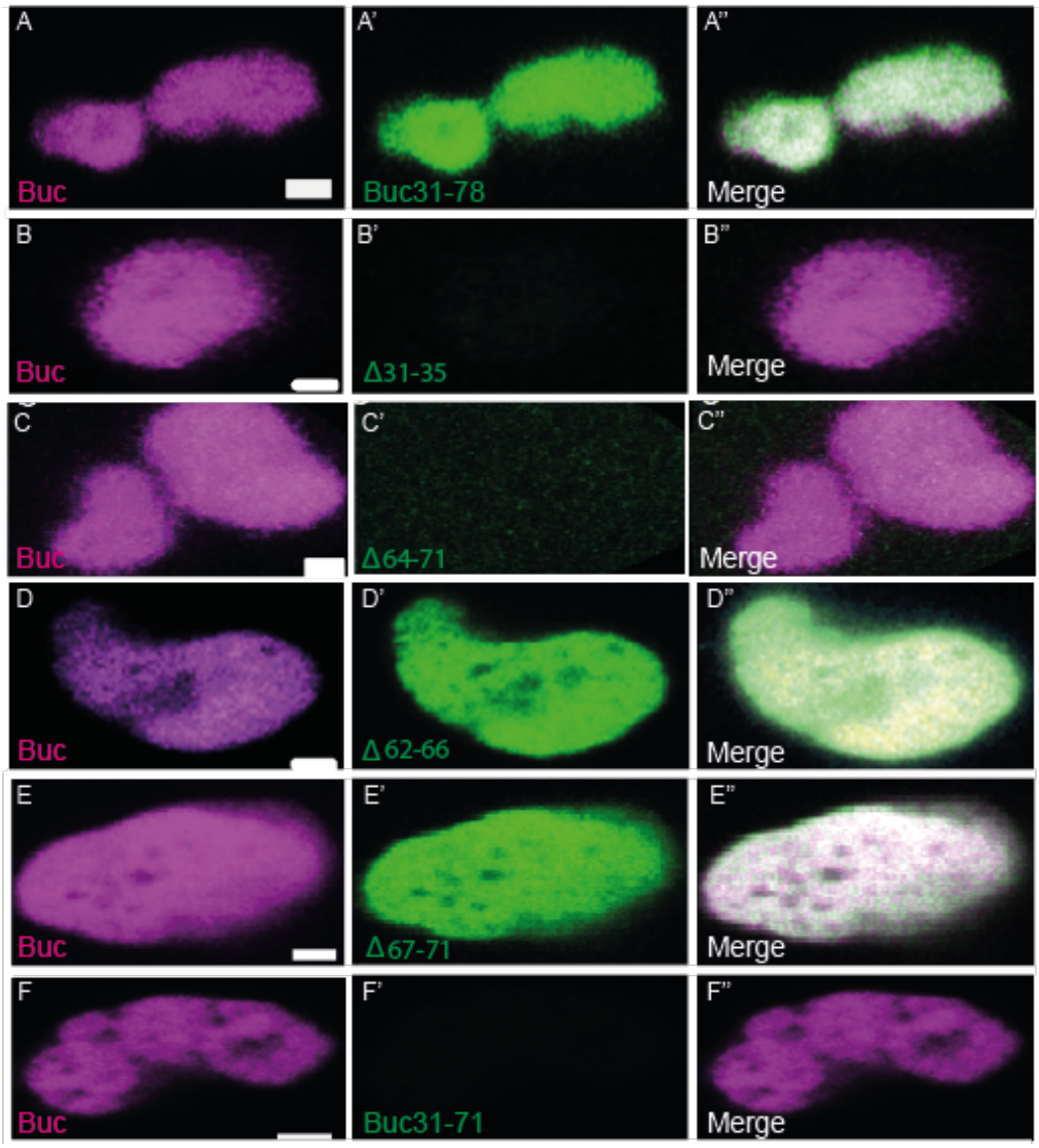

Supplementary figure 7. Colocalization of deletion constructs of BucLoc mapping in Figure 5 with Buc-GFP.

(A-A'') shows colocalization of transgenic Buc-GFP (magneta) and BucLoc-m-cherry fusion (aa31-78) (green). (B-B'') Shows colocalization of transgenic Buc-GFP (magneta) and Buc31-78 (Δ 31-35)-m-cherry fusion (green). (C-C'') Shows colocalization of transgenic Buc-GFP (magneta) and Buc31-78 (Δ 64-71)-m-cherry fusion (green). (D-D'') Shows colocalization of transgenic Buc-GFP (magneta) and Buc31-78 (Δ 62-66)-m-cherry fusion (green). (E-E'') Shows colocalization of transgenic Buc-GFP (magneta) and Buc31-78 (Δ67-71)-m-cherry fusion (green). (F-F'') Shows colocalization of transgenic Buc-GFP (magneta) and Buc31-71-m-cherry fusion (green). Embryos were injected at 1-cell stage with RNA encoding BucLoc-m-cherry fusions and imaged at high stage. The pictures are representing magnified germ plasm spots. Scale bars: 2 µm.

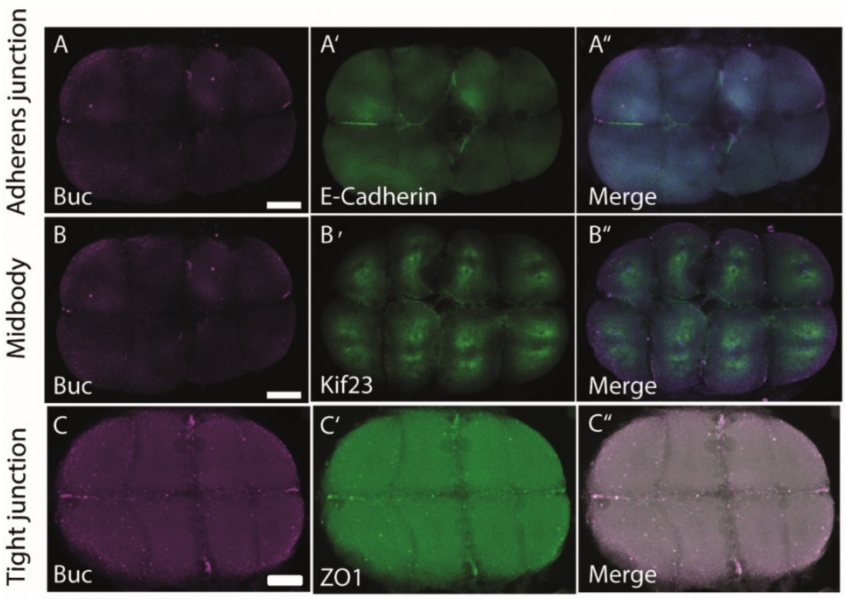

Supplementary figure 8. Tight junction protein ZO1 colocalizes with Buc.

Colocalization analysis of Buc with different cellular structure markers. (A, B, C) Show animal view of immunostained 8-cell stage embryos 1st column - Buc (magenta), 2nd column – respective cellular structure (green), 3rd column – merge. (A-A'') Immunostaining for Buc and adherens junction marker E-cadherin; (B-B'') Buc and midbody marker Kif23; (C-C'') Buc and tight junction marker Zonula occludens 1 (ZO1). Scale bars: 50 µm.

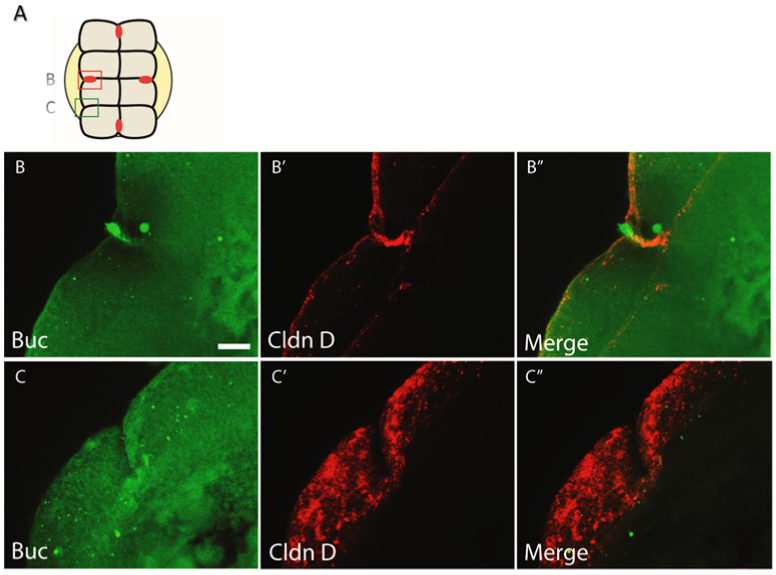

Supplementary figure 9. Immunostaining shows colocalization of Buc and *cldn-d*.

Zebrafish embryo at 8- cell stage was double stained with Buc and Cldn-d antibodies and their colocalization was analysed using confocal microscopy. A) A representative cartoon showing an embryo at 8- cell stage. (B-B'') Colocalization of Buc and Cldn-d at the middle cleavage furrow (the upper red rectangle in A). (C-C'') Localization of Buc and Cldn-d at the lower cleavage furrow (the lower green rectangle in A). Scale bar: 10 µm.

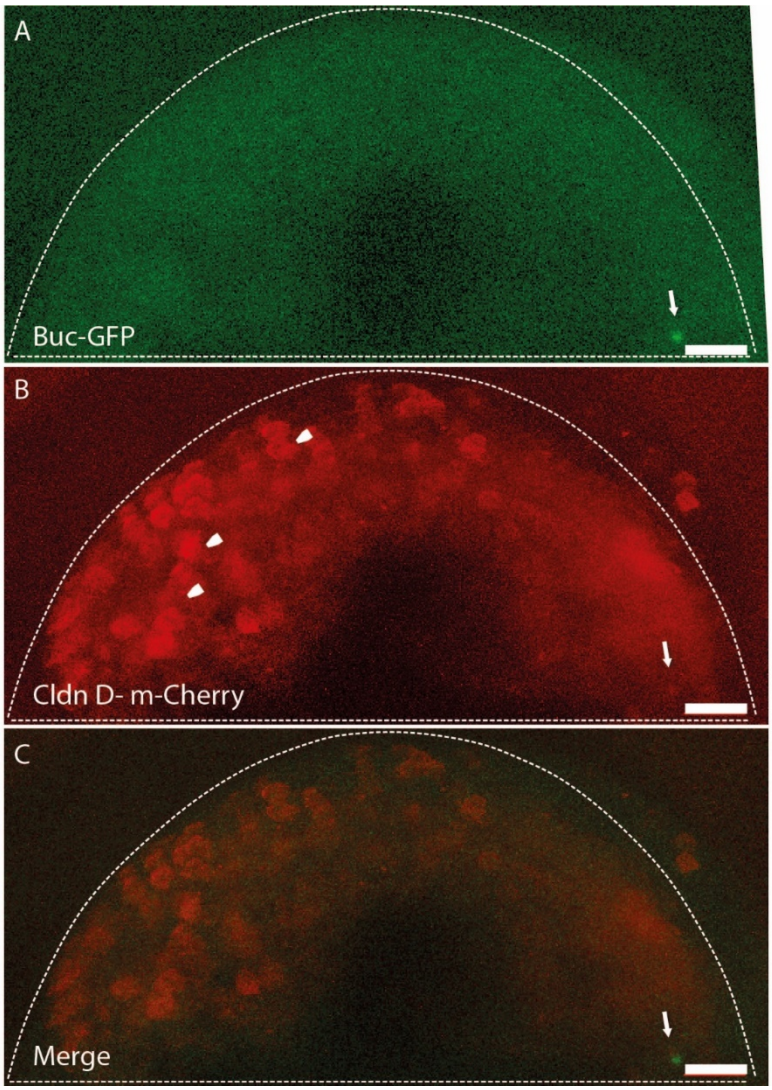

Supplementary figure 10. Overexpression of Cldn-d shows colocalization of Buc and *cldn-d*.

Cldn-d- m-Cherry RNA was injected into 1-cell stage embryos from Buc-GFP transgenic line and their colocalization was analysed using confocal microscopy. A) Embryo is shown from the lateral view approximately at 2 hpf, outlined by the white dashed line. The arrow shows Buc-GFP aggregate (Green). B) Expression of *cldn-d* (Red). Note the ubiquitous expression of m-Cherry signal and at the same time its colocalization with Buc (white arrow). C) Merge of A and B. Scale bar: 50 µm.

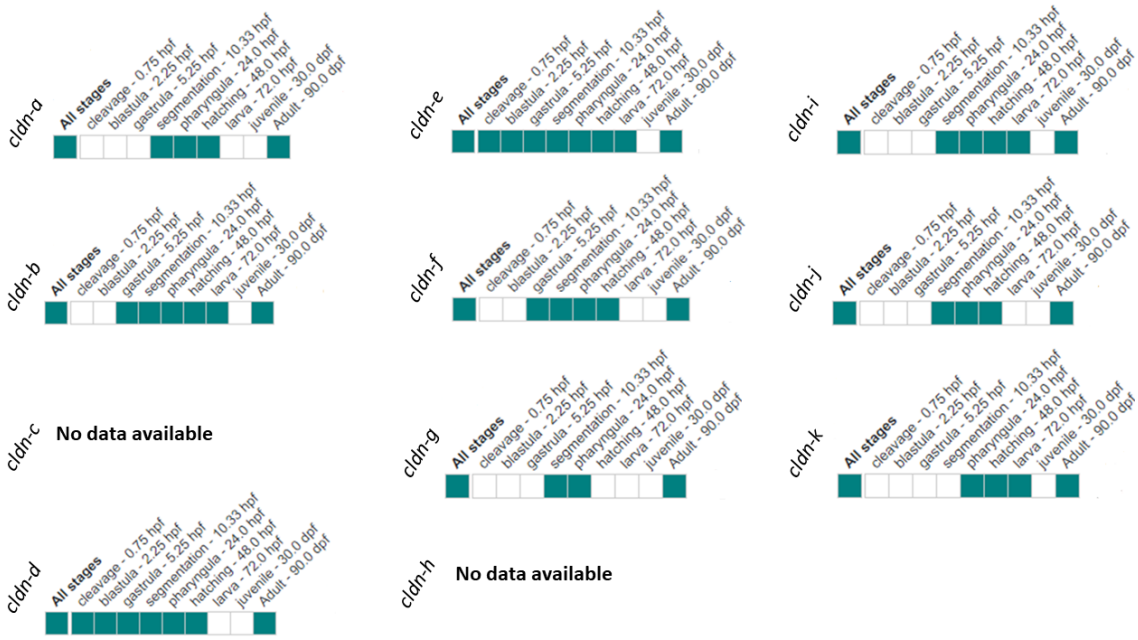

Supplementary figure 11. Expression data of zebrafish cldns available on https://zfin.org/.

Expression of cldns at different developmental stages is shown in zebrafish. The green boxes represent annotated expression and the white boxes show no expression. Note only cldn-d and cldn-e showed expression at early developmental stages. The data is updated as on (date February 28th, 2021).

Supplementary table 1. 213 BucLoc interaction candidates selected from 3464 proteins identified by mass spectrometry analysis.

Identified Protein	Accession Number	GFP Co-IP	Buc-GFP Co-IP	BucLoc-GFP Co-IP
PREDICTED: protein PRRC2C [Danio rerio]	gi|528511146	79.6	1278.6	817.9
PREDICTED: zinc finger protein 318-like isoform X1 [Danio rerio]	gi|528497145	12.4	666.7	512.8
Cluster of PREDICTED: protein PRRC2B isoform X4 [Danio rerio] (gi|528481247)	gi|528481247 [2]	22.6	480.1	320.0
large proline-rich protein BAT2 [Danio rerio]	gi|319738640 (+2)	71.6	362.1	280.0
PREDICTED: msx2-interacting protein isoform X1 [Danio rerio]	gi|326678004 (+2)	63.3	434.0	257.4

PREDICTED: microtubule-actin cross-linking factor 1, isoforms 1/2/3/5 isoform X1 [Danio rerio]	gi|528510265	0.0	546.5	218.8
uncharacterized protein LOC792544 [Danio rerio]	gi|194353937	15.8	83.1	201.9
Cluster of PREDICTED: OTU domain-containing protein 4 isoformX1 [Danio rerio] (gi|528518829)	gi|528518829 [2]	83.8	417.6	189.9
PREDICTED: YLP motif-containing protein 1 isoform X2 [Danio rerio]	gi|528511017	36.9	232.6	185.5
PREDICTED: symplekin isoform X2 [Danio rerio]	gi|326668188 (+1)	52.9	218.7	184.5
PREDICTED: microtubule-associated protein futsch-like [Danio rerio]	gi|528497151	1.7	123.8	181.0
retinoblastoma-binding protein 6 isoform 1 [Danio rerio]	gi|302632528 (+4)	13.0	75.0	159.1
Cluster of PREDICTED: membrane-associated guanylate kinase, WW and PDZ domain-containing protein 1 [Danio rerio] (gi|528488944)	gi|528488944 [4]	62.6	191.7	157.7
guanine nucleotide-binding protein subunit beta-2-like 1 [Danio rerio]	gi|18859301	53.1	208.3	149.1
PREDICTED: uncharacterized protein LOC767754 isoform X1 [Danio rerio]	gi|528467168 (+2)	45.1	104.3	134.7
Cluster of eukaryotic translation initiation factor 4A, isoform 1A [Danio rerio] (gi|38198643)	gi|38198643 [3]	43.2	230.2	127.8
PERQ amino acid-rich with GYF domain-containing protein 2 [Danio rerio]	gi|71834468	55.0	261.2	123.5
Cluster of zinc finger CCCH domain-containing protein 13 [Danio rerio] (gi|319738618)	gi|319738618	39.2	118.6	120.6
Cluster of PREDICTED: cell cycle associated protein 1b isoform X1 [Danio rerio] (gi|528508316)	gi|528508316 [3]	39.1	262.3	117.6

Cluster of PREDICTED: eukaryotic translation initiation factor 4E transporter isoform X1 [Danio rerio] (gi|528482894)	gi|528482894 [2]	6.5	204.5	114.7
PREDICTED: cytoskeleton-associated protein 5 isoform X1 [Danio rerio]	gi|528520895	2.9	71.0	110.6
regulation of nuclear pre-mRNA domain containing 2a [Danio rerio]	gi|41053979	0.0	65.7	96.8
Cluster of LIM domain only 7b [Danio rerio] (gi|319996634)	gi|319996634 [2]	5.5	182.2	89.9
GPI-anchored membrane protein 1 [Danio rerio]	gi|51011059	17.0	206.9	89.8
PREDICTED: trinucleotide repeat-containing gene 6B protein [Danio rerio]	gi|528495941	0.0	130.1	84.6
Cluster of glutathione S-transferase pi [Danio rerio] (gi|18858197)	gi|18858197	7.1	32.3	82.7
Cluster of PREDICTED: pyrroline-5-carboxylate reductase isoform X1 [Danio rerio] (gi|528495079)	gi|528495079 [2]	28.1	108.1	81.0
ATP synthase subunit O, mitochondrial [Danio rerio]	gi|51467909	4.7	21.0	76.8
pre-mRNA cleavage complex 2 protein Pcf11 [Danio rerio]	gi|55925534	0.9	100.4	75.3
PREDICTED: DNA-directed RNA polymerase II subunit RPB1 isoform X2 [Danio rerio]	gi|528496057 (+1)	0.0	58.5	72.8
Cluster of ataxin-2 [Danio rerio] (gi|190358425)	gi|190358425 [2]	30.9	149.0	70.6
5'-3' exoribonuclease 1 [Danio rerio]	gi|289577074 (+1)	1.4	114.6	65.5
voltage-dependent anion-selective channel protein 2 [Danio rerio]	gi|41054601 (+1)	16.5	33.7	65.5
Cluster of splicing factor 45 [Danio rerio] (gi|41055474)	gi|41055474 [2]	13.5	132.2	57.6
voltage-dependent anion-selective channel protein 1 [Danio rerio]	gi|47777306	17.5	42.1	57.0

PREDICTED: protein FAM208A [Danio rerio]	gi|528517763	1.9	70.5	54.5
single-stranded DNA-binding protein, mitochondrial [Danio rerio]	gi|62955585	11.5	24.0	54.4
PREDICTED: tyrosine 3-monooxygenase/tryptophan 5-monooxygenase activation protein, zeta polypeptide isoform X1 [Danio rerio]	gi|528509453	3.6	13.6	53.7
non-POU domain-containing octamer-binding protein [Danio rerio]	gi|42415509	23.4	96.3	52.9
Cluster of PREDICTED: fish-egg lectin isoform X1 [Danio rerio] (gi|528491480)	gi|528491480 [5]	7.2	64.2	52.2
alpha-2-macroglobulin-like precursor [Danio rerio]	gi|320118891	0.0	17.3	50.3
Cluster of PREDICTED: chromodomain helicase DNA binding protein 4 isoform X1 [Danio rerio] (gi|528509046)	gi|528509046 [4]	1.7	30.1	49.5
14-3-3 protein epsilon [Danio rerio]	gi|47086819	4.6	12.4	47.8
Cluster of uncharacterized protein LOC100141336 precursor [Danio rerio] (gi|168823478)	gi|168823478 [5]	11.2	41.2	47.5
PREDICTED: protein SCAF11 isoform X1 [Danio rerio]	gi|528475676 (+2)	0.9	52.1	45.5
PREDICTED: cytoplasmic dynein 2 heavy chain 1-like, partial [Danio rerio]	gi|528502710	20.8	42.4	44.2
Cluster of PREDICTED: pericentriolar material 1 protein isoform X7 [Danio rerio] (gi|528467744)	gi|528467744 [3]	1.7	12.9	44.1
alpha-2-macroglobulin-like [Danio rerio]	gi|319655740 (+2)	2.9	18.7	43.1
PREDICTED: ubiquitin carboxyl-terminal hydrolase 10 isoformX1 [Danio rerio]	gi|326669691	1.0	138.2	42.9

PREDICTED: cleavage stimulation factor subunit 2-like isoform X1 [Danio rerio]	gi|326673799	11.3	86.7	40.3
Cluster of PREDICTED: alpha-2-macroglobulin isoformX1 [Danio rerio] (gi|326665588)	gi|326665588 [2]	8.9	60.0	39.8
PREDICTED: eukaryotic translation initiation factor 4 gamma 3 [Danio rerio]	gi|528517986	3.0	151.5	39.8
Ndufa9 protein [Danio rerio]	gi|157423514 (+2)	9.6	22.4	39.6
Zgc:158157 protein [Danio rerio]	gi|55250357	0.0	63.4	39.5
Cluster of myosin light chain alkali, smooth-muscle isoform [Danio rerio] (gi|47174755)	gi|47174755 [6]	8.7	17.3	39.1
Cluster of PREDICTED: uncharacterized protein LOC100000125 isoform X2 [Danio rerio] (gi|528510415)	gi|528510415 [3]	6.1	103.3	38.8
signal-induced proliferation-associated 1-like protein 1 [Danio rerio]	gi|529250122	2.8	31.4	38.7
eukaryotic translation initiation factor 4E-1B [Danio rerio]	gi|18858611	11.8	92.6	37.4
Cyc1 protein [Danio rerio]	gi|51327354 (+1)	11.5	32.9	35.8
complement component 1 Q subcomponent-binding protein, mitochondrial [Danio rerio]	gi|324021711 (+1)	9.0	19.2	35.8
LOC449616 protein [Danio rerio]	gi|213624848 (+2)	0.0	92.5	35.8
PREDICTED: cyclin-dependent kinase 13 [Danio rerio]	gi|326679472	5.8	67.7	33.7
Cluster of CWF19-like protein 2 [Danio rerio] (gi|76253886)	gi|76253886 [2]	0.0	28.5	32.6
nanog homeobox [Danio rerio]	gi|528505177 (+1)	3.9	60.8	32.4
PREDICTED: zinc finger CCCH domain-containing protein 4-like isoform X1 [Danio rerio]	gi|528501822	0.0	18.3	31.6

Cluster of PREDICTED: unconventional myosin-Va [Danio rerio] (gi|326680074)	gi|326680074 [4]	3.7	20.9	31.4
PREDICTED: protein FAM208A-like [Danio rerio]	gi|528516938	0.0	23.0	31.2
glutamate dehydrogenase 1b [Danio rerio]	gi|41282194	0.0	27.4	31.0
S-phase kinase-associated protein 1 [Danio rerio]	gi|41152201	14.5	29.8	30.8
PREDICTED: tyrosine-protein phosphatase non-receptor type 13 isoform X1 [Danio rerio]	gi|528513092 (+4)	6.4	107.4	30.7
Cluster of ADP-ribosylation factor 1 like [Danio rerio] (gi|41393117)	gi|41393117 [2]	0.0	11.2	30.1
Si:dkey-16k6.1 protein [Danio rerio]	gi|45767805 (+1)	2.4	7.8	29.8
Cluster of ras homolog gene family, member Ad [Danio rerio] (gi|50539958)	gi|50539958 [3]	1.2	16.1	29.4
tight junction protein ZO-2 isoform 1 [Danio rerio]	gi|320118869 (+2)	0.0	13.5	29.2
Cluster of uncharacterized protein LOC569235 precursor [Danio rerio] (gi|350536793)	gi|350536793 [3]	13.0	42.7	29.2
ATP-dependent RNA helicase DDX42 [Danio rerio]	gi|302318882	0.0	73.3	27.9
Cluster of PREDICTED: hypothetical protein LOC565404 [Danio rerio] (gi|189517232)	gi|189517232 [5]	6.7	58.2	27.5
PREDICTED: telomerase-binding protein EST1A-like isoform X1 [Danio rerio]	gi|326671361 (+1)	0.0	90.3	27.4
PREDICTED: ATP synthase subunit b, mitochondrial isoform X1 [Danio rerio]	gi|528487650 (+1)	3.5	9.1	27.1
mitochondrial import inner membrane translocase subunit Tim13 [Danio rerio]	gi|50539998	0.0	10.2	26.9
PREDICTED: RNA-binding protein 27 isoform X2 [Danio rerio]	gi|528491090 (+1)	5.8	32.9	26.7

PREDICTED: nudC domain-containing protein 1 isoform X1 [Danio rerio]	gi|528509803	2.7	11.2	26.6
regulation of nuclear pre-mRNA domain-containing protein 1B [Danio rerio]	gi|41054665 (+3)	0.0	63.3	25.4
nuclear pore complex protein Nup133 [Danio rerio]	gi|47087231	0.0	8.9	25.1
PREDICTED: RNA-binding protein 6 isoform X1 [Danio rerio]	gi|528483145	0.0	25.4	24.6
Cluster of PREDICTED: RNA-binding protein 26 [Danio rerio] (gi|528481486)	gi|528481486 [2]	2.5	30.2	24.6
glutamate dehydrogenase 1a [Danio rerio]	gi|47086875	0.0	11.1	24.5
Cluster of Bub3 protein [Danio rerio] (gi|53734038)	gi|53734038 [2]	3.2	16.2	23.8
Cluster of PREDICTED: cat eye syndrome critical region protein 2 isoform X2 [Danio rerio] (gi|528521383)	gi|528521383 [2]	0.0	46.3	23.6
LYR motif-containing protein 4 [Danio rerio]	gi|256000753	0.0	7.7	23.4
mitochondrial inner membrane protein [Danio rerio]	gi|47777298 (+1)	3.5	15.4	22.5
Abcf2 protein [Danio rerio]	gi|42542861 (+1)	7.3	27.2	22.5
DNA-directed RNA polymerase II subunit RPB2 [Danio rerio]	gi|302488402	0.0	33.2	22.5
Cluster of SNW domain-containing protein 1 [Danio rerio] (gi|50838798)	gi|50838798	7.9	39.3	22.4
PREDICTED: NFX1-type zinc finger-containing protein 1-like [Danio rerio]	gi|528483584	5.8	39.3	22.4
periphilin-1 [Danio rerio]	gi|121583944 (+1)	1.4	33.7	22.3
PREDICTED: unconventional myosin-IXa isoform X1 [Danio rerio]	gi|528486090 (+1)	0.0	56.0	22.2

PREDICTED: histone-lysine N-methyltransferase SETD1A isoform X1 [Danio rerio]	gi|326666050	0.0	38.1	21.9
PREDICTED: death-inducer obliterator 1-like [Danio rerio]	gi|528516988	0.0	59.7	21.9
Cluster of LOC100000597 protein [Danio rerio] (gi|66910514)	gi|66910514 [5]	0.0	10.2	21.7
dolichyl-diphosphooligosaccharide--protein glycosyltransferase subunit DAD1 [Danio rerio]	gi|154426290	0.0	10.2	21.1
protein QIL1 [Danio rerio]	gi|113678245	4.2	10.2	21.1
PREDICTED: E3 ubiquitin-protein ligase TTC3 isoform X2 [Danio rerio]	gi|528491184	2.8	70.6	21.0
serine/threonine-protein phosphatase 2A 56 kDa regulatory subunit delta isoform [Danio rerio]	gi|50726892	0.0	5.5	20.9
cytochrome b-c1 complex subunit Rieske, mitochondrial [Danio rerio]	gi|157073897	0.0	6.1	20.7
Cluster of Protein regulator of cytokinesis 1 [Danio rerio] (gi|28279644)	gi|28279644 [2]	7.5	61.7	20.4
PREDICTED: E3 ubiquitin-protein ligase HERC2, partial [Danio rerio]	gi|528483182	0.0	8.5	20.0
Cluster of LOC563225 protein [Danio rerio] (gi|115292012)	gi|115292012 [2]	7.9	17.8	19.7
Cluster of eukaryotic translation initiation factor 4B [Danio rerio] (gi|47550837)	gi|47550837 [6]	0.0	41.9	19.6
high mobility group protein B2 [Danio rerio]	gi|82658290	0.9	5.7	19.4
Icln protein [Danio rerio]	gi|44890532 (+2)	7.6	23.6	19.3
nuclear pore complex protein Nup160 [Danio rerio]	gi|41054908	0.0	5.3	19.3
Cluster of TNF receptor-associated protein 1 [Danio rerio] (gi|165972373)	gi|165972373 [2]	0.0	71.3	18.8

Cluster of PREDICTED: microtubule-associated serine/threonine-protein kinase 3-like [Danio rerio] (gi|528470977)	gi|528470977 [2]	0.0	25.5	18.8
M-phase phosphoprotein 8 [Danio rerio]	gi|187607764	2.4	42.2	18.7
PREDICTED: PHD finger protein 3 isoform X1 [Danio rerio]	gi|528498598 (+1)	0.0	18.4	18.5
PREDICTED: sideroflexin-3 isoform X1 [Danio rerio]	gi|528497698	1.9	7.2	18.2
Cluster of Epithelial cell adhesion molecule [Danio rerio] (gi|44890710)	gi|44890710 [2]	1.8	13.9	18.0
Sept2 protein [Danio rerio]	gi|115313325 (+3)	0.0	13.3	17.6
Cluster of PREDICTED: regulation of nuclear pre-mRNA domain-containing protein 2 isoform X1 [Danio rerio] (gi|528502856)	gi|528502856 [2]	0.0	12.6	17.5
Zgc:77560 protein [Danio rerio]	gi|42542976 (+1)	2.4	66.6	17.4
Cluster of PREDICTED: nucleolar pre-ribosomal-associated protein 1-like [Danio rerio] (gi|528501168)	gi|528501168 [2]	2.9	20.9	17.3
ras-related protein Rab-14 [Danio rerio]	gi|41393147	0.0	5.1	16.8
NADH dehydrogenase [ubiquinone] 1 beta subcomplex subunit 10 [Danio rerio]	gi|41152268	3.5	17.2	16.8
Cluster of oxoglutarate (alpha-ketoglutarate) dehydrogenase (lipoamide) [Danio rerio] (gi|254028264)	gi|254028264 [2]	0.0	5.6	16.6
Pard3 protein [Danio rerio]	gi|190339230 (+4)	0.9	32.3	16.6
DNA-directed RNA polymerase II subunit RPB3 [Danio rerio]	gi|269784633	0.0	22.8	16.3

RecName: Full=Protein CASC3; AltName: Full=Cancer susceptibility candidate gene 3 protein homolog; AltName: Full=Metastatic lymph node protein 51 homolog; Short=DrMLN51; Short=Protein MLN 51 homolog	gi|123886565 (+1)	6.3	28.9	16.1
Cluster of serine/threonine kinase 36 (fused homolog, Drosophila) [Danio rerio] (gi|320043268)	gi|320043268	6.0	13.9	16.0
cytotoxic granule-associated RNA binding protein 1 [Danio rerio]	gi|47086779	6.4	16.9	16.0
Cluster of PREDICTED: uncharacterized protein LOC393431 isoform X1 [Danio rerio] (gi|528486792)	gi|528486792	0.0	9.1	16.0
Cluster of nuclear receptor corepressor 2 [Danio rerio] (gi|380420327)	gi|380420327 [4]	0.0	57.7	15.9
Cas-Br-M (murine) ecotropic retroviral transforming sequence-like 1 [Danio rerio]	gi|41055074	3.3	20.8	15.7
PREDICTED: polyribonucleotide 5'-hydroxyl-kinase Clp1-like [Danio rerio]	gi|189528302	0.0	53.2	15.4
uncharacterized protein LOC556124 [Danio rerio]	gi|157909776	1.4	30.5	15.2
succinate dehydrogenase [ubiquinone] iron-sulfur subunit, mitochondrial precursor [Danio rerio]	gi|148922926	5.4	11.3	14.9
Cluster of cAMP-dependent protein kinase catalytic subunit alpha [Danio rerio] (gi|130493522)	gi|130493522 [3]	0.0	8.8	14.9
serine/threonine-protein kinase 3 [Danio rerio]	gi|41054445 (+1)	3.6	49.0	14.8
uncharacterized protein LOC541537 [Danio rerio]	gi|62122901	0.0	7.4	14.6
chromodomain-helicase-DNA-binding protein 8 [Danio rerio]	gi|320461545 (+2)	0.0	22.7	14.6

PREDICTED: splicing factor, arginine/serine-rich 15 [Danio rerio]	gi|528492333	0.0	20.4	14.4
zinc finger HIT domain-containing protein 3 [Danio rerio]	gi|41053670	3.5	33.1	14.0
eukaryotic translation initiation factor 6 [Danio rerio]	gi|41055624 (+2)	0.0	9.1	13.9
PREDICTED: nuclear pore complex protein Nup153 isoform X1 [Danio rerio]	gi|528510621	0.0	17.5	13.7
PREDICTED: uncharacterized protein LOC436879 isoform X4 [Danio rerio]	gi|528517594	0.0	11.1	13.3
Zgc:111960 protein [Danio rerio]	gi|166796880	0.0	11.6	13.2
very low-density lipoprotein receptor precursor [Danio rerio]	gi|169646705 (+4)	0.0	5.1	13.0
C-terminal binding protein 1 [Danio rerio]	gi|40254690	3.3	11.6	12.9
claudin-like protein ZF-A89 [Danio rerio]	gi|30725822	0.0	5.2	12.8
Cluster of PREDICTED: C2 domain-containing protein 3 [Danio rerio] (gi|528501432)	gi|528501432	0.0	9.2	12.7
PREDICTED: histone deacetylase 1 isoform X1 [Danio rerio]	gi|528510099	2.6	29.6	12.0
peptidyl-prolyl cis-trans isomerase-like 1 [Danio rerio]	gi|77683061	1.9	18.6	11.9
Cluster of ras-related C3 botulinum toxin substrate 1 [Danio rerio] (gi|54792776)	gi|54792776 [2]	3.5	11.7	11.9
PREDICTED: uncharacterized protein KIAA0556-like [Danio rerio]	gi|528520519	0.0	14.9	11.8
PREDICTED: trinucleotide repeat-containing gene 6B protein-like isoform X2 [Danio rerio]	gi|528472879 (+1)	0.0	23.4	11.7
nuclear pore complex protein Nup107 [Danio rerio]	gi|71834480	1.8	6.9	11.3

Cluster of PREDICTED: tight junction protein ZO-1-like [Danio rerio] (gi|528521995)	gi|528521995	0.0	12.5	11.3
DIS3-like exonuclease 1 [Danio rerio]	gi|160333118	0.0	32.6	11.3
PREDICTED: PAB-dependent poly(A)-specific ribonuclease subunit 2-like isoform X2 [Danio rerio]	gi|528518391 (+1)	0.0	13.3	11.2
Cluster of PREDICTED: PERQ amino acid-rich with GYF domain-containing protein 1-like isoform X1 [Danio rerio] (gi|528492127)	gi|528492127 [2]	0.0	13.3	11.2
uncharacterized protein LOC550263 [Danio rerio]	gi|62955177	0.0	14.9	11.2
Cluster of PREDICTED: serine/threonine-protein kinase TAO2-like [Danio rerio] (gi|125812164)	gi|125812164	0.0	17.9	10.7
PREDICTED: uncharacterized protein LOC503771 isoform X3 [Danio rerio]	gi|528519733	0.0	17.1	10.6
Cluster of LOC559853 protein, partial [Danio rerio] (gi|79151969)	gi|79151969 [2]	0.0	38.9	10.4
PREDICTED: serine/threonine-protein kinase LATS1 isoform X1 [Danio rerio]	gi|528510786	0.0	20.4	10.2
PREDICTED: cyclin-dependent kinase 12 [Danio rerio]	gi|528509066	0.9	29.5	10.0
poly(rC)-binding protein 2 [Danio rerio]	gi|41055221	0.0	12.7	9.9
nanog homeobox [Danio rerio]	gi|148357118	0.0	28.5	9.9
Cluster of TIA1 cytotoxic granule-associated RNA binding protein [Danio rerio] (gi|37681959)	gi|37681959 [4]	4.8	33.1	9.9
protein mago nashi homolog [Danio rerio]	gi|62955377	3.8	15.8	9.8
nucleoporin 98 [Danio rerio]	gi|320118905 (+1)	0.0	7.5	9.7

uncharacterized protein LOC100126100 precursor [Danio rerio]	gi|157954446 (+1)	2.9	22.5	9.7
N-acetyltransferase 10 [Danio rerio]	gi|41055301	4.7	15.0	9.7
OCIA domain-containing protein 1 [Danio rerio]	gi|41053513 (+1)	0.0	5.8	9.5
cytochrome c oxidase subunit II [Danio rerio]	gi|8395615	2.4	5.1	9.5
PREDICTED: transcription factor 19 [Danio rerio]	gi|292624089	0.0	17.6	9.4
signal recognition particle 9 [Danio rerio]	gi|41055367	0.0	5.1	9.4
actin related protein 2/3 complex subunit 4 [Danio rerio]	gi|45387521	0.0	7.4	9.1
PREDICTED: lysine-specific demethylase 6A isoform X1 [Danio rerio]	gi|528490350 (+1)	0.0	26.6	8.8
exosome complex exonuclease RRP4 [Danio rerio]	gi|339717151	2.9	22.8	8.8
PREDICTED: bromodomain adjacent to zinc finger domain, 2A isoform X1 [Danio rerio]	gi|528517226 (+1)	0.0	8.0	8.7
PREDICTED: AF4/FMR2 family member 4 isoform X1 [Danio rerio]	gi|528514500 (+3)	2.6	13.3	8.6
Cluster of PREDICTED: kinesin family member 13A [Danio rerio] (gi|528505240)	gi|528505240 [5]	0.0	5.4	8.4
exosome complex exonuclease RRP45 [Danio rerio]	gi|54400656	0.0	20.2	8.4
exosome complex component MTR3 [Danio rerio]	gi|66472734	1.0	14.4	8.1
MGC174638 protein [Danio rerio]	gi|156230391 (+2)	0.0	7.8	8.0
Cluster of cyclin-L1 [Danio rerio] (gi|41054323)	gi|41054323	3.6	13.3	7.7
Xrcc5 protein [Danio rerio]	gi|133777834	0.0	12.9	7.7

sorting and assembly machinery component 50 homolog B [Danio rerio]	gi|55925219	0.0	5.2	7.4
Cluster of PREDICTED: rho GTPase-activating protein 21 isoform X1 [Danio rerio] (gi|528470502)	gi|528470502 [2]	0.0	10.9	7.4
60S ribosomal protein L29 [Danio rerio]	gi|51010951	2.9	11.6	7.1
immediate early response 3-interacting protein 1 precursor [Danio rerio]	gi|356991159	0.0	5.1	7.0
transmembrane and coiled-coil domains 1 [Danio rerio]	gi|50540216 (+1)	1.9	8.7	7.0
PREDICTED: wu:fc48e01 [Danio rerio]	gi|125820176	0.0	18.4	6.8
Zgc:123096 protein, partial [Danio rerio]	gi|50417024 (+1)	0.0	6.1	6.6
PREDICTED: protein TANC1-like isoform X2 [Danio rerio]	gi|528481904 (+1)	0.0	9.1	6.4
Centrin2 [Danio rerio]	gi|161213715 (+1)	1.9	14.9	6.3
PREDICTED: dehydrogenase/reductase SDR family member 7B isoform X1 [Danio rerio]	gi|528473478	0.0	10.8	6.3
cyclin T2b [Danio rerio]	gi|47086855	2.7	16.8	6.3
U4/U6.U5 tri-snRNP-associated protein 1 [Danio rerio]	gi|50540414	0.0	15.6	5.9
PREDICTED: uveal autoantigen with coiled-coil domains and ankyrin repeats [Danio rerio]	gi|292616084 (+1)	0.0	6.6	5.9
C-Myc-binding protein [Danio rerio]	gi|91176306	0.0	15.4	5.9
transcription elongation factor B polypeptide 1 [Danio rerio]	gi|52219182 (+1)	0.0	7.7	5.9
Cluster of cytochrome c oxidase assembly factor 5 [Danio rerio] (gi|238859533)	gi|238859533	0.0	5.1	5.9

PREDICTED: uncharacterized protein DKFZp762I1415-like [Danio rerio]	gi|68399071	0.0	5.1	5.9
Ku70 autoantigen [Danio rerio]	gi|114215700 (+2)	1.6	7.4	5.7
uncharacterized protein LOC100216070 [Xenopus (Silurana) tropicalis]	gi|213983243 (+1)	0.0	11.3	5.6
RNA-binding protein 8A [Danio rerio]	gi|61651846	2.4	9.0	5.6
G kinase anchoring protein 1 [Danio rerio]	gi|32451811 (+3)	0.0	17.8	5.6
PREDICTED: nuclear receptor coactivator 3 [Danio rerio]	gi|326671802	0.0	14.8	5.3
Cluster of PREDICTED: mps one binder kinase activator-like 1B-like [Danio rerio] (gi|292614396)	gi|292614396 [5]	0.0	9.1	5.1
coiled-coil-helix-coiled-coil-helix domain-containing protein 2, mitochondrial [Danio rerio]	gi|41152140	0.0	8.1	5.1
store-operated calcium entry-associated regulatory factor precursor [Danio rerio]	gi|115495791 (+2)	0.0	13.2	5.0

Supplementary table 2. Data for 16-cell injection assay.

Cldn-dΔYV	***R1***	***R2***	***R3***	***R4***
total	38	20	20	16
same	21	8	12	9
down	10	10	6	7

uninejcted	***R1***	***R2***	***R3***	***R4***
total		20	21	16
same		18	20	16
down		0	0	0

Cldn-d	**R1**	**R2**	**R3**	**R4**

total	20	16	13
same	19	8	13
down	0	3	0

R: Replicate total: total number of embryos same: embryos did not lose germ plasm spot down: embryos lost a germ plasm spot

Note: Buc spots were counted twice in each embryo, right after injection (16 cell stage) and at 2 hpf.

Digital appendix

For a full list of the 3464 proteins identified by mass spectrometry analysis please open the Excel file.

References

Alberti, S., Halfmann, R., King, O., Kapila, A., & Lindquist, S. (2009). A Systematic Survey Identifies Prions and Illuminates Sequence Features of Prionogenic Proteins. *Cell*, *137*(1), 146–158. https://doi.org/10.1016/j.cell.2009.02.044

Anne Ephrussi, R. L. (1992). Induction of germ cell formation by oskar. *Nature*, *359*, 710–713.

Beutel, O., Maraspini, R., Pombo-García, K., Martin-Lemaitre, C., & Honigmann, A. (2019). Phase Separation of Zonula Occludens Proteins Drives Formation of Tight Junctions. *Cell*, *179*(4), 923-936.e11. https://doi.org/10.1016/j.cell.2019.10.011

Boke, E., Ruer, M., Wühr, M., Coughlin, M., Lemaitre, R., Gygi, S. P., Alberti, S., Drechsel, D., Hyman, A. A., & Mitchison, T. J. (2016). Amyloid-like Self-Assembly of a Cellular Compartment. *Cell*, *166*(3), 637–650. https://doi.org/10.1016/j.cell.2016.06.051

Bontems, F., Stein, A., Marlow, F., Lyautey, J., Gupta, T., Mullins, M. C., & Dosch, R. (2009). Bucky Ball Organizes Germ Plasm Assembly in Zebrafish. *Current Biology*, *19*(5), 414–422. https://doi.org/10.1016/j.cub.2009.01.038

Brizuela, B. J., Wessely, O., & De Robertis, E. M. (2001). Overexpression of the Xenopus tight-junction protein claudin causes randomization of the left-right body axis. *Developmental Biology*, *230*(2), 217–229. https://doi.org/10.1006/dbio.2000.0116

Campbell, P. D., Heim, A. E., Smith, M. Z., & Marlow, F. L. (2015). Kinesin-1 interacts with bucky ball to form germ cells and is required to pattern the zebrafish body axis. *Development (Cambridge)*, *142*(17), 2996–3008. https://doi.org/10.1242/dev.124586

Canever, H., Sipieter, F., & Borghi, N. (2020). When Separation Strengthens Ties. *Trends in Cell Biology*, *30*(3), 169–170. https://doi.org/10.1016/j.tcb.2019.12.002

Citi, S. (2020). Cell Biology: Tight Junctions as Biomolecular Condensates. *Current Biology*, *30*(2), R83–R86. https://doi.org/10.1016/j.cub.2019.11.060

Conchillo-Solé, O., de Groot, N. S., Avilés, F. X., Vendrell, J., Daura, X., & Ventura, S. (2007). AGGRESCAN: A server for the prediction and evaluation of “hot spots” of aggregation in polypeptides. *BMC Bioinformatics*, *8*. https://doi.org/10.1186/1471-2105-8-65

Dodson, A. E., & Kennedy, S. (2020). Phase Separation in Germ Cells and Development. *Developmental Cell*, *55*(1), 4–17. https://doi.org/10.1016/j.devcel.2020.09.004

Dosch, R. (2015). Next generation mothers: Maternal control of germline development in zebrafish. *Critical Reviews in Biochemistry and Molecular Biology*, *50*(1), 54–68. https://doi.org/10.3109/10409238.2014.985816

Ewen-Campen, B., Schwager, E. E., & Extavour, C. G. M. (2010). The molecular machinery of germ line specification. *Molecular Reproduction and Development*, *77*(1), 3–18. https://doi.org/10.1002/mrd.21091

Família, C., Dennison, S. R., Quintas, A., & Phoenix, D. A. (2015). Prediction of peptide and protein propensity for amyloid formation. *PLoS ONE*, *10*(8), 1–16. https://doi.org/10.1371/journal.pone.0134679

Fernandez-Escamilla, A. M., Rousseau, F., Schymkowitz, J., & Serrano, L. (2004). Prediction of sequence-dependent and mutational effects on the aggregation of peptides and proteins. *Nature Biotechnology*, *22*(10), 1302–1306. https://doi.org/10.1038/nbt1012

Furuse, M., Fujita, K., Hiiragi, T., Fujimoto, K., & Tsukita, S. (2014). *Claudin-1 and -2 : Novel Integral Membrane Proteins Localizing at Tight Junctions with No Sequence Similarity to Occludin*. *141*(7), 1539–1550.

Gasior, P., & Kotulska, M. (2014). FISH Amyloid - a new method for finding amyloidogenic segments in proteins based on site specific co-occurence of aminoacids. *BMC Bioinformatics*, *15*(1), 1–8. https://doi.org/10.1186/1471-2105-15-54

Heasman, J., Quarmby, J., & Wylie, C. C. (1984). The mitochondrial cloud of Xenopus oocytes: The source of germinal granule material. *Developmental Biology*, *105*(2), 458–469. https://doi.org/10.1016/0012-1606(84)90303-8

Heim, A. E., Hartung, O., Rothhämel, S., Ferreira, E., Jenny, A., & Marlow, F. L. (2014). Oocyte polarity requires a Bucky ball-dependent feedback amplification loop. *Development (Cambridge)*, *141*(4), 842–854. https://doi.org/10.1242/dev.090449

Houston, D. W. (2013). Regulation of cell polarity and RNA localization in vertebrate oocytes. In *International Review of Cell and Molecular Biology* (1st ed., Vol. 306). Elsevier Inc. https://doi.org/10.1016/B978-0-12-407694-5.00004-3

Houwing, S., Kamminga, L. M., Berezikov, E., Cronembold, D., Girard, A., van den Elst, H., Filippov, D. V., Blaser, H., Raz, E., Moens, C. B., Plasterk, R. H. A., Hannon, G. J., Draper, B. W., & Ketting, R. F. (2007). A Role for Piwi and piRNAs in Germ Cell Maintenance and Transposon Silencing in Zebrafish. *Cell*, *129*(1), 69–82. https://doi.org/10.1016/j.cell.2007.03.026

Itoh, M., Furuse, M., & Morita, K. (2014). *Direct Binding of Three Tight Junction-associated and ZO-3 , with the COOH Termini of Claudins*. *147*(6), 1351–1363.

Jeske, M., Müller, C. W., & Ephrussi, A. (2017). The LOTUS domain is a conserved DEAD-box RNA helicase regulator essential for the recruitment of Vasa to the germ plasm and nuage. *Genes and Development*, *31*(9), 939–952. https://doi.org/10.1101/gad.297051.117

Jesuthasan, S. (1998). Furrow-associated microtubule arrays are required for the cohesion of zebrafish blastomeres following cytokinesis. *Journal of Cell Science*, *111*(24), 3695–3703.

Juliano, C. E., Swartz, S. Z., & Wessel, G. M. (2010). A conserved germline multipotency program. *Development*, *137*(24), 4113–4126. https://doi.org/10.1242/dev.047969

Kiener, T. K., Sleptsova-Friedrich, I., & Hunziker, W. (2007). Identification, tissue distribution and developmental expression of tjp1/zo-1, tjp2/zo-2 and tjp3/zo-3 in the zebrafish, Danio rerio. *Gene Expression Patterns*, *7*(7), 767–776. https://doi.org/10.1016/j.modgep.2007.05.006

Kim-Ha, J., Webster, P. J., Smith, J. L., & Macdonald, P. M. (1993). Multiple RNA regulatory elements mediate distinct steps in localization of oskar mRNA. *Development*, *119*(1), 169–178.

Kistler, K. E., Trcek, T., Hurd, T. R., Chen, R., Liang, F. X., Sall, J., Kato, M., & Lehmann, R. (2018). Phase transitioned nuclear oskar promotes cell division of drosophila primordial germ cells. *ELife*, *7*, 1–35. https://doi.org/10.7554/eLife.37949

Knaut, H., Pelegri, F., Bohmann, K., Schwarz, H., & Nüsslein-Volhard, C. (2000). Zebrafish vasa RNA but not its protein is a component of the germ plasm and segregates asymmetrically before germline specification. *Journal of Cell Biology*, *149*(4), 875–888. https://doi.org/10.1083/jcb.149.4.875

Kolosov, D., Bui, P., Chasiotis, H., & Kelly, S. P. (2013). Claudins in teleost fishes. *Tissue Barriers*, *1*(3), e25391. https://doi.org/10.4161/tisb.25391

Krishnakumar, P., Riemer, S., Perera, R., Lingner, T., Goloborodko, A., Khalifa, H., Bontems, F., Kaufholz, F., El-Brolosy, M. A., & Dosch, R. (2018). Functional equivalence of germ plasm organizers. *PLoS Genetics*, *14*(11), 1–29. https://doi.org/10.1371/journal.pgen.1007696

Liu, K. C., Jacobs, D. T., Dunn, B. D., Fanning, A. S., & Cheney, R. E. (2012). Myosin-X functions in polarized epithelial cells. *Molecular Biology of the Cell*, *23*(9), 1675–1687. https://doi.org/10.1091/mbc.E11-04-0358

Marlow, F. L., & Mullins, M. C. (2008). Bucky ball functions in Balbiani body assembly and animal-vegetal polarity in the oocyte and follicle cell layer in zebrafish. *Developmental Biology*, *321*(1), 40–50. https://doi.org/10.1016/j.ydbio.2008.05.557

Mccarthy, K. M., Francis, S. A., Mccormack, J. M., Lai, J., Rogers, R. A., Skare, I. B., & Lynch, R. D. (2000). *Inducible expression of claudin-1-myc but not occludin-VSV-G results in aberrant tight junction strand formation in MDCK cells*. *3398*, 3387–3398.

McWilliam, H., Li, W., Uludag, M., Squizzato, S., Park, Y. M., Buso, N., Cowley, A. P., & Lopez, R. (2013). Analysis Tool Web Services from the EMBL-EBI. *Nucleic Acids Research*, *41*(Web Server issue), 597–600. https://doi.org/10.1093/nar/gkt376

Moravec, C. E., & Pelegri, F. (2020). The role of the cytoskeleton in germ plasm aggregation and compaction in the zebrafish embryo. In *Current Topics in Developmental Biology* (1st ed., Vol.

140). Elsevier Inc. https://doi.org/10.1016/bs.ctdb.2020.02.001

Nair, S., Marlow, F., Abrams, E., Kapp, L., Mullins, M. C., & Pelegri, F. (2013). The Chromosomal Passenger Protein Birc5b Organizes Microfilaments and Germ Plasm in the Zebrafish Embryo. *PLoS Genetics*, *9*(4). https://doi.org/10.1371/journal.pgen.1003448

Olsen, L. C., Aasland, R., & Fjose, A. (1997). A vasa-like gene in zebrafish identifies putative primordial germ cells. *Mechanisms of Development*, *66*(1–2), 95–105. https://doi.org/10.1016/S0925-4773(97)00099-3

Otto, S. P., & Goldstein, D. B. (1992). Recombination and the evolution of diploidy. *Genetics*, *131*(3), 745–751.

Pelegri, F., Knaut, H., Maischein, H. M., Schulte-Merker, S., & Nüsslein-Volhard, C. (1999). A mutation in the zebrafish maternal-effect gene nebel affects furrow formation and vasa RNA localization. *Current Biology*, *9*(24), 1431–1440. https://doi.org/10.1016/S0960-9822(00)80112-8

Pflanz, R., Voigt, A., Yakulov, T., & Jäckle, H. (2015). Drosophila gene tao-1 encodes proteins with and without a Ste20 kinase domain that affect cytoskeletal architecture and cell migration differently. *Open Biology*, *5*(1). https://doi.org/10.1098/rsob.140161

Raz, E. (2003). Primordial germ-cell development: The zebrafish perspective. *Nature Reviews Genetics*, *4*(9), 690–700. https://doi.org/10.1038/nrg1154

Ressom, R. E., & Dixon, K. E. (1988). Relocation and reorganization of germ plasm in Xenopus embryos after fertilization. *Development*, *103*(3), 507–518.

Riemer, S., Bontems, F., Krishnakumar, P., Gömann, J., & Dosch, R. (2015). A functional Bucky ball-GFP transgene visualizes germ plasm in living zebrafish. *Gene Expression Patterns*, *18*(1–2), 44–52. https://doi.org/10.1016/j.gep.2015.05.003

Roovers, E. F., Kaaij, L. J. T., Redl, S., Bronkhorst, A. W., Wiebrands, K., de Jesus Domingues, A. M., Huang, H. Y., Han, C. T., Riemer, S., Dosch, R., Salvenmoser, W., Grün, D., Butter, F., van Oudenaarden, A., & Ketting, R. F. (2018). Tdrd6a Regulates the Aggregation of Buc into Functional Subcellular Compartments that Drive Germ Cell Specification. *Developmental Cell*, *46*(3), 285-301.e9. https://doi.org/10.1016/j.devcel.2018.07.009

Schwayer, C., Shamipour, S., Pranjic-Ferscha, K., Schauer, A., Balda, M., Tada, M., Matter, K., & Heisenberg, C. P. (2019). Mechanosensation of Tight Junctions Depends on ZO-1 Phase Separation and Flow. *Cell*, *179*(4), 937-952.e18. https://doi.org/10.1016/j.cell.2019.10.006

Seydoux, G. (2018). The P Granules of C. elegans: A Genetic Model for the Study of RNA–Protein Condensates. *Journal of Molecular Biology*, *430*(23), 4702–4710. https://doi.org/10.1016/j.jmb.2018.08.007

Škugor, A., Tveiten, H., Johnsen, H., & Andersen, Ø. (2016). Multiplicity of Buc copies in Atlantic salmon contrasts with loss of the germ cell determinant in primates, rodents and axolotl. *BMC Evolutionary Biology*, *16*(1), 1–12. https://doi.org/10.1186/s12862-016-0809-7

So, C., Cheng, S., & Schuh, M. (2021). Phase Separation during Germline Development. *Trends in Cell Biology*, *xx*(xx), 1–15. https://doi.org/10.1016/j.tcb.2020.12.004

Strasser, M. J., Mackenzie, N. C., Dumstrei, K., Nakkrasae, L. I., Stebler, J., & Raz, E. (2008). Control over the morphology and segregation of Zebrafish germ cell granules during embryonic development. *BMC Developmental Biology*, *8*, 1–16. https://doi.org/10.1186/1471-213X-8-58

Strome, S., & Updike, D. (2015). Specifying and protecting germ cell fate. *Nature Reviews Molecular Cell Biology*, *16*(7), 406–416. https://doi.org/10.1038/nrm4009

Strome, S., & Wood, W. B. (1983). Generation of asymmetry and segregation of germ-line granules in early C. elegans embryos1. Strome, S. & Wood, W. B. Generation of asymmetry and segregation of germ-line granules in early C. elegans embryos. Cell 35, 15–25 (1983). *Cell*, *35*(1), 15–25. https://doi.org/10.1016/0092-8674(83)90203-9

Tanaka, T., & Nakamura, A. (2008). The endocytic pathway acts downstream of Oskar in Drosophila germ plasm assembly. *Development*, *135*(6), 1107–1117. https://doi.org/10.1242/dev.017293

Trcek, T., & Lehmann, R. (2019). Germ granules in Drosophila. *Traffic*, *20*(9), 650–660. https://doi.org/10.1111/tra.12674

Tristan Aguero, Susannah Kassmer, Ramiro Alberio, Andrew Johnson, and M. L. K. (2017). Mechanisms of Vertebrate Germ Cell Determination. In *Adv Exp Med Biol*. https://doi.org/10.1007/978-3-319-46095-6

Vicente-Manzanares, M., Ma, X., Adelstein, R. S., & Horwitz, A. R. (2009). Non-muscle myosin II takes centre stage in cell adhesion and migration. *Nature Reviews Molecular Cell Biology*, *10*(11), 778–790. https://doi.org/10.1038/nrm2786

Welch, E., & Pelegri, F. (2014). Cortical depth and differential transport of vegetally localized dorsal and germ line determinants in the zebrafish embryo. *BioArchitecture*, *5*(1–2), 13–26. https://doi.org/10.1080/19490992.2015.1080891

Westerfield M. (2000). *No TitleThe zebrafish book: A guide for the laboratory use of zebrafish(Daniorerio)* (4th ed.). Eugene: University of OregonPress.

Wolke, U., Weidinger, G., Köprunner, M., & Raz, E. (2002). Multiple levels of posttranscriptional control lead to germ line-specific gene expression in the zebrafish. *Current Biology*, *12*(4), 289–294. https://doi.org/10.1016/S0960-9822(02)00679-6

Yabe, T., Ge, X., & Pelegri, F. (2007). The zebrafish maternal-effect gene cellular atoll encodes the centriolar component sas-6 and defects in its paternal function promote whole genome duplication. *Developmental Biology*, *312*(1), 44–60. https://doi.org/10.1016/j.ydbio.2007.08.054

Yoon, C., Kawakami, K., & Hopkins, N. (1997). Zebrafish vasa homologue RNA is localized to the cleavage planes of 2- and 4-cell-stage embryos and is expressed in the primordial germ cells. *Development*, *124*(16), 3157–3165.

2.3. Bucky ball Interacts with ZO2a and ZO2b to Direct the Localization of Germ Plasm to the Tight Junctions in Zebrafish

This manuscript was a follow up of the previous chapter and was aimed at characterizing the binding partners of Buc that localizes GP at the TJs. Here, Buc is presented as a proline rich protein containing multiple PxxP motifs, which are well known to interact with the SH3 domain, which is also a well-studied protein-protein interaction model. Each ZO protein, which is a TJ scaffold protein, contains a SH3 domain. Therefore, all ZO proteins were tested here and I discovered that Buc interacts with the SH3 domain of ZO2a and ZO2b. Detailed mutational analyses identified the essential PxxP motifs for the interaction and localization of Buc. Results from this manuscript allows us to draw the complete localization pathway of GP in zebrafish.

Authors: ***Nadia Rostam****,*, Roshan Priyarangana Perera, Gerd Vorbrüggen , Roland Dosch.*

**Corresponding author: Nadia Rostam (nrostam@gwdg.de).*

Status: To be submitted, 2022.

Author contributions: Conceptualization: NR, RD; Methodology: NR, RPP; Validation**:** NR; Formal Analysis: NR, RPP; Investigation: NR; Resources: RD; Writing – Original Draft: NR, GV; Writing – Review & Editing: NR, RD, GV; Visualization: NR; Supervision: RD; Project Administration: RD; Funding Acquisition: RD.

My specific contribution in the data: All the experiments are performed by me and all the figures are produced by me.

Bucky ball Interacts with ZO2a and ZO2b to Direct the Localization of Germ Plasm to the Tight Junctions in Zebrafish

Nadia Rostam [1, 2, *], *Roshan Priyarangana Perera*[3], *Gerd Vorbrüggen* [2], *Roland Dosch* [3.]

[1] *Institute of Human Genetics, University Medical Center, Göttingen, Germany.* [2] *Department of Developmental Biology, Johann-Friedrich-Blumenbach Institute of Zoology and Anthropology, Göttingen Center of Molecular Biosciences, University of Göttingen, Göttingen, Germany.* [3] *Institute for Developmental Biochemistry, University Medical Center, Göttingen, Germany.*

Abstract

Germ plasm formation in zebrafish is controlled by maternal factors which are localized in the Balbiani body (BB) in the oocytes. These factors get transported to the early cleavage furrows during embryogenesis. We have recently shown that zebrafish germplasm is anchored to the tight junctions (TJ) at the embryonic cleavage furrows. However, the exact molecules which are involved in tethering of germ plasm at the TJs remained mysterious. Here we discover that multiple PxxP motifs in the germ plasm organizer Bucky ball (Buc) in zebrafish interacts with the SH3 domains of the TJ proteins ZO2a and ZO2b. We provide evidence that this interaction consequently anchors germ plasm at the TJs. Mutation in the PxxP motifs of Buc disrupts its interaction with the SH3 domains and ultimately its localization to the TJs. In conclusion, here we uncover the detailed molecular pathway for germ plasm localization in zebrafish, which was for decades unknown.

Keywords: Germ plasm localization, zebrafish, SH3 domain, PxxP motif, tight junction.

Introduction

In multicellular organisms a specific subtype of cells emerged that were dedicated to sexual reproduction, the germ cells. During evolution two independent systems developed for the determination of primordial germ cells, the inductive system in which a subset of somatic cells is induced early in the embryo to develop into PGC and the inherited mode is dependent on a maternally derived germ plasm which is deposited into the developing egg (Extavour and Akam 2003; Dosch 2015). Germ plasm is composed of a collection of maternally inherited RNA and protein granules that control the formation of germline in many animals including zebrafish (Strome and Updike 2015; Tristan Aguero, Susannah Kassmer, Ramiro Alberio, Andrew Johnson 2017). Only the cells containing germ plasm will become part of the germline, whereas other cells will commit to somatic cell fates. Therefore, proper localization of germ plasm is key for germ cell specification and its removal is critical for the development of the soma. Although several components like Vasa, Nanos and Piwi which control germ cell specification are largely conserved throughout most animal genomes during evolution (Ewen-Campen, Schwager, and Extavour 2010; Juliano, Swartz, and Wessel 2010), the molecular mechanism that controls germ plasm localization is largely unknown. Previously, Bucky ball (Buc) was discovered as the first germ plasm organizer in vertebrates. Buc mutants fail to assemble germ plasm, whereas overexpression of Buc causes ectopic germ cell formation *in vivo*, which was hitherto not shown for any other vertebrate protein (Bontems et al. 2009; Krishnakumar et al. 2018). Most importantly, Buc always colocalizes with the germ plasm during oogenesis and embryogenesis. Buc is first localized to the Balbiani body (BB) in the oocyte, after fertilization it localizes to the first cleavage furrow and subsequently to four restricted spots at the apical ends of the cleavage furrows at the 4-cells stage. Interestingly, these spots are retained during the following cell divisions, resulting in the original formation of 4 primordial germ cells (PGC). After the midblastula transistion (MBT), germ plasm becomes localized into perinuclear complexes which are inherited symmetrically when the four PGCs start to divide, forming four clusters of PGC that will form the entire germline of the organism (Dosch et al. 2004; Bontems et al. 2009; Riemer et al. 2015; Krishnakumar et al. 2018).

We previously showed that the localization of Buc to the four cleavage furrows entirely depends on its amino acid sequence (Bontems et al. 2009). Most recently, we isolated a motif

of 77 amino acids in Buc, which is necessary and sufficient for its localization, named BucLoc (Rostam et al. 2021). Moreover, we exploited Buc in a structure-function analysis to investigate the molecular process of germ plasm localization in zebrafish. We purified this motif from zebrafish embryos and analyzed its interaction partners by mass-spectrometry. We identified tight junction (TJ) components as Buc interaction candidates (Rostam et al. 2021). Remarkably, we also found that TJ proteins colocalize with germ plasm and electron microscopy showed TJ-like structures at the early cleavage furrows. Additionally, we showed that germ plasm localizes to the TJs during early embryonic development in zebrafish and that overexpression of the TJ receptor protein Cldn-d produces extra germ plasm spots in zebrafish embryos (Rostam et al. 2021). However, the exact molecular mechanism and protein interaction partners by which germ plasm localizes at the TJs remains to be unknown, which we aim to explore here.

Tight junctions compose of transmembrane proteins like Claudin and cytoplasmic proteins including Zonula occludens (ZO) proteins (Furuse 2010). There are five ZO proteins in the zebrafish genome, which are ZO1a, -1b -2a, -2b, and -3 (Kiener, Sleptsova-friedrich, and Hunziker 2007). These proteins are scaffold proteins that connect transmembrane proteins to the cytoskeleton (Fanning et al. 1998; Itoh et al. 1999). We have previously shown that ZO1 colocalizes with Buc (Rostam et al. 2021), here we show the detailed protein machinery which anchors Buc at the TJs. We analyze the interaction between Buc and the these TJ proteins and we show that Buc interacts specifically with the SH3 domain of ZO2a and ZO2b. We then present Buc as a protein with multiple PxxP motifs (named P1- P6), which are the key for its interaction with ZO2 proteins. Among the several PxxP motifs, we identified three motifs as key motifs for the localization of Buc at the cleavage furrows and showed that these PxxP motifs also mediate the direct interaction with the SH3 domain of ZO2a and ZO2b. Furthermore, we investigated the specificity of this interaction and characterized a motif which is specific for the interaction with ZO2a, a motif which is specific for the interaction with ZO2b, and a motif which interacts with both proteins. Systematic mutagenesis of single prolines at these PxxP motifs abolish the interaction of Buc with both ZO2 proteins and consequently its localization. Taken together, here we discovered that Buc is directly interacting with TJ proteins via their SH3 domain, suggesting a novel mechanism for the recruitment of germ plasm. We believe these results uncovered a novel role of the SH3

domains as hubs for the recruitment of zebrafish germplasm to the tight junctions, which was previously unknown in vertebrate reproduction.

Results

Localization of Buc to germ plasm depends on proline rich domains

The highly conserved amino-terminal BuLoc (aa11-88) domain of Buc is essential for its localization to the four germ plasm aggregates at the cleavage furrows at the 4-cells stage (Rostam et al. 2021). The sequence of this domain reveals an uncommon enrichment of proline residues either as single prolines or in the form of proline motifs of the sequence PxxP (Figure 1A). To address the role of these prolines in germ plasm localization, we initially used the minimal localization sequence of Buc (aa31-78) (Figure 1A, B; Suppl. Figure 1), that we have recently shown to be sufficient to localize heterologous proteins like GFP (Rostam et al. 2021). The mRNA of variants of this domain coupled to mCherry were injected into 1-cell embryos and their colocalization to the germ plasm was quantified at 2-3 hpf. The exchange of two single prolines (P61A and P65A) to alanine had no effect on the localization to the germ plasm. However, the simultaneous exchange of one proline within the two PxxP motifs (P2 and P3; Figure 1A) to alanine (P35A, P42A) reduced germ plasm localization by more than 70%. To investigate the individual role of the two PxxP motifs within the minimal BucLoc peptide, germ plasm localization was analysed using variants in which only a single proline was exchanged to alanine (P35A or P42A). Whereas the mutation of the P2 motif (P35A) almost completely abolished germ plasm localization, the mutation within the P3 motif (P42A) had no effect. These results clearly showed an essential role of the PxxP motifs for germ plasm localization and that the PxxP motifs have specific non-redundant functions.

Based on the observed specificity of the PxxP motifs, we next analysed the role of the five PxxP motifs (P1-P5; Figure 1A) within the entire BucLoc domain (aa11-88) (Figure 1A, C; Suppl. Figure 2). Indeed, mutation of a single proline within the P2 domain reduces the germ plasm localization of the entire BucLoc domain only partially (P2; Figure 1C). As our results suggested that P3 is dispensable for germ plasm localization, we investigated a potential combinatorial mode of P2 with P1, P4 and P5. The mutation of two PxxP motifs P2, P4 or P2, P5 (P35A, P77A or P35A, P83A; Figure 1C) did not block germ plasm localization completely.

Even the mutation of the three PxxP motifs P1, P2 and P4 (P19A, P35A, P77A) had no additional effect. However, the mutation of P2, P4 and P5 (P35A, P77A, P83A) strongly interfered germ plasm localization of the entire BucLoc domain (Figure 1C). Taken together, these results suggest that P1 and P3 are dispensable for germ plasm localization at the cleavage furrows, whereas P2, P4 and P5 function in a combinatorial mode. However, our data do not allow to distinguish if the position of the PxxP motifs within the BucLoc domain is important or if the individual sequences of the PxxP motif control the observed specificity.

Buc interacts with the SH3 domains of ZO proteins

The germ plasm localization experiments revealed a critical role of the PxxP motifs within the BucLoc domain which represents the minimal binding motif for SH3 domains (Teyra et al. 2017). This finding suggested that the Buc PxxP motifs may facilitate the localization at the cleavage furrows by a direct interaction with TJ proteins containing a SH3 domain. As the TJ complex component Z02 was co-immunoprecipitated with Buc (Rostam et al. 2021), we analyzed if full length Buc can interact with the SH3 domain of zebrafish ZO proteins. To test this hypothesis we initially tested if Buc can interact with the SH3 domain of ZO proteins *in vivo* using the BiFC assay (Perera and Dosch, 2021). In this assay, two non-fluorescent Venus fragments were expressed separately fused to the interaction candidates. Fluorescence can only be observed when the Venus fragments get into close contact via the interaction of the two proteins tested. We discovered that full length Buc interacts with the SH3 domains of ZO2a and ZO2b with similar intensity, but not with ZO1a, ZO1b or ZO3 (Figure 2). No significant difference was seen between the interaction of Buc with ZO2a and ZO2b and the interaction was detectable independent of the position of the Venus half sites (VN vs VC) relative to the SH3 domain. These results showed that full length Buc can specifically interact with the SH3 domain of the maternally provided TJ proteins ZO2a and ZO2b *in vivo,* thereby independently verifying the interaction of Buc with ZO2 by co-immunoprecipitation (Rostam et al. 2021).

Specificity of Buc and ZO2 interaction is mediated by a combinatorial mode of PxxP motifs

Since we found that full length Buc interacts with the SH3 domain of ZO2a and ZO2b, we investigated next if the specificity of this interaction is mediated by the individual PxxP motifs

of BucLoc domain. Therefore, we used the BiFC assay to test BucLoc variants with single proline to alanine exchanges in the P2, P4 and P5 motifs shown before to be essential for germ plasm localization. The interaction with ZO2a was affected by the individual mutation of P2 (P35A) or P4 (P77A), but not P5 (P83A) (Figure 3A). Whereas the combined proline to alanine exchanges in P2 and P5 (P35A, P83A) had no additional effect, a simultaneous exchange within P2 and P4 (P35A, P77A) almost completely blocked the interaction of Buc with the SH3 domain of ZO2a (Figure 3A). Contrarily, the interaction of Buc with the SH3 domain of ZO2b is dependent on the P4-and P5-motifs, as this interaction was strongly reduced by single exchanges in P4 (P77A) and P5 (P83A) but not in P2 (P35A) (Figure 3B). However, an additional exchange within the P2-motif in the P2 and P4 double mutant (P35A, P77A) and P2 and P5 double mutant (P35A, P83A) resulted in a further significant decrease of interaction with ZO2b (Figure 3B), suggesting a supporting role of P2. To test the role of the PxxP individually, we split P2 from P4 and P5 and tested their interaction with the SH3 domain of ZO2a and ZO2b separately. This experiment used short peptides of about 30 aa. Results revealed that indeed the P2-motif interacts specifically with the ZO2a SH3-domain, whereas the combined P4 and P5- motifs showed a weak but consistent interaction with both ZO2 variants (Suppl. Figure 3). Taken together, these *in vivo* interaction experiments supported the results from our Buc germ plasm localization experiments: P2, P4 and P5 PxxP motifs are essential both for the localization to the germ plasm at the TJs and for the direct interaction with the SH3 domains of ZO2a and ZO2b. Furthermore, the results suggest a combinatorial mode of interaction of the three PxxP motifs with ZO2a and ZO2b, whereby P2 is clearly essential for the interaction with ZO2a as it is sufficient for the interaction (Suppl. Figure 1) and its mutation blocks the localization of the minimal BucLoc domain to the germ plasm (Figure 1B). Mutation of P4 significantly reduced interaction with both ZO2a and ZO2b and P5 is required for the binding of Buc to the SH3 domain of ZO2b. The presence of at least three independent SH3 interaction domains with different specificities in the BucLoc domain suggests the possibility of a simultaneous interaction of Buc with the two ZO2 proteins at the TJs.

Discussion

Here we explored the protein machinery targeting germ plasm to the cleavage furrows in zebrafish and found that Buc interacts specifically with ZO2a and ZO2b which are key components of the TJ complex. This interaction is driven by multiple PxxP motifs localized in the conserved N-terminal localization domain of Buc and the SH3 domain in each of the ZO2 isoforms. We identified the exact PxxP motifs specific to each interaction and could show that the identical PxxP motifs are also essential for the localization of the germ plasm at the cleavage furrows from 4-cells stage onwards. These results strongly support the model that germ plasm aggregation at the forming TJs is directly mediated by the SH3 domain of ZO2 protein variants and the PxxP motifs of Buc. Furthermore, based on the three PxxP motifs shown to directly interact with ZO2a and ZO2b proteins, Buc could function as a hub for aggregation by binding ZO proteins in a combinatorial manner. To our knowledge our results represent the first example for the essential role of a SH3 domain-mediated protein-protein interaction in germ plasm formation.

Buc as aggregation hub at the TJs of the cleavage furrows

Bucky ball is essential for germ plasm assembly in the BB (Bontems et al. 2009) and its overexpression results in extra germ cell formation in zebrafish embryos. In addition to this, it is known that endogenous Buc accumulates at the cleavage furrows from the 4-cells stage onwards. This anchorage at only four cleavage furrows results in the preservation of only four PGC up to the 512 cells stage. Only after the MBT, at cell cycle 10, germ plasm is released and subsequently symmetrically inherited as perinuclear clusters forming four clusters of PGCs by the subsequent germ cell divisions (Knaut et al. 2000; Dosch 2015; Wolke et al. 2002).

We have recently shown that Buc colocalizes with the TJs at the cleavage furrows (Rostam et al. 2021); however, the mechanism and the direct interaction partners of Buc directing germ plasm to the TJs was still unknown. Here, we identified the direct TJ interaction partners of Buc, which are ZO2a and ZO2b. We show that the SH3 domains of these two proteins interact with the PxxP motifs of Buc and this provides the molecular base for germ plasm localization in zebrafish. Sequence comparison with 15 related Buc proteins revealed a conserved 100 amino acid N-terminus, which was named BUVE motif (Buc-Velo) (Bontems et al. 2009).

Within this conserved domain, we previously found that the so called BucLoc domain, which is composed of 77 amino acids, is sufficient for the localization of Buc (Rostam et al. 2021). The N-terminus of Buc contains six PxxP motifs, with five of them located in the BucLoc region. PxxP motifs are well documented to interact with the SH3 domains, which are protein binding specific sequences between 50 and 70 amino acids long (Mayer and Eck 1995). We show here that three of the six PxxP motifs in Buc are essential for the specific interaction with the SH3 domains of ZO2a and ZO2b proteins. Our data further support the idea that the three PxxP motifs function in a combinatorial way with distinct specificities for ZO2a and ZO2b. The occurrence of three PxxP motifs could either allow the interaction with ZO proteins in a combinatorial way or alternatively could enable the parallel binding of more than one ZO protein at the same time as shown in our model (Figure 4). Such a concurrent binding could enhance the formation of the germ plasm aggregates at the newly forming tight junctions at the cleavage furrows. Our results represent a novel mechanism for the aggregation of the germ plasm at the cleavage furrows, which does explain asymmetric distribution of the four germ plasm spots during the following cell divisions up to the MBT.

However, it is still not fully understood by which mechanism Buc is transported towards the cleavage furrows or whether the activity of TJ proteins are required for the aggregation of Buc (See suppl. Figure 4 for a related experiment). We have previously found Myosin Light Chain, which is a subunit of the Non-Muscle Myosin II (NMII) protein, as an interacting partner of Buc (Rostam et al. 2021). It is described that NMII phosphorylated by ROCK (p-NMII) (Amano et al. 1996; Miranda-Rodríguez et al. 2017) colocalizes with germ plasm RNAs at the 2- and 4-cell stage in zebrafish embryos (Nair et al. 2013). It has been suggested that inhibition of RhoA/ROCK disturbs the localization of germ plasm, through the destruction of correct localization of furrow microtubular array (FMA) at the cleavage furrows (Miranda-Rodríguez et al. 2017). Interestingly, also Kinesin-1 Kif5Ba interacts with Buc, and mutant analyses suggest that kif5Ba is required to recruit Buc to the cleavage furrows and thereby specifying PGCs (Campbell et al. 2015).

Taken together these interactions and functional data support the idea that germ plasm aggregation at the TJs at the cleavage furrows depend on cytoskeletal structures and associated motor proteins. Further experiments are required to investigate if another subset of the identified PxxP motifs in the Buc conserved in the N-terminal region are involved in

these processes by the interaction with additional SH3 domain harbouring proteins. In addition, the PxxP motifs might be as well involved in the assembly of the BB, as the interaction with various proteins could be the basis for the observed phase separation during BB formation by the Buc homologue Xvelo in *Xenopus laevis* (Boke et al. 2016).

Conclusion

In this study, we discovered the direct interaction partners of Buc which anchors germ plasm at the TJs in zebrafish, ZO2a and ZO2b. We identified multiple PxxP motifs in Buc which specifically interact with these TJ proteins and target the localization of Buc. We believe our data do not only provide fascinating results to vertebrate reproduction biology, but also add additional knowledge to the broad range of biochemical functions of the SH3 domains.

Acknowledgements

We are thankful to Prof. E. A. Wimmer for providing the facilities to perform this research and G. Kracht for technical assistance.

Author contributions

Conceptualization: NR, RD, Methodology: NR, RPP, Validation**:** NR, Formal Analysis: NR, RPP, Investigation: NR, Resources: RD, Writing – Original Draft: NR, GV, Writing – Review & Editing: NR, RD, GV. Visualization: NR, Supervision: RD, Project Administration: RD, Funding Acquisition: RD.

Declaration of interests

The authors declare no competing interests.

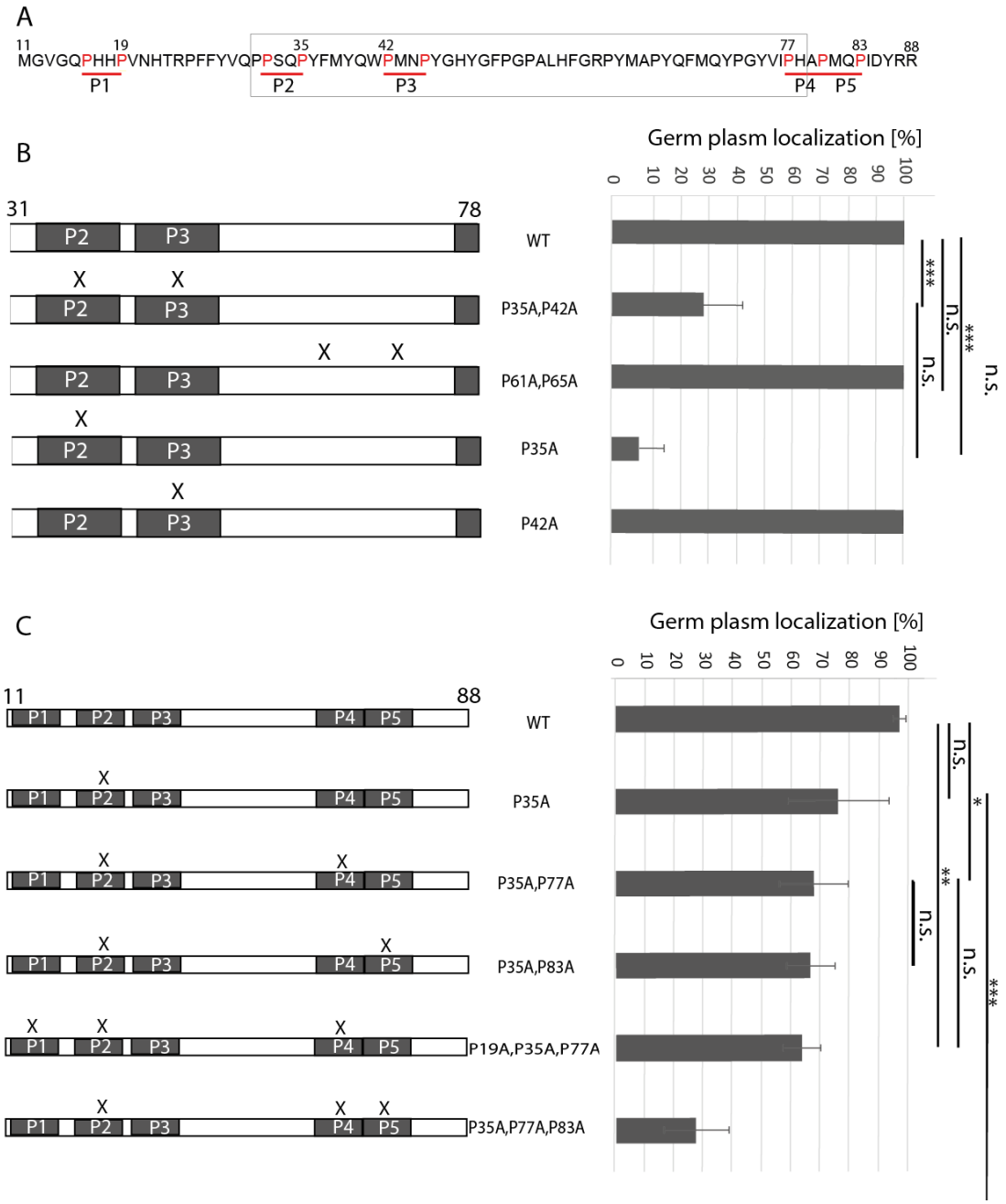

Figure 1. Triple mutation in P2, P4, and P5 abolishes localization of BucLoc (Buc11-88).

A) aa sequence of BucLoc with PxxP motifs named from P1 to P5. The numbers represent aa numbers in Buc protein. Mutations were introduced at aa (19, 35, 42, 77, 88). B) Localization of minimal BucLoc domain (Buc31- 78). Schematic representation of Buc31-78 is shown on the left side with all mutated variants tested. Grey boxes represent the PxxP motifs in Buc31-78. Each mutation is denoted by a letter X, depicting a single mutation of a proline residue into alanine, transforming a PxxP into AxxP or PxxA. Quantification of localization of Buc31-78 variants is shown on the right side. Mutating P2 almost completely abolished the localization of Buc31-78 (5.12 ± 0.08%) (n: 62) compared to the WT (100 ± 0.00%) (P-value: 0.00005) (n: 62), with no significant difference when a second mutation in P3 added to it (28% ± 0.14%) (n: 58). There was no significant difference between mutated P3 (100 ± 0.00%) (n: 58) or control non- PxxP motif prolines (P61A, P65A) (100 ± 0.00%) (n: 60) compared to the WT (100 ± 0.00%). C) Localization of BucLoc. Schematic representation of BucLoc is shown on the left

side and quantification of localization of BucLoc mutant variants is shown on the right side. Single mutation in P2 did not influence the localization of BucLoc (76.12 ± 17.43%) (n:58) compared to the WT (96.96 ± 2.40%) (P-value: 0.16) (n: 87). There was significant difference in the presence of double mutant P2, P4 (67.70 ± 11.71%) (n: 76) or P4, P5 (66.57 ± 8.19%) (n: 67) in comparison to WT (P-value: 0.02,0.007, respectively). No significant difference was recorded between P2, P4 double mutant and P1, P2, P4 triple mutant (63.56 ± 6.23%) (n: 79) (P-value: 0.68). A significant difference was seen between P2, P4 double mutant and P2, P4, P5 triple mutant (27.40 ± 11.02%) (n: 128) (P-value: 0.005). Triple mutation P2, P4, P5 showed significantly the least localization potency compared to the WT (P-value: 0.00009). Error bars represent standard deviation (SD). *: P ≤ 0.05, **: P ≤ 0.01, ***: P ≤ 0.001, n.s.: non-significant.

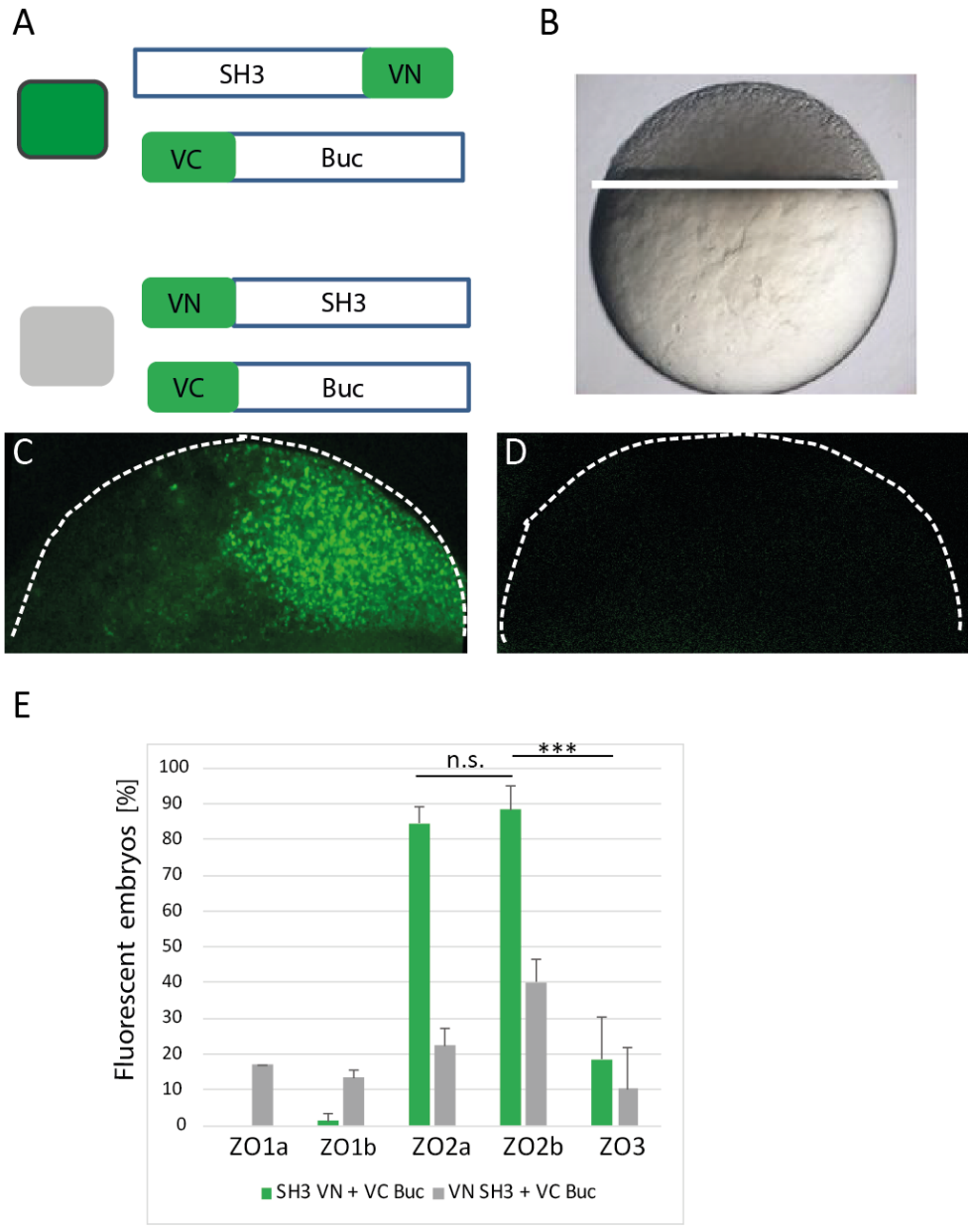

Figure 2. Buc interacts with ZO2a and ZO2b.

A) Schematic representation of tested BiFC combinations. Embryos were injected at 1- cell stage with Buc RNA and one of the SH3 RNAs at a time and examined for fluorescent signal approximately 4 hpf (B). C) Exemplary embryo showing fluorescent signal at 4 hpf, injected with RNA from Buc and SH3 ZO2a. D) Exemplary embryo showing no fluorescent signal at 4 hpf, injected with RNA from Buc and SH3 ZO1a. (E) Quantification of interaction between Buc and different SH3 domains. SH3- VN of ZO2a and ZO2b showed the highest interaction value with Buc (85 ± 0.04% and 88 ± 0.06%, respectively) (n: 90, 112, respectively) with no significant difference between them (P-value: 0.37). ZO2a (SH3- VN) interacted significantly higher with Buc than SH3- VN of ZO1a (0 ±, 0.00%) (n: 81) ZO1b (1.25 ± 0.02%) (n: 84) and ZO3 (19 ± 0.11%) (n: 80) (P- value: 0,000000070,0000001, 0,0001, respectively). Error bars represent SD. ***: P ≤ 0.001, n.s.: non-significant.

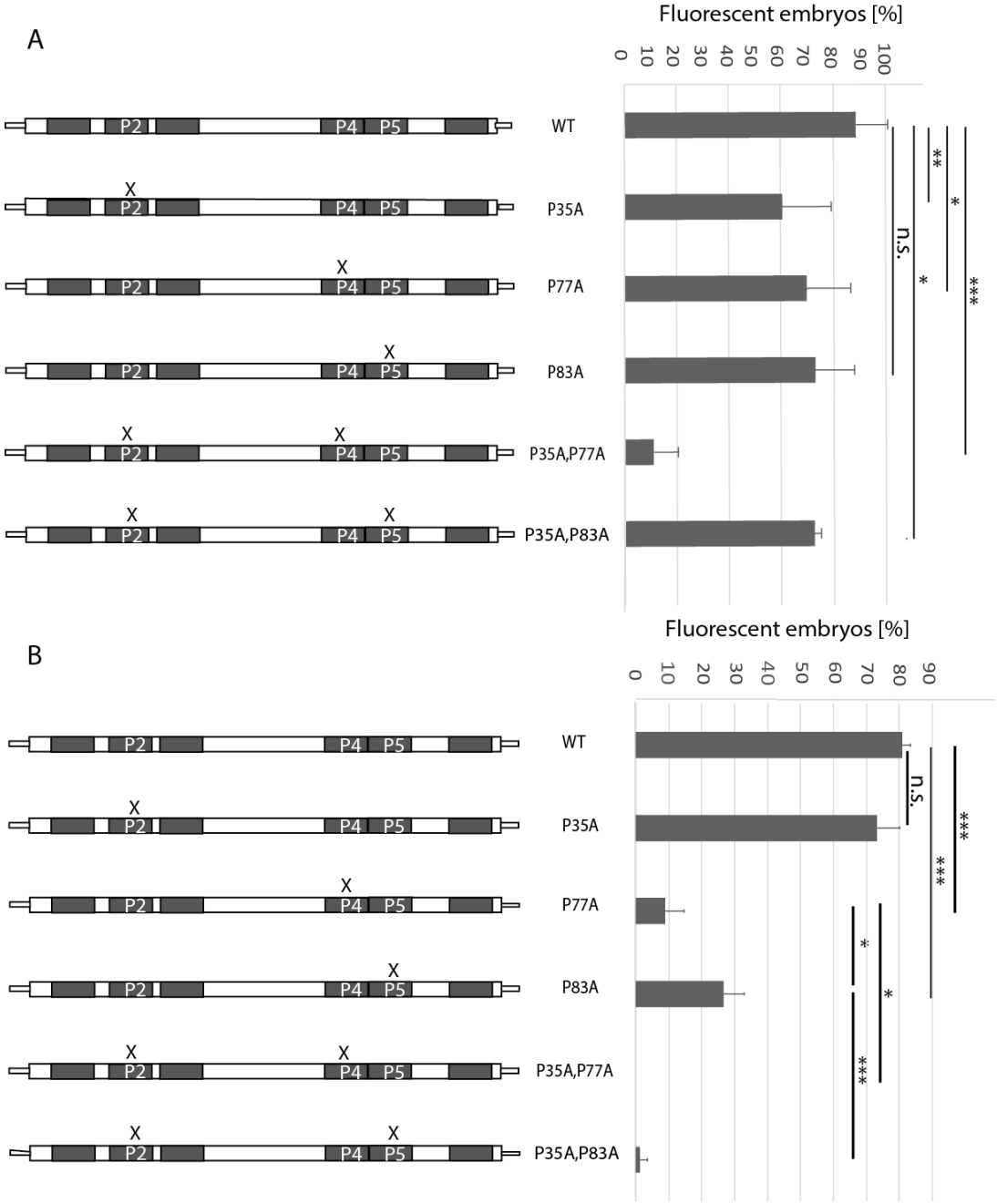

Figure 3. Specificity of Buc ZO interaction is mediated by a combinatorial mode of PxxP motifs. The schemes on the left side show full length Buc containing 6 PxxP motifs. Key motifs based on the localization assay are labelled (P2, P4, P5). Quantification of the interaction of Buc variants is shown on the right side. (A) Interaction with ZO2a SH3 domain. Single mutation in P2 (60 ± 0.18%) (n: 125) or P4 (70 ± 0.17%) (n: 137) significantly decreased the interaction of Buc with ZO2a compared to the WT (89 ± 0.12%) (n: 151) (P-value: 0.0061 and 0.02, respectively), while single mutation in P5 had no influence (70.44 ± 0.15) (n: 96 (P-value: 0.07)). Double mutation in P2, P4 almost completely abolished this interaction (11 ± 0.09%) (n: 157) compared to the WT (P-value: 0,0000000007). B) Interaction of Buc with ZO2b SH3 domain. Single mutation in P2 did not influence the interaction with ZO2b (73 ± 6.75%) (n: 69) compared to the WT Buc (81 ±. 2.61) (n: 79) (P-value: 0.11). Single mutation in P4 (8.94 ± 5.68%) (n: 79) or P5 (26.71 ± 6.19%) (n: 79) significantly decreased this interaction compared to the WT (P-value: 0,000001 and 0,00001, respectively). Double mutation in P2, P4 (0.00 ± 0.00%) (n: 84) or P2, P5 (1.25 ± 2.16%) (n: 80) almost completely abolished the interaction compared to the WT (P-value: 0,000000002, 0,00000001, respectively), with no significant difference between them (P-value: 0.35). Error bars represent SD. *: P ≤ 0.05, **: P ≤ 0.01, ***: P ≤ 0.001, n.s.: non-significant.

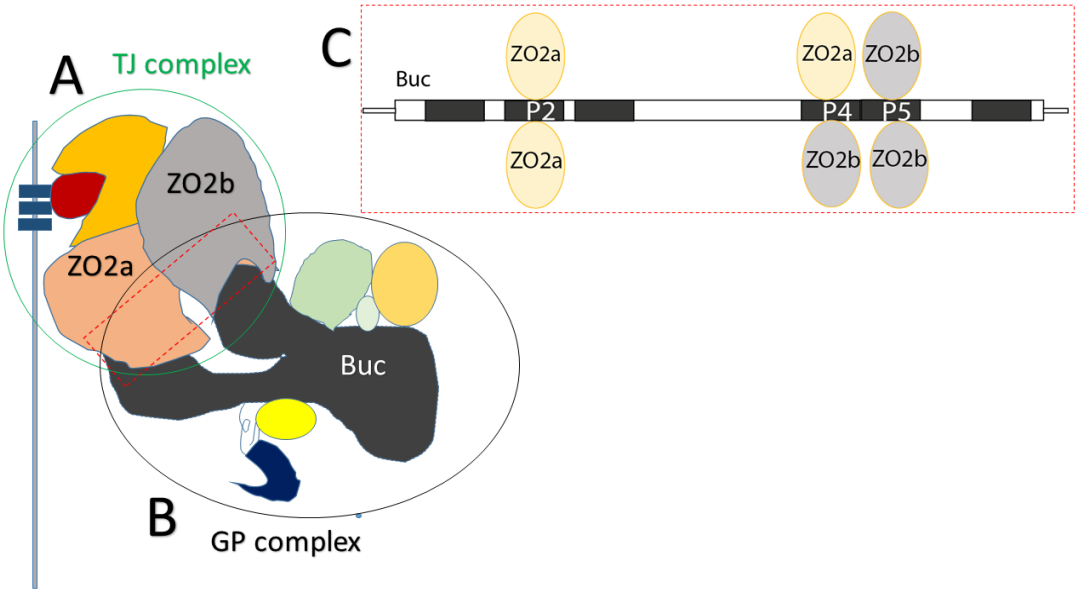

Figure 4. Model for germ plasm localization in zebrafish.

(A) Representation of tight junction (TJ) protein complex at an early zebrafish cleavage furrow (green circle). TJ proteins complex includes transmembrane and cytoplasmic proteins including ZO2a and ZO2b. B) Representation of germ plasm (GP) complex, outlined by the grey oval shape. GP consists of various protein and RNA molecules, including Buc as a central player. Note the overlap between these two complexes (dashed red rectangle). C) Magnification of the dashed red rectangle between (A) and (B). Buc interacts with ZO2a and ZO2b through its PxxP motifs (P2, P4, P5) and this interaction anchors Buc and hence GP to the TJ complex.

Methods

Zebrafish handling and manipulation

All injections were carried out into 1-cell zebrafish (*Danio rerio*) embryos. Fish were maintained as described previously (Westerfield, 2000) and in accordance with regulations from Georg-August university Goettingen, Germany.

Interaction Assay

To investigate the interaction between the SH3 domain and Buc, we used Bimolecular Fluorescent Complementation assay (BiFC) (Krishnakumar et al. 2018; Perera and Dosch, 2021). This assay works by reconstitution of the fluorescent protein Venus from two non-fluorescent halves, which are Venus-N terminal (VN) and Venus-C terminal (VC). Here, we fused the ORF of full length Buc to VC and the SH3 domain of the zebrafish ZO proteins to VN and injected them into 1- cell stage embryos and looked for fluorescence signal in the embryos after around four hours, reflecting the presence of interaction between the two injected constructs.

Mutation strategy to find the key PxxP motifs involved in the localization of Buc

Bucky ball contains six PxxP motifs (Figure 1A). To investigate the role of these motifs, we exchanged a single proline to alanine within the motifs, either mutating one PxxP motif or two or three in combination as shown schematically in figure 1 and 3. All the mutations were introduced with side directed mutagenesis technique and all the constructs were sequenced before injection.

Mutation strategy to find the key PxxP motifs involved in the interaction of Buc with ZO2a and ZO2b

To figure out if interaction of Buc with ZO2a and ZO2b is the key for the localization of Buc and to see whether the same PxxP motifs which are critical for the localization are also involved in its interaction, we performed BiFC assay on mutated Buc protein constructs. For

this, we made the same mutations which we found to be important in the localization assay in VC-Buc. Therefore, single and double mutations in P2, P4, and P5 were introduced by side directed mutagenesis technique in the full length Buc and tested them for interaction with ZO2a and ZO2b separately. All the constructs were sequenced before injection.

Statistics and Quantification assay

At least three replicates were used per each dataset. All the statistical analysis of the experiments has been carried out in Microsoft Excel. T-test was used to calculate the P-values (two tailed t-test). Error bars indicate the standard deviation of averages.

Supplementary data

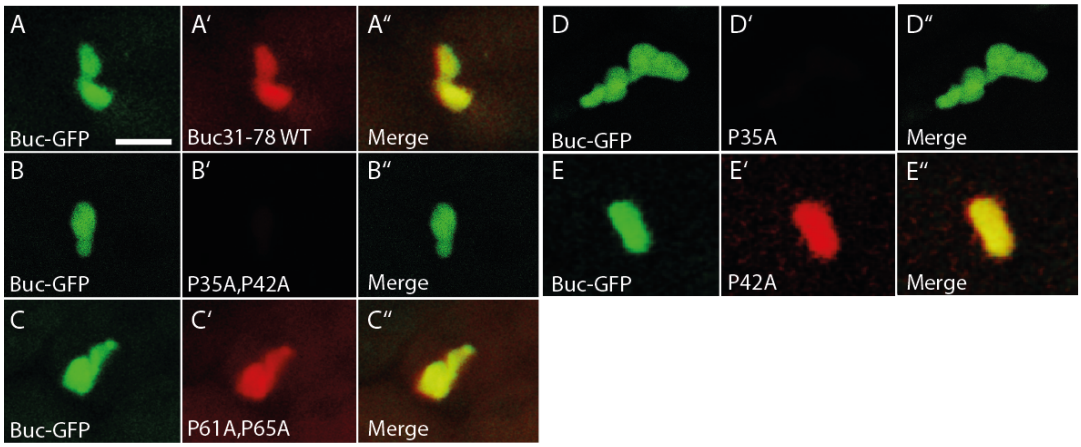

Suppl. Figure 1. **Mutation analysis of minimal BucLoc (aa3- 78) localizaition.**

(A-E) Localization of WT and mutant Buc31- 78constructs. Each construct was tagged to m-Cherry and injected into Buc- GFP transgenic line marking the germ plasm. (A-A'') Localization of Buc- GFP (A) and WT Buc31- 78 (A'), (A'') shows colocalization of A and A'. (B-B'') Localization of Buc- GFP (B) and Buc31- 78 P35A, P42A (B'), (B'') shows colocalization of B and B'. (C-C'') Localization of Buc- GFP (C) and Buc31-78 P61A, P65A (C'), (C'') shows colocalization of C and C'. (D-D'') Localization of Buc- GFP (E) and Buc31- 78 P35A (D'), (D'') shows colocalization of D and D'. (E-E'') Localization of Buc- GFP (E) and Buc31- 78 P42A (E'), (E'') shows colocalization of E and E'. Scale bar: 10µm.

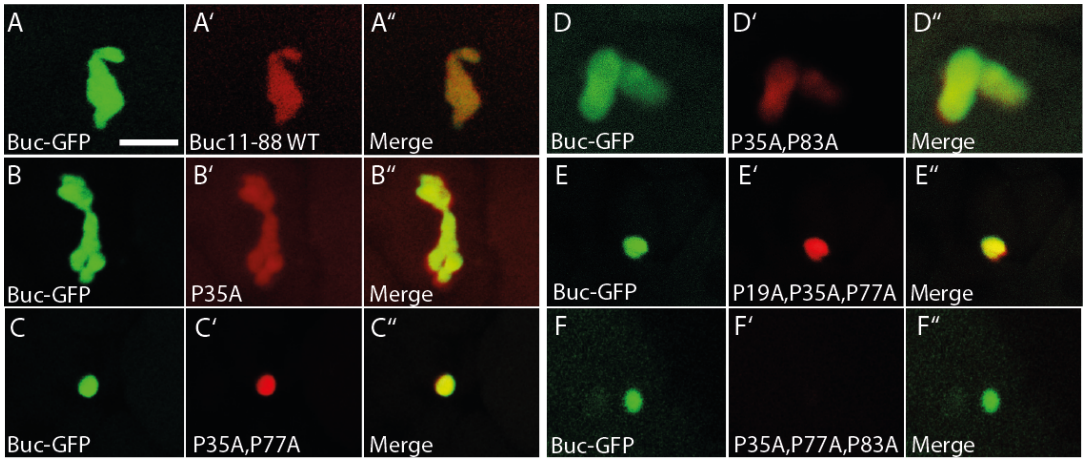

Suppl. Figure 2. Mutation analysis of BucLoc domain (aa11-88).

(A-E) Localization of WT and mutant BucLoc constructs. Each construct was tagged to m-Cherry and injected into Buc- GFP transgenic line to mark the germ plasm. (A-A'') Localization of transgenic Buc-GFP (A) and BucLoc WT (A'), (A'') shows colocalization of A and A'. (B-B'') Localization of transgenic Buc- GFP (B) and BucLoc P35A, (B'), (B'') shows colocalization of B and B'. (C-C'') Localization of transgenic Buc- GFP (C) and BucLoc P35A, P77A (C'), (C'') shows colocalization of C and C'. (D-D'') Localization of transgenic Buc- GFP (D) and BucLoc P35A, P83A (D'), (D'') shows colocalization of D and D'. (E-E'') Localization of transgenic Buc- GFP (E) and BucLoc P19A, P35A, P77A. (E'') shows colocalization of E and E'. (F-F'') Localization of transgenic Buc- GFP (F) and BucLoc P35A, P77A, P83A (F'), (F'') shows colocalization of F and F'. Scale bar: 10µm.

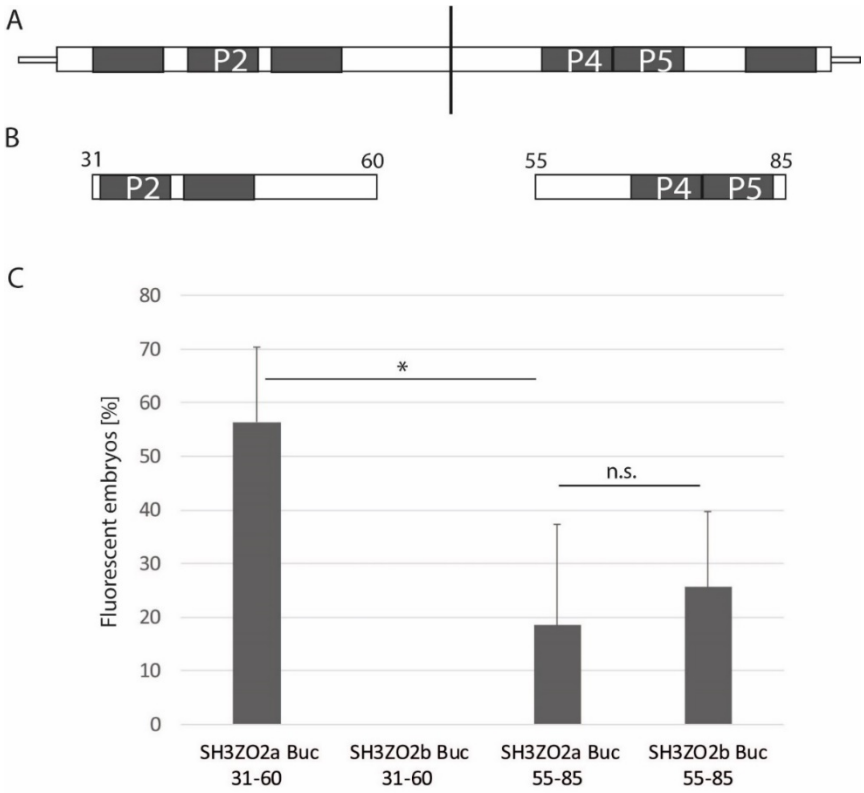

Suppl. Figure 3. Splitting PxxP motifs revealed their specific interaction with ZO2a and ZO2b.

(A) Schematic representation of split PxxP motifs into two peptides, the first one contains P1 and the second one contains P4 and P5. (B) The first peptide is composed of 30 amino acids (aa31- aa60). The second peptide is composed of 31 amino acids (aa55- aa85). Grey boxes represent the PxxP motifs in each peptide. The peptides were tagged to VC. (C) Quantification of interaction with ZO2a and ZO2b. The first peptide only interacted with ZO2a (56.42 ± 14.03) (n: 100) and not with ZO2b (0.00 ± 0.00%) (n: 139). While the second peptide interacted with both ZO2a (18.54 ± 18.83) (n: 56) and ZO2b (25.57 ± 14.14%) (n: 129) with no significant difference between them (P-value: 0.51). There was significant difference between the interaction of ZO2a with the first peptide and the second peptide (P-value: 0.01). Error bars represent SD. *: P ≤ 0.05. n.s.: non-significant.

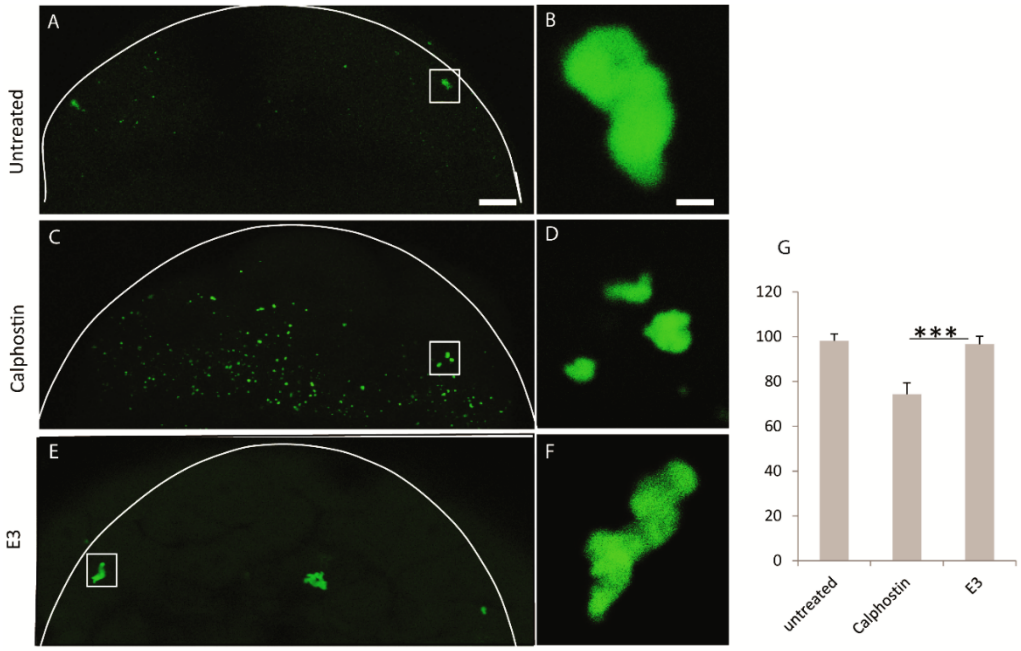

Suppl. Figure 4. Inhibiting ZO phosphorylation disturbs Buc aggregation.

The importance of TJ protein ZO1 in the aggregation of Buc was evaluated using the phosphorylation inhibitor Calphostin. (A) An untreated embryo from the lateral view at 2hpf. (B) A germ plasm spot from (A), the magnified rectangle. (C) A calphostin treated Embryo at 2hpf. (D) A magnified germ plasm spot from (C). (E) Embryo treated with E3 medium (control). (F) A magnified germ plasm spot from (E). (G) Quantification of embryos showing intact germ plasm spots. The percentages of untreated embryos showing intact germ plasm spots (98.75 ± 2.1%) and embryos treated with E3 (96.66 ± 3.5%) were significantly higher than the percentage of embryos treated with calphostin (74.29 ± 5.13%); P=0.0002, 0.0007 respectively. Scale bars (A): 50µm, (B): 2µm. Error bars represent SD. ***: P ≤ 0.001.

References

Amano, Mutsuki, Masaaki Ito, Kazushi Kimura, Yuko Fukata, Kazuyasu Chihara, Takeshi Nakano, Yoshiharu Matsuura, and Kozo Kaibuchi. 1996. “Phosphorylation and Activation of Myosin by Rho-Associated Kinase (Rho- Kinase).” *Journal of Biological Chemistry* 271 (34): 20246–49. https://doi.org/10.1074/jbc.271.34.20246.

Boke, Elvan, Martine Ruer, Martin Wühr, Margaret Coughlin, Regis Lemaitre, Steven P. Gygi, Simon Alberti, David Drechsel, Anthony A. Hyman, and Timothy J. Mitchison. 2016. “Amyloid-like Self-Assembly of a Cellular Compartment.” *Cell* 166 (3): 637–50. https://doi.org/10.1016/j.cell.2016.06.051.

Bontems, Franck, Amandine Stein, Florence Marlow, Jacqueline Lyautey, Tripti Gupta, Mary C. Mullins, and Roland Dosch. 2009. “Bucky Ball Organizes Germ Plasm Assembly in Zebrafish.” *Current Biology* 19 (5): 414–22. https://doi.org/10.1016/j.cub.2009.01.038.

Campbell, Philip D., Amanda E. Heim, Mordechai Z. Smith, and Florence L. Marlow. 2015. “Kinesin-1 Interacts with Bucky Ball to Form Germ Cells and Is Required to Pattern the Zebrafish Body Axis.” *Development (Cambridge)* 142 (17): 2996–3008. https://doi.org/10.1242/dev.124586.

Dosch, Roland. 2015. “Next Generation Mothers: Maternal Control of Germline Development in Zebrafish.” *Critical Reviews in Biochemistry and Molecular Biology* 50 (1): 54–68. https://doi.org/10.3109/10409238.2014.985816.

Dosch, Roland, Daniel S. Wagner, Keith A. Mintzer, Greg Runke, Anthony P. Wiemelt, and Mary C. Mullins. 2004. “Maternal Control of Vertebrate Development before the Midblastula Transition: Mutants from the Zebrafish I.” *Developmental Cell* 6 (6): 771–80. https://doi.org/10.1016/j.devcel.2004.05.002.

Ewen-Campen, Ben, Evelyn E. Schwager, and Cassandra G.M. Extavour. 2010. “The Molecular Machinery of Germ Line Specification.” *Molecular Reproduction and Development* 77 (1): 3–18. https://doi.org/10.1002/mrd.21091.

Extavour, Cassandra G., and Michael Akam. 2003. “Mechanisms of Germ Cell Specification across the Metazoans: Epigenesis and Preformation.” *Development* 130 (24): 5869–84. https://doi.org/10.1242/dev.00804.

Fanning, Alan S., Brian J. Jameson, Lynne A. Jesaitis, and James Melvin Anderson. 1998. “The Tight Junction Protein ZO-1 Establishes a Link between the Transmembrane Protein Occludin and the Actin Cytoskeleton.” *Journal of Biological Chemistry* 273 (45): 29745–53. https://doi.org/10.1074/jbc.273.45.29745.

Furuse, Mikio. 2010. “Molecular Basis of the Core Structure of Tight Junctions.” *Cold Spring Harbor Perspectives in Biology* 2 (1). https://doi.org/10.1101/cshperspect.a002907.

Itoh, Masahiko, Mikio Furuse, Kazumasa Morita, Koji Kubota, Mitinori Saitou, and Shoichiro Tsukita. 1999. “And ZO-3 , with the COOH Termini of Claudins.” *Cell* 147 (6): 1351–63.

Juliano, Celina E., S. Zachary Swartz, and Gary M. Wessel. 2010. “A Conserved Germline Multipotency Program.” *Development* 137 (24): 4113–26. https://doi.org/10.1242/dev.047969.

Kiener, Tanja K, Inna Sleptsova-friedrich, and Walter Hunziker. 2007. “Identification , Tissue Distribution and Developmental Expression of Tjp1 / Zo-1 , Tjp2 / Zo-2 and Tjp3 / Zo-3 in the Zebrafish , Danio Rerio B Percent AA Identity” 7: 767–76. https://doi.org/10.1016/j.modgep.2007.05.006.

Knaut, Holger, Francisco Pelegri, Kerstin Bohmann, Heinz Schwarz, and Christiane Nüsslein-Volhard. 2000. “Zebrafish Vasa RNA but Not Its Protein Is a Component of the Germ Plasm and Segregates Asymmetrically before Germline Specification.” *Journal of Cell Biology* 149 (4): 875–88. https://doi.org/10.1083/jcb.149.4.875.

Krishnakumar, Pritesh, Stephan Riemer, Roshan Perera, Thomas Lingner, Alexander Goloborodko, Hazem Khalifa, Franck Bontems, Felix Kaufholz, Mohamed A. El-Brolosy, and Roland Dosch. 2018. “Functional Equivalence of Germ Plasm Organizers.” *PLoS Genetics* 14 (11): 1–29. https://doi.org/10.1371/journal.pgen.1007696.

Mayer, Bruce J, and Michael J Eck. 1995. “Minding Your p ’ s and q ’ s” 5 (4): 364–67.

Miranda-Rodríguez, Jerónimo Roberto, Enrique Salas-Vidal, Hilda Lomelí, Mario Zurita, and Denhi Schnabel. 2017. “RhoA/ROCK Pathway Activity Is Essential for the Correct Localization of the Germ Plasm MRNAs in Zebrafish Embryos.” *Developmental Biology* 421 (1): 27–42. https://doi.org/10.1016/j.ydbio.2016.11.002.

Nair, Sreelaja, Florence Marlow, Elliott Abrams, Lee Kapp, Mary C. Mullins, and Francisco Pelegri. 2013. “The Chromosomal Passenger Protein Birc5b Organizes Microfilaments and Germ Plasm in the Zebrafish Embryo.” *PLoS Genetics* 9 (4). https://doi.org/10.1371/journal.pgen.1003448.

Riemer, Stephan, Franck Bontems, Pritesh Krishnakumar, Jasmin Gömann, and Roland Dosch. 2015. “A Functional Bucky Ball-GFP Transgene Visualizes Germ Plasm in Living Zebrafish.” *Gene Expression Patterns* 18 (1–2): 44–52. https://doi.org/10.1016/j.gep.2015.05.003.

Perera, Roshan Priyarangana , Dosch, Roland. 2021. “In Vivo Imaging of Protein Interactions in the Germplasm with Bimolecular Fluorescent Complementation.” In *Methods Mol Biol* ., 2218: 303-317. https://doi.org/10.1007/978-1-0716-0970-5_24.

Rostam, Nadia, Goloborodko, Alexander, Riemer, Stephan, Hertel, Andres, Riedel, Dietmar, Vorbrüggen, Gerd and Dosch, Roland. 2021. “Author Information Affiliations.”

Strome, Susan, and Dustin Updike. 2015. “Specifying and Protecting Germ Cell Fate.” *Nature Reviews Molecular Cell Biology* 16 (7): 406–16. https://doi.org/10.1038/nrm4009.

Teyra, Joan, Haiming Huang, Shobhit Jain, Xinyu Guan, Aiping Dong, Yanli Liu, Wolfram Tempel, et al. 2017. “Comprehensive Analysis of the Human SH3 Domain Family Reveals a Wide Variety of Non-Canonical Specificities.” *Structure* 25 (10): 1598-1610.e3. https://doi.org/10.1016/j.str.2017.07.017.

Tristan Aguero, Susannah Kassmer, Ramiro Alberio, Andrew Johnson, and Mary Lou King. 2017. *Mechanisms of Vertebrate Germ Cell Determination*. *Adv Exp Med Biol*. https://doi.org/10.1007/978-3-319-46095-6.

Westerfield M. (2000). *No TitleThe zebrafish book: A guide for the laboratory use of zebrafish(Danio rerio)* (4th ed.). Eugene: University of OregonPress.

Wolke, Uta, Gilbert Weidinger, Marion Köprunner, and Erez Raz. 2002. “Multiple Levels of Posttranscriptional Control Lead to Germ Line-Specific Gene Expression in the Zebrafish.” *Current Biology* 12 (4): 289–94. https://doi.org/10.1016/S0960-9822(02)00679-6.

3. General discussion

This thesis investigated the molecular mechanism controlling the localization of GP in zebrafish, which let to uncovering the entire pathway regarding this and finding an alternative way of fixation of zebrafish embryos for the purpose of immunostaining. Here, Buc was used as a molecular proxy to investigate GP, as zebrafish organizer of GP and its assembly. Results revealed that GP is anchored at early TJs in the embryos of this organism. In addition, this thesis found that Buc interacts through its multiple PxxP motifs with the SH3 domain of the tight junction proteins ZO2a and ZO2b, localizing GP at the TJs. Detailed mutation analyses of the PxxP motifs pinpointed the essential motifs for the interaction and hence the localization of Buc at the TJs. Furthermore, Cldn-d is discovered as the TJ receptor protein for tethering of Buc at the TJs. Overexpression of Cldn-d resulted in the formation of ectopic GP aggregates and interfering the function of TJ proteins disturbed the localization of GP.

3.1 Improvement in the fixation methods for immunohistochemistry in zebrafish research

The function of genes at the tissue and organ levels is mostly determined by immunohistochemistry and live-imaging investigations of protein expression and localization. While *in vivo* imaging of fusion proteins allows researchers to understand their spatiotemporal expression and localization, endogenous protein expression and subcellular localization needs to be confirmed by immunohistochemistry. In theory, immunostaining is simple; yet, attaining good immunostaining for each antibody necessitates a variety of protocol adjustments, such as selecting of appropriate fixative agents and antigen retrieval with suitable buffers (Shi, Cote, and Taylor 2001; D'Amico, Skarmoutsou, and Stivala 2009).

Antibodies that can be used to designate zebrafish are scarce, making immunostaining difficult. Several research have been performed to discover optimal protocols for immunolabeling in zebrafish (Jessica Sullivan-Brown, Margaret E. Bisher 2011; Inoue and Wittbrodt 2011; Bensimon-Brito et al. 2016; Copper et al. 2018). However, glyoxal fixation was never tested on zebrafish, which has recently been rediscovered in tissue culture, mouse, rat, and Drosophila, adding to the list of useful antibodies for these organisms (Richter et al. 2018). This thesis compared a zebrafish staining procedure that uses glyoxal as a fixative agent to one that uses PFA.

Results indicated that glyoxal fixation improves the antigenicity of TJ proteins in zebrafish. Moreover, this fixation method is advantageous over the conventional PFA fixation method in many ways. Glyoxal fixation needs considerably shorter time and overcomes the toxicity outcome of PFA. In addition, embryos which are fixed with glyoxal maintain a much better texture and give a clearer visualisation and much less

background signal during imaging. I believe this method is valuable and requires to be further tested for a wider range of antibodies in zebrafish.

3.2 Germplasm localization in Zebrafish and its relation to TJs

The role of TJ proteins in GP localization has previously never described. Germplasm in zebrafish is first localized in the BB in the oocyte, then at the first cleavage furrow during the first embryonic division and later it localizes at four distinct spots at the apical ends of the cleavage furrows from four cells stage onward. This pattern of localization is retained during further embryonic divisions and from this stage on Germplasm stays at the same four spots and never passes to the new progenies of cells as the embryo continuously divides. The first four cells of the embryo will stay as the only germplasm storage cells as embryonic development proceeds, which means every further cell division stays asymmetric so that daughter cells never carry the cytoplasmic part which contains GP. This asymmetric division guarantees the formation of germ line and soma. However, the cellular structure which control this process was unknown. A mass spectrometry analysis identified us NMMII and TJ proteins as the interaction partners of Buc, which is the major GP organizer in zebrafish, which was the start point of this thesis. Later, colocalization of Buc and ZO1 and Cldn was also recorded by immunohistochemistry. Furthermore, electron microscopy showed TJ like structures at early cleavage furrows were GP is located. These results all together confirmed that Buc localizes at TJs and at the same time showed a role of TJ in GP formation which was not known before. The identified Buc localization domain 'BucLoc' contains all the necessary interaction sites to localize GP to the TJs through interaction with the SH3 domain of the ZO2 proteins in zebrafish.

3.3 Protein interactome of Buc

Bucky ball is essential for GP assembly in the BB and its overexpression results in extra germ cell formation in zebrafish embryos (Bontems et al. 2009). However, the exact mechanism by which Buc induces extra germ cell formation is unknown. In addition to this, it is known that endogenous Buc accumulates at embryonic cleavage furrows. However, very little is known about the protein interactome of Buc which leads to its recruitment to the cleavage furrows (Bontems et al. 2009). In 2015, Campbell *et. al.* discovered Kinesin-1 Kif5Ba as a binding partner of Buc, which is also maternally expressed in zebrafish, and showed its role in germline specification *in vivo*. Campbell and other authors claimed that Mkif5Ba is required to recruit Buc to the cleavage furrows and thereby specifying PGCs, suggesting a first insight into the anchorage of Buc to the cleavage furrows through cytoskeletal structures (Campbell et al. 2015).

Two years after, another study found that RhoA/ROCK pathway activity is essential for the correct localization of the GP mRNAs in zebrafish embryos (Miranda-Rodríguez et al. 2017). This study suggested that inhibition of RhoA/ROCK disturbs the localization of GP through the destruction of correct localization of furrow microtubule array (FMA) at the cleavage furrows, providing another evidence for the involvement of cytoskeleton in GP localization in zebrafish. The first described cytoskeletal structure tethering GP in zebrafish was previously also described as furrow-associated microtubule-array (FMA) (Jesuthasan 1998; Pelegri et al. 1999).

We found Myosin Light Chain, which is a subunit of the Non-Muscle Myosin II (NMII) protein as another interacting partner of Buc (Rostam et al. 2021a, submitted). NMII is known to associate with various cellular structures (Liu et al. 2012; Vicente-Manzanares et al. 2009; Nair et al. 2013) and it is described to get activated upon phosphorylation by ROCK (Amano et al. 1996; Miranda-Rodríguez et al. 2017). Interestingly, phosphorylated NMII (p-NMII) is known to colocalize with GP RNAs at the 2- and 4-cell stage in zebrafish embryos(Nair et al. 2013) and we also found that p-NMII colocalizes with Buc (Rostam et al. 2021a, submitted). These results suggest a model in which GP is anchored to the cleavage furrows through the interaction of Buc with cytoskeletal structures. We believe that Buc acts as a nucleator for the assembly of other GP components.

As FMA disassembles after the third cleavage, the molecular identity of the cellular structure anchoring GP after the eight-cell stage was still unresolved. Here, I show that Buc localizes to the TJ at the cleavage furrows, suggesting that this cellular structure is responsible of the association of Buc to the FMA (Rostam et al. 2021a, submitted). In addition, I identified the direct TJ interaction partners of Buc, which are ZO2a and ZO2b. We show that the SH3 domains of these two proteins interact with the PxxP motifs of Buc protein and this provides the molecular control for GP localization in zebrafish.

SH3 (Src homology region 3) domains are well known models of protein-protein interaction, known to interact with proline rich domains which have PXXP core motifs, where P indicates proline and X denotes any amino acid (Mayer and Eck 1995). SH3 was first identified as a conserved region at the N terminal non catalytic part of the Src protein tyrosine kinases (Mayer, Hamaguchi, and Hanafusa 1988). It is a short domain composed of about 60 amino acids and it is an evolutionary conserved domain through yeast to mammals (Musacchio et al. 1992; Erpel, Superti-Furga, and Courtneidige 1995). Eventually, these domains were characterised in many other proteins having various roles in a broad range of intracellular and cell-environment signalling, starting from cell growth and differentiation, cytoskeletal arrangement till immune response and protein turnover (ärkkäinen et al. 2006; Mayer 2001; Li 2005; Kaneko, Li, and Li 2008). About 300 SH3 domains are recorded in the human genome (Kärkkäinen et al. 2006).

The identification of SH3 domain interaction with Buc which I present here provides, on the one hand, valuable details of interacting molecules involved in the anchorage of GP in zebrafish. This is for the first time that is shown that a well-known protein interaction model, SH3 domain vs PxxP motifs, plays a role in GP localization. On the other hand, this adds novel data to the biochemistry of this famous model of protein interaction. I believe, the data presented here broadens the ligand pool and the cellular function of the SH3 domain family.

3.4 Buc uses multiple PxxP motifs to interact with ZO2a and ZO2b

We found that BucLoc domain, which is composed of 78 amino acids is sufficient for the localization of Buc. Buc contains six PxxP motives, with five of them located in the BucLoc region. We named them as P-motives, P1, P2, P3, P4, P5 and P6. It is previously shown that Buc interacts with other proteins of the GP such as VASA and Tudor, here I found that Buc interacts with SH3 domains. This is for the first time that interaction of Buc to a cellular structure component is shown, after the discovery of its interaction with kif5a and FMA, providing the molecular base for the localization of Buc at TJs.

Two main classes of legand sequences have been identified to interact with SH3 domain, classI: +xxPxxP and classII: PxxPx+. As we can see from these data, having a positively charged residue (arginine or lysine) is very important in making the interaction with SH3 domain and based on this class I and class II are identified. However, it is reported that some legends do not fall into this classification Xin et al. 2013; Tonikian et al. 2009; Chen at al. 2009). It is described that nearly 25% of human proteins are containing proline rich sequences, it was mysterious how the few hundred SH3 domains in the human protein pool can recognize their target proline motifs to specifically perform their respective cellular function (Kärkkäinen et al. 2006). This argument has been rather clarified by discovering that some of these SH3 domains bind to non-PxxP proline regions, and hence making their selection more specific (Li 2005; Kaneko, Li, and Li 2008).

The same argument has been also mentioned in *C. elegans*. It is suggested that in organisms like *C. elegans* where many SH3 domains exist, specificity is more difficult and it would be more competitive to the SH3 domains to bind to their legands if they only belong to the regular few identified classes of PxxP motifs, and specifically if two SH3 domains want to bind to the same protein. Therefore, *C. elegans* developed a new strategy to overcome this problem, in which different PxxP containing sequences outside of the class I and II pattern exist which indeed interact with various SH3 domains. This ultimately increases the specificity of the interaction and decreases the competitive binding energy. I agree that this process is an evolutionary consequence of adaptation of *C. elegans* to the competition where several SH3 domains exist in the same organism. Here I discovered a novel zebrafish protein which I believe used the same mechanism of evolution.

Zebrafish is having different isoforms of SH3 domains of tight junction ZO proteins, ZO1a/b, ZO2a/b and ZO3 (Kiener, Sleptsova-friedrich, and Hunziker 2007), making them more diverse and therefore less specific. Here I show that zebrafish Buc protein is having different PxxP motifs, which I think makes it easier for the protein to select between the diverse SH3 domains of ZO isoforms and hence increase the specificity. This suggests that zebrafish also used its unique strategy to increase the specificity of its SH3 domains to their binding partners. I believe the root for the interaction mechanism involving SH3 domains is conserved through species; however, organism evolved their own way of adaptation and specification in order not to struggle with the lack of specificity (Li 2005; Kaneko, Li, and Li 2008). It is worth mentioning that most of the data, if not all, that are so far available on the SH3 domains and their interactions are based on *in vitro* experiments. The data here provides an insight into how this works in a living organism. It is fascinating that out of five SH3 domains tested three are not interacting with the tested protein. This suggests that specificity of these interactions might be further guaranteed under the normal physiological conditions *in vivo.* It is also possible to claim that multimeric protein complexes which exist *in vivo might* promote SH3 mediated interactions, as suggested before (Mayer 2001; Kaneko, Li, and Li 2008).

Overall, these results discovered a novel role of SH3 domain as hubs in the recruitment of zebrafish germplasm to the TJs, which is for the first time mentioned in vertebrate reproduction. These data suggest that Buc uses its multiple PxxP motifs to select specific SH3 domains of ZO proteins, as there are five ZO proteins in zebrafish and we discovered that Buc only interacts with the SH3 domains of ZO2a and ZO2b. This supports the specificity property of the interaction between proline rich motifs and SH3 domains, as previously described (Kaneko, Li, and Li 2008).

Moreover, it is shown here that three of the six P-motives in Buc are important for interaction with SH3 domains of ZO proteins and its localization, future experiments may investigate the role of the other three motifs in other biological pathways. At this point, I believe that PxxP motifs in Buc are the key for anchoring GP in zebrafish, which is not the same for the other vertebrates. It is shown, for example, that *Xenopus* utilizes a different mechanism for the same process which involves aggregation through the use of the prion like domains of Xvelo (Boke et al. 2016). This suggests that specific molecular pathways exist in vertebrates for the anchorage of GP, hence not every molecular detail is conserved between vertebrates. It seems that Xvelo aggregation and phase separation is the key for anchoring GP in *Xenopus*, while aggregation is a separate process from anchorage of GP in zebrafish.

Here, drug treatment experiments showed the importance of ZO1 phosphorylation in the aggregation of GP in zebrafish, which supports ZO1 colocalization with Buc (Rostam et al. 2021a, submitted). This brings us to drawing the complete GP localization pathway in zebrafish, as I have also shown the role of Cldn-d in this

process (Rostam et al. 2021, submitted). I believe that Buc interacts with ZO2 which subsequently interacts with ZO1 and ZO1 finally interacts with Cldn-d on the membrane and that completes the pathway for GP localization in zebrafish (Rostam atal. 2021b, submitted). Taken together, these data suggest a novel mechanism for GP localization in vertebrates which has not been found before. We show that interaction with TJ proteins is the base for GP localization in zebrafish, which is a completely different process from aggregation of GP granules.

3.5 Role of phase separation in germ plasm assembly

The role of phase separation during germline development has recently become an attractive topic in developmental biology (So, Cheng, and Schuh 2021; Dodson and Kennedy 2020). Since their initial discovery, P granules and many other RNA- rich granules have been mentioned to show liquid-like behaviours (Brangwynne et al. 2009; Brangwynne, Mitchison, and Hyman 2011; Kroschwald et al. 2015). Proteins containing intrinsically disordered regions (IDRs) and prion-like domains (PrDs) are shown to have these properties (Kroschwald et al. 2015), as these proteins tend to aggregate and phase separate other components with them (Prusiner 1998; Shorter and Lindquist 2005). It is previously shown that Buc interacts with zebrafish Tudor homologue Tdrd6 through its C-terminus dimethylated Arginine residues (Roovers et al. 2018) . Using high-resolution microscopy, Roovers et.al. showed that GP RNAs, Tdrd6 and Buc form particles at the 4-cell stage when the GP start to accumulate at the cleavage furrows, in which Buc is localized at the center of the particle and Tdrd6 is situated at the periphery of the particles (Roovers et al. 2018). This implies that Buc coordinates with Tdrd6 to nucleate GP, which is the same action that Osk performs upon interaction with Tudor to aggregate GP (Breitwieser et al. 1996). This proposes a conserved mechanism for GP aggregation between zebrafish and Drosophilla. However, this does not mean that they share the same localization mechanism. We showed that Buc contains Prion like domains, however, we excluded their role in the localization of Buc, suggesting that localization and aggregation are two separate mechanisms in zebrafish (Rostam et al. 2021a, submitted).

Roovers et al. mentioned the importance of Tudor in the formation of GP aggregates and phase separation (Roovers et al. 2018). Our Cldn-d experiments also showed the same effect. When we disturbed TJ protein Cldn-d, Buc aggregation was affected (Rostam et al. 2021a, submitted). It is worth mentioning that formation of TJs is previously suggested to be driven by phase separation of ZO proteins (Beutel et al. 2019) . ZO proteins are IDP proteins and we showed that ZO1 colocalizes with Buc. These results suggest that a set of phase separating proteins come together to form aggregates where also GP components sit. Since disturbing these unknown GP components disturbs GP aggregation, these proteins have roles in bringing GP together.

Therefore, in the case of zebrafish, I believe that TJ proteins, all the interaction partners of Buc found so far, and GP components are all loaded in the BB as phase separated granules and later they get localized to the perspective places in the cell as the embryo develops. As we found that GP is anchored to the TJs, we think binding to TJ proteins is the key for GP anchorage in zebrafish. However, we do not rule out the role of other components such as Tudor, as they can differently play role in the localization process up to the stage where Buc is anchored, but the end point where it gets anchored involves direct interaction with TJ components itself that we show here. This will ultimately prevent symmetric GP distribution in early embryos and therefore allows germ cell specification and somatic tissue segregation.

3.6 Buc and ZO2 as biomolecular condensates

A fundamental question in cell biology is how the densely packed intracellular components coordinate to control the complex biochemical reactions within a cell. Localizing various components reflecting various functions in separate microenvironments with in the cell is one strategy to achieve this. A classical way of doing this is that cells compartmentalize their components into membrane bound organelles such as endoplasmic reticulum and Golgi apparatus. These membranes are selectively permeable, therefore separating the reactions which occur inside them from their surroundings. However, several other compartments are not membrane bounded, such as nucleoli, stress granules and germ granules. These membraneless structures are able to concentrate proteins and RNA molecules. These structures have been recently referred to as 'bimolecular condensates' (Banani et al. 2017). It remained mysterious, however, how these condensates maintain their structure and control their internal biochemical reactions.

Researching this field has recently been paid a lot of attention and phase separation is proposed as a principle to explain the physical and chemical properties of biomolecular condensates. A well-studied condensate is P-granules in *C. elegans*, which is shown to form by liquid-liquid phase separation (Brangwynne et al. 2009). BB is also investigated in this term and it is described that BB in *Xenopus* forms amyloid structures, which is a different physical feature compared to the P-granules of *C. elegans*. Xvelo, the homologue of Buc in zebrafish, is the most prevalent protein in the BB of *Xenopus* and it is shown that prion like domains in Xvelo drives the phase separation of the BB (Boke et al. 2016). Buc is also shown to aggregate and to possess gel like behaviours (Krishnakumar et al. 2018). However, it is mentioned that different condensates with different physical properties first emerge as liquid droplets at and tend to solidify with time forming pathogenic aggregates, which is the principle for neurodegenerative disorders and cancer (Spann et al. 2019). To conclude, I believe investigating the role of phase separation and condensate

formation during embryonic development might move the field further forward and bring novel insights to our understanding of developmental biology.

Outlook

This work brings in two major outlooks for future research:

First: This research identified the cellular structure which anchors GP in zebrafish, the TJs. Future research might investigate the mechanism by which GP is transported to the TJs.

Second: This thesis shows the interaction between Buc and ZO proteins, which are also recently described as phase separating molecules (Beutel et al. 2019; Schwayer et al. 2019). This proposes that two sets of phase separating compartments come together in a system, which can be explained as a multivalency-driven form of phase separation which is previously described (Banani et al. 2017). It will be interesting to find out how these condensates come together.

Is it Buc which concentrates ZO2 or it is ZO2 which concentrates Buc? Do they share the same condensate or they are separate but miscible compartments? Buc is shown to concentrate Tudor, in particles where Buc localizes at the center of the particle and Tudor surrounding it. This means Buc acts as a scaffold protein in this case and Tudor is a client for Buc, a principle which is described previously (Banani et al. 2016). If we take this scenario in the case of Buc and ZO2 interaction, we could suggest that Buc concentrates ZO, thereby ZO2 molecules can be clients for Buc. Especially as Buc has separate motifs to bind ZO2a and ZO2b, it is highly likely that Buc recruits ZO2a and ZO2b to its condensate. However, as ZO proteins are known to phase separate independently, it is also possible that they form separate condensates and get mixed with Buc containing condensates as they favour each other because of the interacting domains in them. What Happens if Buc does not contain PxxP motifs? Would it still favour ZO2? The data here provides the first insights into a 'No' to this question.

The question which remains to be answered in more detail, is what is the significance of being Buc and ZO2 droplets together? Could Buc induce TJ formation in zebrafish, or is it TJ proteins which assemble GP? Future studies might investigate these aspects.

References

Amano M, Ito M, Kimura K, Fukata Y, Chihara K, Nakano T, Matsuura Y, Kaibuchi K. Phosphorylation and activation of myosin by Rho-associated kinase (Rho-kinase). J Biol Chem. 1996 Aug 23;271(34):20246-9. doi:

10.1074/jbc.271.34.20246. PMID: 8702756.

Banani SF, Rice AM, Peeples WB, Lin Y, Jain S, Parker R, Rosen MK. Compositional Control of Phase-Separated Cellular Bodies. Cell. 2016 Jul 28;166(3):651-663. doi: 10.1016/j.cell.2016.06.010. Epub 2016 Jun 30. PMID: 27374333; PMCID: PMC4967043.

Bensimon-Brito A, Cardeira J, Dionísio G, Huysseune A, Cancela ML, Witten PE. Revisiting in vivo staining with alizarin red S--a valuable approach to analyse zebrafish skeletal mineralization during development and regeneration. BMC Dev Biol. 2016 Jan 19;16:2. doi: 10.1186/s12861-016-0102-4. PMID: 26787303; PMCID: PMC4719692.

Berchowitz LE, Kabachinski G, Walker MR, Carlile TM, Gilbert WV, Schwartz TU, Amon A. Regulated Formation of an Amyloid-like Translational Repressor Governs Gametogenesis. Cell. 2015 Oct 8;163(2):406-18. doi: 10.1016/j.cell.2015.08.060. Epub 2015 Sep 24. PMID: 26411291; PMCID: PMC4600466.

Beutel O, Maraspini R, Pombo-García K, Martin-Lemaitre C, Honigmann A. Phase Separation of Zonula Occludens Proteins Drives Formation of Tight Junctions. Cell. 2019 Oct 31;179(4):923-936.e11. doi: 10.1016/j.cell.2019.10.011. PMID: 31675499.

Boke E, Ruer M, Wühr M, Coughlin M, Lemaitre R, Gygi SP, Alberti S, Drechsel D, Hyman AA, Mitchison TJ. Amyloid-like Self-Assembly of a Cellular Compartment. Cell. 2016 Jul 28;166(3):637-650. doi: 10.1016/j.cell.2016.06.051. PMID: 27471966; PMCID: PMC5082712.

Bontems F, Stein A, Marlow F, Lyautey J, Gupta T, Mullins MC, Dosch R. Bucky ball organizes germ plasm assembly in zebrafish. Curr Biol. 2009 Mar 10;19(5):414-22. doi: 10.1016/j.cub.2009.01.038. Epub 2009 Feb 26. PMID: 19249209.

Brangwynne CP, Eckmann CR, Courson DS, Rybarska A, Hoege C, Gharakhani J, Jülicher F, Hyman AA. Germline P granules are liquid droplets that localize by controlled dissolution/condensation. Science. 2009 Jun 26;324(5935):1729-32. doi: 10.1126/science.1172046. Epub 2009 May 21. PMID: 19460965.

Brangwynne CP, Mitchison TJ, Hyman AA. Active liquid-like behavior of nucleoli determines their size and shape in Xenopus laevis oocytes. Proc Natl Acad Sci U S A. 2011 Mar 15;108(11):4334-9. doi: 10.1073/pnas.1017150108. Epub 2011 Feb 28. PMID: 21368180; PMCID: PMC3060270.

Breitwieser W, Markussen FH, Horstmann H, Ephrussi A. Oskar protein interaction with Vasa represents an essential step in polar granule assembly. Genes Dev. 1996 Sep 1;10(17):2179-88. doi: 10.1101/gad.10.17.2179. PMID: 8804312.

Buehr ML, Blackler AW. Sterility and partial sterility in the South African clawed toad following the pricking of the egg. J Embryol Exp Morphol. 1970 Apr;23(2):375-84. PMID: 5465209.

Campbell PD, Heim AE, Smith MZ, Marlow FL. Kinesin-1 interacts with Bucky ball to form germ cells and is required to pattern the zebrafish body axis. Development. 2015 Sep 1;142(17):2996-3008. doi: 10.1242/dev.124586. Epub 2015 Aug 7. PMID: 26253407; PMCID: PMC4582183.

Chen JK, Tanaka A, Schreiber SL, Lane WS, Braucr AW. Biased Combinatorial Libraries; Novel Ligands for the SH3 Domain of Phosphatidylinositol 3-Kinase. Journal of the American Chemical Society. 1993 Dec;115 (26): 12591–92. doi: 10.1021/ja00079a051

Copper JE, Budgeon LR, Foutz CA, van Rossum DB, Vanselow DJ, Hubley MJ, Clark DP, Mandrell DT, Cheng KC. Comparative analysis of fixation and embedding techniques for optimized histological preparation of zebrafish. Comp Biochem Physiol C Toxicol Pharmacol. 2018 Jun;208:38-46. doi: 10.1016/j.cbpc.2017.11.003. Epub 2017 Nov 20. PMID: 29157956; PMCID: PMC5936644.

Crow JF. Advantages of sexual reproduction. Dev Genet. 1994;15(3):205-13. doi: 10.1002/dvg.1020150303. PMID: 8062455.

D'Amico F, Skarmoutsou E, Stivala F. State of the art in antigen retrieval for immunohistochemistry. J Immunol Methods. 2009 Feb 28;341(1-2):1-18. doi: 10.1016/j.jim.2008.11.007. Epub 2008 Dec 6. PMID: 19063895.

Dosch R, Wagner DS, Mintzer KA, Runke G, Wiemelt AP, Mullins MC. Maternal control of vertebrate development before the midblastula transition: mutants from the zebrafish I. Dev Cell. 2004 Jun;6(6):771-80. doi: 10.1016/j.devcel.2004.05.002. PMID: 15177026.

Dosch R. Next generation mothers: Maternal control of germline development in zebrafish. Crit Rev Biochem Mol Biol. 2015 Jan-Feb;50(1):54-68. doi: 10.3109/10409238.2014.985816. Epub 2014 Nov 21. PMID: 25413788.

Erpel T, Superti-Furga G, Courtneidge SA. Mutational analysis of the Src SH3 domain: the same residues of the ligand binding surface are important for intra- and intermolecular interactions. EMBO J. 1995 Mar 1;14(5):963-75. PMID: 7534229; PMCID: PMC398168.

Ewen-Campen B, Schwager EE, Extavour CG. The molecular machinery of germ line specification. Mol Reprod Dev. 2010 Jan;77(1):3-18. doi: 10.1002/mrd.21091. PMID: 19790240.

Extavour CG, Akam M. Mechanisms of germ cell specification across the metazoans: epigenesis and preformation. Development. 2003 Dec;130(24):5869-84. doi: 10.1242/dev.00804. PMID: 14597570.

Hashimoto Y, Maegawa S, Nagai T, Yamaha E, Suzuki H, Yasuda K, Inoue K. Localized maternal factors are required for zebrafish germ cell formation. Dev Biol. 2004 Apr 1;268(1):152-61. doi: 10.1016/j.ydbio.2003.12.013. PMID: 15031112.

Hashimoto Y, Suzuki H, Kageyama Y, Yasuda K, Inoue K. Bruno-like protein is localized to zebrafish germ plasm during the early cleavage stages. Gene Expr Patterns. 2006 Jan;6(2):201-5. doi: 10.1016/j.modgep.2005.06.006. Epub 2005 Sep 15. PMID: 16168720.

Heasman J, Quarmby J, Wylie CC. The mitochondrial cloud of Xenopus oocytes: the source of germinal granule material. Dev Biol. 1984 Oct;105(2):458-69. doi: 10.1016/0012-1606(84)90303-8. PMID: 6541166.

Howley C, Ho RK. mRNA localization patterns in zebrafish oocytes. Mech Dev. 2000 Apr;92(2):305-9. doi: 10.1016/s0925-4773(00)00247-1. PMID: 10727871.

Illmensee K, Mahowald AP. Transplantation of posterior polar plasm in Drosophila. Induction of germ cells at the anterior pole of the egg. Proc Natl Acad Sci U S A. 1974 Apr;71(4):1016-20. doi: 10.1073/pnas.71.4.1016. PMID: 4208545; PMCID: PMC388152.

Inoue D, Wittbrodt J. One for all--a highly efficient and versatile method for fluorescent immunostaining in fish embryos. PLoS One. 2011;6(5):e19713. doi: 10.1371/journal.pone.0019713. Epub 2011 May 13. PMID: 21603650; PMCID: PMC3094454.

Jesuthasan S. Furrow-associated microtubule arrays are required for the cohesion of zebrafish blastomeres following cytokinesis. J Cell Sci. 1998 Dec 18;111 (Pt 24):3695-703. PMID: 9819360.

Juliano CE, Swartz SZ, Wessel GM. A conserved germline multipotency program. Development. 2010 Dec;137(24):4113-26. doi: 10.1242/dev.047969. PMID: 21098563; PMCID: PMC2990204.

Kaneko T, Li L, Li SS. The SH3 domain--a family of versatile peptide- and protein-recognition module. Front Biosci. 2008 May 1;13:4938-52. doi: 10.2741/3053. PMID: 18508559.

Kaneko T, Li L, Li SS. The SH3 domain--a family of versatile peptide- and protein-recognition module. Front Biosci. 2008 May 1;13:4938-52. doi: 10.2741/3053. PMID: 18508559.

Kärkkäinen S, Hiipakka M, Wang JH, Kleino I, Vähä-Jaakkola M, Renkema GH, Liss M, Wagner R, Saksela K. Identification of preferred protein interactions by phage-display of the human Src homology-3 proteome. EMBO Rep. 2006 Feb;7(2):186-91. doi: 10.1038/sj.embor.7400596. PMID: 16374509; PMCID: PMC1369250.

Kato M, Han TW, Xie S, Shi K, Du X, Wu LC, Mirzaei H, Goldsmith EJ, Longgood J, Pei J, Grishin NV, Frantz DE, Schneider JW, Chen S, Li L, Sawaya MR, Eisenberg D, Tycko R, McKnight SL. Cell-free formation of RNA granules: low complexity sequence domains form dynamic fibers within hydrogels. Cell. 2012 May 11;149(4):753-67. doi: 10.1016/j.cell.2012.04.017. PMID: 22579281; PMCID: PMC6347373.

Kloc M, Bilinski S, Etkin LD. The Balbiani body and germ cell determinants: 150 years later. Curr Top Dev Biol. 2004;59:1-36. doi: 10.1016/S0070-2153(04)59001-4. PMID: 14975245.

Knaut H, Pelegri F, Bohmann K, Schwarz H, Nüsslein-Volhard C. Zebrafish vasa RNA but not its protein is a component of the germ plasm and segregates asymmetrically before germline specification. J Cell Biol. 2000 May 15;149(4):875-88. doi: 10.1083/jcb.149.4.875. PMID: 10811828; PMCID: PMC2174565.

Kosaka K, Kawakami K, Sakamoto H, Inoue K. Spatiotemporal localization of germ plasm RNAs during zebrafish oogenesis. Mech Dev. 2007 Apr;124(4):279-89. doi: 10.1016/j.mod.2007.01.003. Epub 2007 Jan 13. PMID: 17293094.

Krishnakumar P, Riemer S, Perera R, Lingner T, Goloborodko A, Khalifa H, Bontems F, Kaufholz F, El-Brolosy MA, Dosch R. Functional equivalence of germ plasm organizers. PLoS Genet. 2018 Nov 6;14(11):e1007696. doi: 10.1371/journal.pgen.1007696. PMID: 30399145; PMCID: PMC6219760.

Kroschwald S, Maharana S, Mateju D, Malinovska L, Nüske E, Poser I, Richter D, Alberti S. Promiscuous interactions and protein disaggregases determine the material state of stress-inducible RNP granules. Elife. 2015 Aug 4;4:e06807. doi: 10.7554/eLife.06807. PMID: 26238190; PMCID: PMC4522596.

Li SS. Specificity and versatility of SH3 and other proline-recognition domains: structural basis and implications for cellular signal transduction. Biochem J. 2005 Sep 15;390(Pt 3):641-53. doi: 10.1042/BJ20050411. PMID: 16134966; PMCID: PMC1199657.

Li SS. Specificity and versatility of SH3 and other proline-recognition domains: structural basis and implications for cellular signal transduction. Biochem J. 2005 Sep 15;390(Pt 3):641-53. doi: 10.1042/BJ20050411. PMID: 16134966; PMCID: PMC1199657.

Liu KC, Jacobs DT, Dunn BD, Fanning AS, Cheney RE. Myosin-X functions in polarized epithelial cells. Mol Biol Cell. 2012 May;23(9):1675-87. doi: 10.1091/mbc.E11-04-0358. Epub 2012 Mar 14. PMID: 22419816; PMCID: PMC3338435.

Mayer BJ, Eck MJ. SH3 domains. Minding your p's and q's. Curr Biol. 1995 Apr 1;5(4):364-7. doi: 10.1016/s0960-9822(95)00073-x. PMID: 7542990.

Mayer BJ, Hamaguchi M, Hanafusa H. A novel viral oncogene with structural similarity to phospholipase C. Nature. 1988 Mar 17;332(6161):272-5. doi: 10.1038/332272a0. PMID: 2450282.

Mayer BJ. SH3 domains: complexity in moderation. J Cell Sci. 2001 Apr;114(Pt 7):1253-63. PMID: 11256992.

McCarthy KM, Francis SA, McCormack JM, Lai J, Rogers RA, Skare IB, Lynch RD, Schneeberger EE. Inducible expression of claudin-1-myc but not occludin-VSV-G results in aberrant tight junction strand formation in MDCK

cells. J Cell Sci. 2000 Oct;113 Pt 19:3387-98. PMID: 10984430.

Miranda-Rodríguez JR, Salas-Vidal E, Lomelí H, Zurita M, Schnabel D. RhoA/ROCK pathway activity is essential for the correct localization of the germ plasm mRNAs in zebrafish embryos. Dev Biol. 2017 Jan 1;421(1):27-42. doi: 10.1016/j.ydbio.2016.11.002. Epub 2016 Nov 9. PMID: 27836552.

Musacchio A, Gibson T, Lehto VP, Saraste M. SH3--an abundant protein domain in search of a function. FEBS Lett. 1992 Jul 27;307(1):55-61. doi: 10.1016/0014-5793(92)80901-r. PMID: 1639195.

Nair S, Marlow F, Abrams E, Kapp L, Mullins MC, Pelegri F. The chromosomal passenger protein birc5b organizes microfilaments and germ plasm in the zebrafish embryo. PLoS Genet. 2013 Apr;9(4):e1003448. doi: 10.1371/journal.pgen.1003448. Epub 2013 Apr 18. PMID: 23637620; PMCID: PMC3630083.

Nakamura A, Shirae-Kurabayashi M, Hanyu-Nakamura K. Repression of early zygotic transcription in the germline. Curr Opin Cell Biol. 2010 Dec;22(6):709-14. doi: 10.1016/j.ceb.2010.08.012. PMID: 20817425.

Pelegri F, Knaut H, Maischein HM, Schulte-Merker S, Nüsslein-Volhard C. A mutation in the zebrafish maternal-effect gene nebel affects furrow formation and vasa RNA localization. Curr Biol. 1999 Dec 16-30;9(24):1431-40. doi: 10.1016/s0960-9822(00)80112-8. PMID: 10607587.

Pelegri F. Maternal factors in zebrafish development. Dev Dyn. 2003 Nov;228(3):535-54. doi: 10.1002/dvdy.10390. PMID: 14579391.

Pepling ME, Wilhelm JE, O'Hara AL, Gephardt GW, Spradling AC. Mouse oocytes within germ cell cysts and primordial follicles contain a Balbiani body. Proc Natl Acad Sci U S A. 2007 Jan 2;104(1):187-92. doi: 10.1073/pnas.0609923104. Epub 2006 Dec 22. PMID: 17189423; PMCID: PMC1765432.

Prusiner SB. Prions. Proc Natl Acad Sci U S A. 1998 Nov 10;95(23):13363-83. doi: 10.1073/pnas.95.23.13363. PMID: 9811807; PMCID: PMC33918.

Raz E. Primordial germ-cell development: the zebrafish perspective. Nat Rev Genet. 2003 Sep;4(9):690-700. doi: 10.1038/nrg1154. PMID: 12951570.

Richter KN, Revelo NH, Seitz KJ, Helm MS, Sarkar D, Saleeb RS, D'Este E, Eberle J, Wagner E, Vogl C, Lazaro DF, Richter F, Coy-Vergara J, Coceano G, Boyden ES, Duncan RR, Hell SW, Lauterbach MA, Lehnart SE, Moser T, Outeiro TF, Rehling P, Schwappach B, Testa I, Zapiec B, Rizzoli SO. Glyoxal as an alternative fixative to formaldehyde in immunostaining and super-resolution microscopy. EMBO J. 2018 Jan 4;37(1):139-159. doi: 10.15252/embj.201695709. Epub 2017 Nov 16. PMID: 29146773; PMCID: PMC5753035.

Riemer S, Bontems F, Krishnakumar P, Gömann J, Dosch R. A functional Bucky ball-GFP transgene visualizes germ plasm in living zebrafish. Gene Expr Patterns. 2015 May-Jul;18(1-2):44-52. doi: 10.1016/j.gep.2015.05.003. Epub 2015 Jul 2. PMID: 26143227.

Riemer S. Analyzing the Molecular Mechanism of Bucky Ball Localization during Germ Cell Specification in Zebrafish. Dissertation, 2014 Oct.

Rongo C, Lehmann R. Regulated synthesis, transport and assembly of the Drosophila germ plasm. Trends Genet. 1996 Mar;12(3):102-9. doi: 10.1016/0168-9525(96)81421-1. PMID: 8868348.

Roovers EF, Kaaij LJT, Redl S, Bronkhorst AW, Wiebrands K, de Jesus Domingues AM, Huang HY, Han CT, Riemer S, Dosch R, Salvenmoser W, Grün D, Butter F, van Oudenaarden A, Ketting RF. Tdrd6a Regulates the Aggregation of Buc into Functional Subcellular Compartments that Drive Germ Cell Specification. Dev Cell. 2018 Aug 6;46(3):285-301.e9. doi: 10.1016/j.devcel.2018.07.009. PMID: 30086300; PMCID: PMC6084408.

Rostam N, Goloborodko A, Riemer S, Hertel A, Riedel D, Vorbrüggen G, and Dosch R. 2021a. Germ plasm anchors at tight junctions in the early zebrafish embryo (submitted).

Rostam N, Perera R, Vorbrüggen G, Dosch R. 2021b. Bucky ball Interacts with ZO2a and ZO2b to Direct the Localization of Germ Plasm to the Tight Junctions in Zebrafish (submitted).

Saitou M. Germ cell specification in mice. Curr Opin Genet Dev. 2009 Aug;19(4):386-95. doi: 10.1016/j.gde.2009.06.003. Epub 2009 Jul 16. PMID: 19616424.

Schwayer C, Shamipour S, Pranjic-Ferscha K, Schauer A, Balda M, Tada M, Matter K, Heisenberg CP. Mechanosensation of Tight Junctions Depends on ZO-1 Phase Separation and Flow. Cell. 2019 Oct 31;179(4):937-952.e18. doi: 10.1016/j.cell.2019.10.006. PMID: 31675500.

Selman K, Wallace RA, Sarka A, Qi X. Stages of oocyte development in the zebrafish, Brachydanio rerio. J Morphol. 1993 Nov;218(2):203-224. doi: 10.1002/jmor.1052180209. PMID: 29865471.

Shi SR, Cote RJ, Taylor CR. Antigen retrieval techniques: current perspectives. J Histochem Cytochem. 2001 Aug;49(8):931-7. doi: 10.1177/002215540104900801. PMID: 11457921.

Shorter J, Lindquist S. Prions as adaptive conduits of memory and inheritance. Nat Rev Genet. 2005 Jun;6(6):435-50. doi: 10.1038/nrg1616. PMID: 15931169.

Smith LD. The role of a "germinal plasm" in the formation of primordial germ cells in Rana pipiens. Dev Biol. 1966 Oct;14(2):330-47. doi: 10.1016/0012-1606(66)90019-4. PMID: 6008350.

Spannl S, Tereshchenko M, Mastromarco GJ, Ihn SJ, Lee HO. Biomolecular condensates in neurodegeneration and cancer. Traffic. 2019 Dec;20(12):890-911. doi: 10.1111/tra.12704. PMID: 31606941.

Strome S, Updike D. Specifying and protecting germ cell fate. Nat Rev Mol Cell Biol. 2015 Jul;16(7):406-16. doi: 10.1038/nrm4009. PMID: 26122616; PMCID: PMC4698964.

Sullivan-Brown J, Bisher ME, Burdine RD. Embedding, serial sectioning and staining of zebrafish embryos using JB-4 resin. Nat Protoc. 2011 Jan;6(1):46-55. doi: 10.1038/nprot.2010.165. Epub 2010 Dec 16. PMID: 21212782; PMCID: PMC3122109.

Suzuki H, Maegawa S, Nishibu T, Sugiyama T, Yasuda K, Inoue K. Vegetal localization of the maternal mRNA encoding an EDEN-BP/Bruno-like protein in zebrafish. Mech Dev. 2000 May;93(1-2):205-9. doi: 10.1016/s0925-4773(00)00270-7. PMID: 10781958.

Taguchi A, Takii M, Motoishi M, Orii H, Mochii M, Watanabe K. Analysis of localization and reorganization of germ plasm in Xenopus transgenic line with fluorescence-labeled mitochondria. Dev Growth Differ. 2012 Oct;54(8):767-76. doi: 10.1111/dgd.12005. PMID: 23067138.

Tonikian R, Xin X, Toret CP, Gfeller D, Landgraf C, Panni S, Paoluzi S, Castagnoli L, Currell B, Seshagiri S, Yu H, Winsor B, Vidal M, Gerstein MB, Bader GD, Volkmer R, Cesareni G, Drubin DG, Kim PM, Sidhu SS, Boone C. Bayesian modeling of the yeast SH3 domain interactome predicts spatiotemporal dynamics of endocytosis proteins. PLoS Biol. 2009 Oct;7(10):e1000218. doi: 10.1371/journal.pbio.1000218. Epub 2009 Oct 20. PMID: 19841731; PMCID: PMC2756588.

Urven LE, Yabe T, Pelegri F. A role for non-muscle myosin II function in furrow maturation in the early zebrafish embryo. J Cell Sci. 2006 Oct 15;119(Pt 20):4342-52. doi: 10.1242/jcs.03197. PMID: 17038547.

Vicente-Manzanares M, Ma X, Adelstein RS, Horwitz AR. Non-muscle myosin II takes centre stage in cell adhesion

and migration. Nat Rev Mol Cell Biol. 2009 Nov;10(11):778-90. doi: 10.1038/nrm2786. PMID: 19851336; PMCID: PMC2834236.

Wakahara M. Partial characterization of "primordial germ cell-forming activity" localized in vegetal pole cytoplasm in anuran eggs. J Embryol Exp Morphol. 1977 Jun;39:221-33. PMID: 560424.

Weismann A. 1983. “The Germ-Plasm: A Theory of Heredity.” Charles Scribner’s Sons.

Xin X, Gfeller D, Cheng J, Tonikian R, Sun L, Guo A, Lopez L, Pavlenco A, Akintobi A, Zhang Y, Rual JF, Currell B, Seshagiri S, Hao T, Yang X, Shen YA, Salehi-Ashtiani K, Li J, Cheng AT, Bouamalay D, Lugari A, Hill DE, Grimes ML, Drubin DG, Grant BD, Vidal M, Boone C, Sidhu SS, Bader GD. SH3 interactome conserves general function over specific form. Mol Syst Biol. 2013;9:652. doi: 10.1038/msb.2013.9. PMID: 23549480; PMCID: PMC3658277.

Yoon C, Kawakami K, Hopkins N. Zebrafish vasa homologue RNA is localized to the cleavage planes of 2- and 4-cell-stage embryos and is expressed in the primordial germ cells. Development. 1997 Aug;124(16):3157-65. PMID: 9272956.